The Spin Structure of Nucleon and High Energy Reactions

Yamanishi, Teruya

(Degree)
博士（学術）

(Date of Degree)
1994-03-31

(Date of Publication)
2012-06-20

(Resource Type)
doctoral thesis

(Report Number)
甲1311

(JaLCDOI)
https://doi.org/10.11501/3078439

(URL)
https://hdl.handle.net/20.500.14094/D1001311

博士論文

The Spin Structure of Nucleons and High Energy Reactions

１９９４年３月

神戸大学大学院自然科学研究科

山　西　輝　也

DOCTORAL THESIS

The Spin Structure of Nucleons and High Energy Reactions

(核子のスピン構造と高エネルギー素粒子反応)

Teruya YAMANISHI

Department of Fundamental Science of Materials

Division of Science of Materials

The Graduate School of Science and Technology

Kobe University

March 1994

ACKNOWLEDGMENTS

I wish to express my gratitude to Professor Toshiyuki Morii for invaluable suggestions, comments, instructions and careful reading of this manuscript. I am so much obliged to Professor Keizo Kobayakawa and Mr.Shun'ichi Tanaka for making a number of helpful suggestions and continuous encouragement. Also I would like to thank many of my colleagues at Kobe University. Finally, I am grateful to Professor Akira Masaike, Drs.Seiji Makino and Naohito Saito at Kyoto University for enlightening me on interesting experimental data and encouraging discussions on spin–dependent gluon distributions.

ABSTRACT

The spin–dependent distribution functions of quarks and gluons in a proton are studied so as to explain the EMC $g_1^p(x)$ data by introducing a new model which possesses both characteristics of the static quark model and the parton model. The x dependence of not only the EMC $g_1^p(x)$ data but also the recent SMC $g_1^d(x)$ data are reproduced well. It is shown that the polarized gluons through the $U_A(1)$ anomaly of QCD play a significant role and the resultant sum of quark spin in a proton becomes 0.381, that is, almost 3/4 of the proton spin is carried by quarks. The first moment of the polarized gluon density in a proton becomes quite large, $\Delta G(Q^2 = 10.7$ GeV$^2) = 6.32$. To examine whether this result is reasonable or not, we apply the model to other processes, *i.e.* inclusive π^0–, γ– and J/ψ–productions in polarized hadron–polarized hadron reactions and study the two–spin asymmetry $A_{LL}^{\pi^0}(\overset{(-)}{p}p)$, $A_{LL}^{\gamma}(\overset{(-)}{p}p)$ and $A_{LL}^{J/\psi}(pp)$ for these processes. It is shown that the model can reproduce the experimental data for inclusive π^0–production rather well even if the first moment of our polarized gluons is large. In addition, the effect of the polarized gluons on these processes is investigated for several typical spin–dependent gluon distributions. Furthermore, to extract more directly the information on the spin–dependent gluon distribution in a proton, we study the spin–dependent differential cross section for deep inelastic J/ψ leptoproductions, which will be tested in the forthcoming HERA experiments. Gluons seem to hold the key to the deep understanding of hadron structures.

Contents

1 INTRODUCTION

1.1 Motivation

In 1964, by studying the classification of a large number of hadrons existing in those days, Gell-Mann[1] and Zweig[2] proposed an interesting composite model called the *quark model*: hadrons are nonrelativistic bound states made of the fundamental building blocks with spin 1/2, *i.e.* quarks. For example, a proton is considered to be a bound state of three constituent quarks, "uud", whose effective masses are of the order of 300 MeV. The model describes well the static properties of hadrons such as the magnetic moments and mass levels of hadrons[3].

In the late sixties SLAC–M.I.T groups observed deep inelastic scatterings (DIS) of incident electron beams with energies between 7 and 17 GeV on proton targets at the Stanford linear accelerator center (SLAC) in order to study the deep structure of hadrons[4]. At large momentum transfer squared Q^2 $(= -q^2)$, they discovered the remarkable phenomenon known as the *Bjorken scaling*. To explain this scaling, Feynman[5], Bjorken and Paschos[6] proposed a simple model called the *parton model*. They considered that at short distances a proton (generally hadron) might be viewed as composed of almost free point–like constituents of spin 1/2, *i.e.* partons. It seems to be quite natural to identify partons as (almost) massless quarks which are called "current quarks". Furthermore, from the analysis of momentum sum rules of hadrons, it has been realized that neutral constituents different from quarks, called "gluons", should exist in hadrons. The parton model, in which a proton is composed of three valence quarks, sea quarks and gluons, explains quite successfully a large amount of experimental data of DIS at high energies. The masses of these (current) quarks are light, especially those of u– and d–quarks are less than 10 MeV.

On the other hand, strong interactions of fundamental particles, quarks, have been success-

fully described by quantum chromodynamics (QCD). Two decades have already passed since the remarkable property of QCD such as the asymptotic freedom was discovered[7]. Nowadays this property allows perturbative treatment of strong interactions at short distances and one can calculate the observables in hard processes based on fundamental particle reactions. However, unfortunately people have not yet definite understanding of the dynamics for the nonperturbative regime of QCD like confinement, though some promising attempts such as lattice gauge theories[8], QCD sum rules[9] etc. are available. Unravelling the mystery of the hadron structure is still a great challenge.

The parton model is very successful for the deep inelastic regions (at large Q^2) while the nonrelativistic quark model works well for the static limit (at small Q^2). However, nobody knows a realistic model of hadrons which explains consistently the physics in these two different kinematical regions and is naturally connected to these two models for respective kinematical regions of Q^2, though QCD is established as the underlying field theory describing the dynamics of quarks and gluons. To study the hadron structure based on the interactions of fundamental constituents and get into the deep understanding of hadron dynamics is our purpose in this work. It is certainly rather difficult to understand the hadron structure consistently in small and large Q^2 regions as long as we remain in the conventional models and analyses. One of the clues to go beyond the present understanding might be obtained by studying the hadron spin structure, the knowledge of which could be grasped by analyzing its spin–dependent structure functions.

About ten years ago, the first polarized DIS experiment measuring the spin–dependent proton structure function $g_1^p(x)$ was done at SLAC[10] by using longitudinally polarized electron beams on longitudinally polarized proton targets. The observed range was in $0.1 < x < 0.7$, where x is a scaling variable of hadron structure functions and is called "Bjorken x" [6]. In those days, the results were consistent with the theoretical prediction of the parton model, *i.e.* the

Ellis–Jaffe sum rule, which was based on the assumption of the exact flavor SU(3) symmetry and no existence of polarized strange quarks [11]. In the meantime, in 1988 the European Muon Collaboration (EMC) measured $g_1^p(x)$ using the muon beams on proton targets[12]. The kinematical region was extended to much smaller range of x than that of the SLAC data, *i.e.* $x \geq 0.015$. In contrast to the SLAC results, the $g_1^p(x)$ of the EMC data was very surprising. Contrary to the expectations of the nonrelativistic quark model in which the proton spin 1/2 is carried entirely by the u– and d–quarks alone, the results, combined with the data of neutron and hyperon β decays, seem to imply that very little of the proton spin is carried by quarks. Furthermore, the data contradict even with the Ellis–Jaffe sum rule. This situation is called the "proton spin crisis". To find a way for getting out of the crisis is very important to understand the hadron structure.

1.2 Brief review of deep inelastic scatterings

Here, we would like to summarize briefly the theoretical background of the spin–dependent structure functions and give the necessary formulas and experimental data before getting into the detailed description of our approach discussed in the present paper. Let us consider the deep inelastic lepton–nucleon scattering (Fig.1)

$$\ell(k) + \mathrm{N}(p) \rightarrow \ell'(k') + X(p_n) \ .$$

Here the kinematic variables are defined in the lab. frame as

$$p_\mu = (M_N, 0, 0, 0) \ , \quad k_\mu = (E, \mathbf{k}) \ , \quad k'_\mu = (E', \mathbf{k}') \ , \tag{1.1}$$

and

$$q = k - k' \ , \quad \nu = p \cdot q / M_N \ , \quad W^2 = p_n^2 = (p+q)^2 \ , \tag{1.2}$$

where q is the momentum transfer in the scattering process, *i.e.* the virtual photon 4–momentum, and ν the energy transfer of the lepton to the nucleon. In the one–photon exchange approxi-

mation, the differential cross section is given by

$$\frac{d^2\sigma}{d\Omega dE'} = \frac{\alpha^2}{q^4}\frac{E'}{E}L_{\mu\nu}W^{\mu\nu} \ , \tag{1.3}$$

with the fine structure constant α. The leptonic tensor $L_{\mu\nu}$ is given by

$$L_{\mu\nu} = 2\left[k_\mu k'_\nu + k'_\mu k_\nu - g_{\mu\nu}(k\cdot k' - m_\ell^2) + i\epsilon_{\mu\nu\rho\sigma}q^\rho s^\sigma\right] \ , \tag{1.4}$$

where $\epsilon_{\mu\nu\rho\sigma}$ is a totally antisymmetric tensor with $\epsilon_{0123} = +1$. s^σ is a dimensionless spin vector of the lepton and is given by $s^\sigma = \frac{1}{m}(k, 0, 0, E)$ for the longitudinal polarization. The hadronic tensor $W_{\mu\nu}$ in eq.(1.3) contains all of the information on the nucleon target and is defined by the Fourier transform of the commutator of two electromagnetic currents sandwiched between one–nucleon states with momentum p and covariant spin S as follows ;

$$\begin{aligned} W_{\mu\nu}(p,q,S) &= \frac{1}{4M_N}\int\frac{d^4x}{2\pi}e^{iq\cdot x}\langle p,S|[J_\mu(x),J_\nu(0)]|p,S\rangle \\ &= W^{(S)}_{\mu\nu} + iW^{(A)}_{\mu\nu} \ . \end{aligned} \tag{1.5}$$

Here $W^{(S)}_{\mu\nu}$ ($W^{(A)}_{\mu\nu}$) denotes the symmetric (antisymmetric) part under $\mu \leftrightarrow \nu$. The requirements of Lorentz invariance, parity, charge conjugation and current conservation ($q^\mu W_{\mu\nu} = 0$) result in

$$W^{(S)}_{\mu\nu} = (g_{\mu\nu} + q_\mu q_\nu/q^2)W_1(\nu,q^2) + (p_\mu - q_\mu p\cdot q/q^2)(p_\nu - q_\nu p\cdot q/q^2)\frac{W_2(\nu,q^2)}{M_N^2} \ , \tag{1.6}$$

and

$$W^{(A)}_{\mu\nu} = \epsilon_{\mu\nu\rho\sigma}q^\rho\left[S^\sigma\left\{M_N G_1(\nu,q^2) + \frac{p\cdot q}{M_N}G_2(\nu,q^2)\right\} - S\cdot q p^\sigma\frac{G_2(\nu,q^2)}{M_N}\right] \ , \tag{1.7}$$

where S^σ denotes the nucleon spin 4–vector. The structure functions W_1 and W_2 are independent of the nucleon polarization, while G_1 and G_2 change sign under reversal of the nucleon polarization. Therefore, $W_{1,\,2}$ and $G_{1,\,2}$ are called the spin–independent and spin–dependent structure functions, respectively.

In terms of $W_{1,\,2}$ and $G_{1,\,2}$, the sum and difference of differential cross sections $d\sigma_{\uparrow\uparrow}$ and $d\sigma_{\uparrow\downarrow}$, where the helicities of the longitudinally polarized beam and target are parallel and antiparallel, respectively, can be written as

$$\begin{aligned}
\frac{d^2\sigma}{d\Omega dE'} &\equiv \frac{1}{4}\left(\frac{d^2\sigma_{\uparrow\uparrow}}{d\Omega dE'} + \frac{d^2\sigma_{\uparrow\downarrow}}{d\Omega dE'} + \frac{d^2\sigma_{\downarrow\downarrow}}{d\Omega dE'} + \frac{d^2\sigma_{\downarrow\uparrow}}{d\Omega dE'}\right) \\
&= \frac{4\alpha^2 E'^2}{Q^4}\left\{2\sin^2\frac{\theta}{2}W_1(\nu,Q^2) + \cos^2\frac{\theta}{2}W_2(\nu,Q^2)\right\}\ , \qquad (1.8) \\
\frac{d^2\Delta\sigma}{d\Omega dE'} &\equiv \frac{1}{4}\left(\frac{d^2\sigma_{\uparrow\uparrow}}{d\Omega dE'} - \frac{d^2\sigma_{\uparrow\downarrow}}{d\Omega dE'} + \frac{d^2\sigma_{\downarrow\downarrow}}{d\Omega dE'} - \frac{d^2\sigma_{\downarrow\uparrow}}{d\Omega dE'}\right) \\
&= \frac{4\alpha^2 E'}{EQ^2}\left\{(E + E'\cos\theta)M_N G_1(\nu,Q^2) - Q^2 G_2(\nu,Q^2)\right\}\ . \qquad (1.9)
\end{aligned}$$

θ is the lepton scattering angle in the lab. frame, and E and E' are the initial and final lepton energies, respectively (see Fig.1). Here we conventionally use Q^2 defined by $Q^2 = -q^2$. G_2 in eq.(1.9) is suppressed with respect to G_1 by a factor $\frac{Q^2}{EM_N} \sim 0.01$, for a typical beam energy of 100 GeV.

In the DIS region, *i.e.* $\nu >$ a few GeV and $Q^2 >$ a few GeV^2 with fixed Q^2/ν (Bjorken limit) [6], $W_{1,\,2}$ and $G_{1,\,2}$ are scaled as follows ;

$$\begin{aligned}
M_N W_1(\nu,Q^2) &\rightarrow F_1(x)\ , \\
\nu W_2(\nu,Q^2) &\rightarrow F_2(x)\ , \qquad (1.10) \\
M_N^2 \nu G_1(\nu,Q^2) &\rightarrow g_1(x)\ , \\
M_N \nu^2 G_2(\nu,Q^2) &\rightarrow g_2(x)\ ,
\end{aligned}$$

where x is a dimensionless scaling variable defined by

$$x = \frac{Q^2}{2M_N\nu}\ , \qquad (1.11)$$

and its allowed range is

$$0 \le x \le 1\ . \qquad (1.12)$$

The scaling property described in eq.(1.10) is called *Bjorken scaling*. The spin–independent structure functions $F_{1,\,2}$ and the spin–dependent ones $g_{1,\,2}$ are defined to be dimensionless. This phenomenon implies that the DIS is viewed as incoherent elastic scatterings of pointlike constituents inside a nucleon [13].

If a lepton is incoherently scattered by a parton carrying a fraction x of the target 4–momentum and if the parton mass and its transverse momentum are negligible, $F_2(x)$ and $g_1(x)$ are described as

$$\begin{aligned} F_2(x) &= \sum_i e_i^2 x \left\{ q_{i\,\uparrow}(x) + q_{i\,\downarrow}(x) + \bar{q}_{i\,\uparrow}(x) + \bar{q}_{i\,\downarrow}(x) \right\} \\ &= \sum_i e_i^2 x q_i(x) \,, \end{aligned} \tag{1.13}$$

and

$$\begin{aligned} g_1(x) &= \frac{1}{2} \sum_i e_i^2 \left\{ q_{i\,\uparrow}(x) - q_{i\,\downarrow}(x) + \bar{q}_{i\,\uparrow}(x) - \bar{q}_{i\,\downarrow}(x) \right\} \\ &= \frac{1}{2} \sum_i e_i^2 \delta q_i(x) \,, \end{aligned} \tag{1.14}$$

with

$$q_i(x) = q_{i\,\uparrow}(x) + q_{i\,\downarrow}(x) + \bar{q}_{i\,\uparrow}(x) + \bar{q}_{i\,\downarrow}(x) \,, \tag{1.15}$$

$$\delta q_i(x) = q_{i\,\uparrow}(x) - q_{i\,\downarrow}(x) + \bar{q}_{i\,\uparrow}(x) - \bar{q}_{i\,\downarrow}(x) \,, \tag{1.16}$$

where the sum is taken over the various species of partons (i=u, d, s, c, $\cdots$) with charge e_i. $q_{i\,\uparrow}$ ($q_{i\,\downarrow}$) represents the parton distribution polarized in parallel (antiparallel) to the nucleon spin and $q_i(x)$ and $\delta q_i(x)$ are the probability that the parton i has momentum fraction x of the nucleon. $q_i(x)$ ($\delta q_i(x)$) is called the spin–independent (spin–dependent) parton distribution function.

It is known that the Bjorken scaling is slightly violated at large Q^2 because of anomalous dimensions for the flavor singlet composite operators appearing in the operator product expansion of the electromagnetic current and in the running of the strong coupling constant α_S

[14]. However, since α_S is small at high energies, the scaling violation calculated from QCD is consistent with experiments [14]. Altarelli and Parisi formulated the Q^2 evolution equations to calculate the magnitude of scaling violations[15].

1.3 Proton spin problem

The spin–independent structure functions, $F_2(x)$, has been extensively investigated so far by many experimentalists and theorists since late 1960s. At present, there have been proposed several kinds of parametrizations of spin–independent parton distributions such as DO[16], DFLM[17], EHLQ[18], KMRS[19] and so on. On the other hand, there exist only a few data of the spin–dependent structure function, $g_1(x, Q^2)$. As mentioned before, in 1988 the EMC Collaboration at CERN measured g_1^p for a proton by using longitudinally polarized muon beams on longitudinally polarized proton targets. By combining this result with the data reported by SLAC Collaboration in early 1980s, we have

$$\int_0^1 g_1^p(x, Q^2 = 10.7\mathrm{GeV}^2)dx = 0.126 \pm 0.010(stat.) \pm 0.015(syst.) \ . \tag{1.17}$$

In the naive parton model, the first moment of g_1^p leads to the following formula with the help of eq.(1.14) ;

$$\begin{aligned} \int_0^1 g_1^p(x, Q^2)dx &= \frac{1}{2}\int_0^1 \left\{\frac{4}{9}\delta u(x, Q^2) + \frac{1}{9}\delta d(x, Q^2) + \frac{1}{9}\delta s(x, Q^2)\right\} dx \\ &= \frac{1}{2}\left\{\frac{4}{9}\Delta u(Q^2) + \frac{1}{9}\Delta d(Q^2) + \frac{1}{9}\Delta s(Q^2)\right\} \\ &= 0.126 \pm 0.010(stat.) \pm 0.015(syst.) \ , \end{aligned} \tag{1.18}$$

at $Q^2 = 10.7$ GeV^2 (hereafter, we denote this value of Q^2 by Q^2_{EMC}). The last equation in eq.(1.18) comes from eq.(1.17). Here $\Delta q_i(Q^2)$ is defined by

$$\Delta q_i(Q^2) = \int_0^1 \delta q_i(x, Q^2)dx \ . \tag{1.19}$$

Δq_i (i=u, d and s) means the amount of the proton spin carried by the quark i.

How can we understand these experimental results? The first moment of $g_1^p(x)$ is expected to be 5/18 in the simple nonrelativistic quark model with the SU(6) symmetric proton wave function[3]. In a more realistic model, where the exact flavor SU(3) symmetry in the baryon-octet β decay and no polarization of strange sea-quarks ($\Delta s = 0$) in a nucleon are assumed, the first moment of $g_1^{p\,(n)}(x)$ is given by

$$\int_0^1 g_1^{p\,(n)}(x,Q^2)dx = \frac{g_A}{12}\left[(\pm)\left\{1-\frac{\alpha_S(Q^2)}{\pi}\right\}+\frac{1}{3}\frac{3F/D-1}{F/D+1}\left\{5-\left(1+4\frac{33-8f}{33-2f}\right)\frac{\alpha_S(Q^2)}{\pi}\right\}\right], \tag{1.20}$$

where QCD radiative corrections are taken into account[20] and + (−) corresponds to the g_1^p for the proton (g_1^n for the neutron). g_A is the ratio of the axial vector to the vector coupling constant in the neutron β decay and f the number of quark flavors. F and D are the antisymmetric and symmetric SU(3) couplings[21]. Eq.(1.20) is called the "Ellis-Jaffe sum rule" [11]. With $F/D = 0.631 \pm 0.018$[22], $g_A = 1.259 \pm 0.006$ and $\alpha_S(Q^2_{EMC}) = 0.27 \pm 0.02$, the Ellis-Jaffe sum rule predicts the first moment of $g_1^p(x, Q^2_{EMC})$ to be 0.189 ± 0.005, which is inconsistent with the experimental data of eq.(1.17).

Now we are interested in the amount of individual terms Δq_i, while the sum of Δq_i means the total amount of a proton spin carried by quarks. There are two other experiments concerned with the magnitude of Δq_i. One is the neutron β decay [22] from which we obtain

$$\begin{aligned}\Delta u - \Delta d &= g_A = F + D \\ &= 1.259 \pm 0.006\ .\end{aligned} \tag{1.21}$$

The other is the semileptonic β decay of hyperons [22], which leads to

$$\Delta u + \Delta d - 2\Delta s = 3F - D = 0.688 \pm 0.035\ . \tag{1.22}$$

Note that eqs.(1.21) and (1.22) do not depend on Q^2 because the corresponding currents would be conserved if quarks were massless and that is enough to derive Ward-identities which forbid

them from being renormalized [23]. Combining these with eqs.(1.18), (1.21) and (1.22), one obtains

$$\begin{aligned}
\frac{1}{2}\Delta u(Q^2_{EMC}) &= 0.391 \pm 0.016 \pm 0.023 \ , \\
\frac{1}{2}\Delta d(Q^2_{EMC}) &= -0.236 \pm 0.016 \pm 0.023 \ , \\
\frac{1}{2}\Delta s(Q^2_{EMC}) &= -0.095 \pm 0.016 \pm 0.023 \ ,
\end{aligned} \tag{1.23}$$

and the amount of the proton spin carried by quarks becomes

$$\begin{aligned}
\frac{1}{2}\Delta\Sigma = \frac{1}{2}\sum_i \Delta q_i(Q^2_{EMC}) &= \frac{1}{2}\left\{\Delta u(Q^2_{EMC}) + \Delta d(Q^2_{EMC}) + \Delta s(Q^2_{EMC})\right\} \\
&= 0.060 \pm 0.047 \pm 0.069 \ .
\end{aligned} \tag{1.24}$$

This implies that very little of the proton spin is carried by quarks and is very different from the result expected from the nonrelativistic quark model and also the parton model. Furthermore, a non–zero value of Δs is very surprising. These results are what is called "proton spin crisis". If we stick to the Ellis–Jaffe sum rule given by eq.(1.20) and use $F/D = 0.631 \pm 0.018$[22], we obtain $\Delta u \simeq 0.97$ and $\Delta d \simeq -0.29$, that is, about 70% of the proton spin is to be carried by quarks.

The unexpected results described above stimulated a great theoretical activity in particle physics. Since the EMC experiments probe the hadron structure at short distances (large Q^2), the amount of the proton spin carried by quarks derived from such experiments is not necessarily the same as the one estimated from the nonrelativistic quark model which works well with the physics associated with long distances (small Q^2). However, even if we bear in mind the difference between a constituent quark and a parton, the experimental results still remain surprising. The referred experiments reveal that the spin structure of the proton is far from trivial. Of course, there exist some arguments on the reliability of the experimental data. Some of them are as follows : (i) the error of $g_1^p(x)$ is underestimated, especially in the extrapolation to $x = 0$[24], (ii) since the SU(3) symmetry is not exact, the estimate of F and D is not

completely reliable[25]. However, we consider the experimental result seriously. And yet, so far there have been various approaches based on the Skyrme model[26], current algebra[27], parton models[28], QCD perturbation theory[29], instantons[30] and so forth. These interpretations, however, are still inconclusive and controversial. Among them, there has been an interesting idea advocated by several people that gluons contribute significantly to the proton spin through the $U_A(1)$ anomaly of QCD[29, 31]. In this model, the first moment of the polarized gluon distribution inside a proton becomes large, typically $5 \sim 6$ at Q^2_{EMC}. Accordingly, the spin-dependent quark distributions are largely affected by gluons and the amount of the proton spin carried by quarks is not necessarily small.

In order to see this explicitly, we rewrite eq.(1.18) as follows

$$\begin{aligned}\int_0^1 g_1^p(x,Q^2)dx &= \frac{1}{2}\left\{\frac{4}{9}\Delta u(Q^2)+\frac{1}{9}\Delta d(Q^2)+\frac{1}{9}\Delta s(Q^2)\right\} \\ &= \frac{1}{12}\left\{\Delta u(Q^2)-\Delta d(Q^2)\right\}+\frac{1}{36}\left\{\Delta u(Q^2)+\Delta d(Q^2)-2\Delta s(Q^2)\right\} \\ &+ \frac{1}{9}\left\{\Delta u(Q^2)+\Delta d(Q^2)+\Delta s(Q^2)\right\}\ , \end{aligned} \tag{1.25}$$

where Δq_i is explicitly defined by the proton matrix element of the axial-vector current as follows

$$2s_\mu \Delta q_i = \langle p,S|\bar{q}_i\gamma_\mu\gamma_5 q_i|p,S\rangle\ . \tag{1.26}$$

The 1st, 2nd and 3rd terms of the r.h.s. in eq.(1.25) is related to the proton matrix element of the axial-vector current

$$j_{5\ \mu}^{(a)} = \bar{q}\gamma_\mu\gamma_5\frac{\lambda^a}{2}q\ , \tag{1.27}$$

with $a = 3$, 8 and 0, respectively, where λ^a represents the Gell-Mann 3×3 matrix in the flavor space. The third term is related to the singlet axial-vector current $j_{5\ \mu}^{(0)}$ in QCD. As is well known, this current is not conserved due to the axial anomaly even in the limit of massless quarks. By taking the axial anomaly into account, the divergence of $j_{5\ \mu}^{(0)}$ is given by

$$\partial^\mu j_{5\ \mu}^{(0)} = N_f\frac{\alpha_S}{4\pi}G^a_{\mu\nu}\tilde{G}^{a\ \mu\nu}\ , \tag{1.28}$$

where N_f is the number of flavors. $G^a_{\mu\nu}$ is the gluon field–strength tensor and $\tilde{G}^a_{\mu\nu}$ is the dual tensor defined as $\tilde{G}^a_{\mu\nu} = \frac{1}{2}\epsilon_{\mu\nu\rho\sigma}G^{a\ \rho\sigma}$. A new current is proposed to ensure its conservation such as

$$\tilde{j}^{(0)}_{5\ \mu} = j^{(0)}_{5\ \mu} - K_\mu \ , \tag{1.29}$$

where

$$K_\mu = \frac{\alpha_S N_f}{2\pi}\epsilon_{\mu\nu\rho\sigma}A^{a\ \nu}(\partial^\rho A^{a\ \sigma} - \frac{1}{3}g_S f_{abc}A^{b\ \rho}A^{c\ \sigma}) \ , \tag{1.30}$$

with A being the gluon field. Note that K_μ is generally not gauge invariant and does not appear in the operator product expansion[23]. However, the proton forward matrix element of K_μ does not depend on the gauge.

The quantity measured in experiments could be considered to be $j^{(0)}_{5\ \mu}$ while the matrix element of the conserved current $\tilde{j}^{(0)}_{5\ \mu}$ can be identified with the true quark contribution $\sum_i \Delta q_i$ to the proton spin since the anomalous dimensions, not the quantities, are the same [32]. Accordingly we can identify the modified current in eq.(1.29) with

$$\sum_i \widetilde{\Delta q_i} = \sum_i \Delta q_i - N_f\frac{\alpha_S}{2\pi}\Delta G \ , \tag{1.31}$$

where ΔG could be interpreted as the spin–dependent gluon distribution:

$$\begin{aligned}\Delta G(Q^2) &= \int_0^1 \left\{G_\uparrow(x,Q^2) - G_\downarrow(x,Q^2)\right\}dx \\ &= \int_0^1 \delta G(x,Q^2)dx \ .\end{aligned} \tag{1.32}$$

According to this consideration, the gluon contributes to the proton spin through the axial anomaly, resulting from non–conservation of the singlet axial–vector current. The quantities in eq.(1.31) depend on the renormalization point and what we observe experimentally implies "renormalized" parton distributions. Therefore, the EMC results in eq.(1.23) can be interpreted as follows ;

$$\frac{1}{2}\widetilde{\Delta u}(Q^2_{EMC}) = \frac{1}{2}\Delta u(Q^2_{EMC}) - \frac{\alpha_S}{4\pi}\Delta G(Q^2_{EMC}) = \ 0.391 \pm 0.016 \pm 0.023 \ ,$$

$$\frac{1}{2}\widetilde{\Delta d}(Q^2_{EMC}) = \frac{1}{2}\Delta d(Q^2_{EMC}) - \frac{\alpha_S}{4\pi}\Delta G(Q^2_{EMC}) = -0.236 \pm 0.016 \pm 0.023 \ , \quad (1.33)$$
$$\frac{1}{2}\widetilde{\Delta s}(Q^2_{EMC}) = \frac{1}{2}\Delta s(Q^2_{EMC}) - \frac{\alpha_S}{4\pi}\Delta G(Q^2_{EMC}) = -0.095 \pm 0.016 \pm 0.023 \ .$$

Since there exist four independent variables in three equations, it is impossible to determine the magnitude of each variable uniquely. However, if the large gluon polarization is taken as $\Delta G(Q^2_{EMC}) \sim 5$, then $\Delta s(Q^2_{EMC})$ turns out to be ~ 0 from eq.(1.33) and the amount of the proton spin carried by quarks becomes almost 70%. This consideration leads us to the conclusion that the EMC data can be reconciled with the Ellis–Jaffe sum rule by adopting a large ΔG.

Now, let us consider the sum rule for the proton spin which is given by

$$\frac{1}{2} = \frac{1}{2}\Delta\Sigma + \Delta G + \langle L_Z \rangle_{q+G} \ , \quad (1.34)$$

where $\langle L_Z \rangle_{q+G}$ implies the orbital angular momentum of quarks and gluons. In the case of large ΔG such as $\Delta G(Q^2_{EMC}) \sim 5$, a large negative orbital angular momentum due to quarks and/or gluons is required to compensate the ΔG ($\langle L_Z \rangle_{q+G} \simeq -\Delta G(Q^2)$). Since $\Delta\Sigma$ has little dependence on Q^2 and $\Delta G(Q^2)$ is nearly propotional to $\log Q^2$, $\langle L_Z \rangle_{q+G}$ must grow logarithmically with Q^2 at perturbative regions. It may be suggested that the direction of the orbital angular momentum due to gluon emissions is antiparallel to the direction of gluon polarization. On the contrary, in the Skyrme model[26], one has $\Delta\Sigma = 0$, $\Delta G = 0$ and $\langle L_Z \rangle_q = \frac{1}{2}$.

The present paper is organized as follows. In section 2 we propose a new model to interpret the EMC $g_1^p(x)$ data by taking into account both characteristics of the nonrelativistic quark model and the parton model. The spin–dependent parton distributions are calculated by developing the Carlitz–Kaur model[33] and considering the $U_A(1)$ anomaly effects. In section 3 we apply the model to hadron–hadron collisions : we calculate the two–spin asymmetries $A_{LL}^{\pi^0}(\overset{(-)}{p}p)$ and compare the results with the experimental data by the E581/704 Collaboration[34]. From

this analysis, it is concluded that the E581/704 data do not necessarily rule out a large gluon polarization but constrain severely the shape of the spin–dependent gluon distribution. In addition, for a future experimental test we calculate the two–spin asymmetries $A_{LL}^{\gamma}(\overset{(-)}{p}p)$ and $A_{LL}^{J/\psi}(pp)$ for γ and J/ψ productions, respectively. In section 4, to get further knowledge of the spin–dependent gluon distribution in a proton, we study the spin–dependent differential cross section for J/ψ leptoproduction which is sensitive to the polarized gluon. Section 5 is devoted to the conclusion and discussion.

2 POLARIZATION OF PARTONS AND SPIN STRUCTURE OF NUCLEONS

In this section we study the EMC $g_1^p(x)$ data in order to get a deep understanding of the proton spin structure.

In the nonrelativistic quark model, a proton is composed of three constituent quarks alone. The model explains well the nonrelativistic properties of hadrons at small Q^2 such as the hadron mass levels, magnetic moments and so on. On the other hand, the parton model in which a proton is constructed by a sum of three valence quarks, sea quarks and gluons, proves extremely effective for the DIS at large Q^2. Therefore, it is expected that a realistic model which describes the hadron dynamics consistently for both small and large Q^2 should contain the characteristics of both the nonrelativistic quark model and the parton model. One of the simple models in line with this view has been proposed in 1977 by Carlitz and Kaur[33]. In the present work we follow the same line and develop their idea to study the EMC data. However, before getting into the description of our model [35], it would be convenient for the reader to summarize briefly the model by Carlitz and Kaur (CK model).

Now, let us go to the CK model. In this model, when a proton interacts with a virtual photon emitted from an incident lepton, the proton first breaks up into two parts : one is a quark which solely interacts with the virtual photon and the other is the remaining constituents which are regarded as a *quasi – particle* called a "core" and work as a spectator. Accordingly, the proton wave function can be written by

$$|p\uparrow\rangle = \frac{1}{2}\left[|\Psi_0\rangle + |\Psi_1\rangle\right] , \tag{2.1}$$

with

$$|\Psi_0\rangle = |I=0, I_3=0|u_V\rangle \otimes |s=0, s_3=0\,|\uparrow\rangle f_0(x) , \tag{2.2}$$

$$
\begin{aligned}
\mid \Psi_1\rangle &= \left[\sqrt{\frac{2}{3}} \mid I=1, I_3=1 \mid d_V\rangle - \frac{1}{\sqrt{3}} \mid I=1, I_3=0 \mid u_V\rangle\right] \\
&\otimes \left[\sqrt{\frac{2}{3}} \mid s=1, s_3=1 \mid \downarrow\rangle - \frac{1}{\sqrt{3}} \mid s=1, s_3=0 \mid \uparrow\rangle\right] f_1(x) \ , \qquad (2.3)
\end{aligned}
$$

where $I = 0, 1$ and $s = 0, 1$ represent the magnitude of the isospin and the spin of the core, respectively, and $I_3(s_3)$ denotes the third component of $I(s)$. In eqs.(2.2) and (2.3), $f_0(x)$ and $f_1(x)$ show the momentum dependent parts of the wave function and they are equal in the SU(6) limit.

Let us define the spin–dependent distribution functions of quarks

$$
\delta q_i(x) = q_{i\uparrow}(x) - q_{i\downarrow}(x) + \bar{q}_{i\uparrow}(x) - \bar{q}_{i\downarrow}(x) \ , \qquad (1.16)
$$

where $q_{i\uparrow}$ ($q_{i\downarrow}$) denotes the distribution of quark i with helicity parallel (antiparallel) to proton helicity. Then, the spin–dependent quark distributions can be related to the spin–independent ones as follows [33]

$$
\begin{aligned}
\delta u_V(x) &= D_f(x)\{u_V(x) - \frac{2}{3} d_V(x)\} \ , \qquad (2.4a) \\
\delta d_V(x) &= D_f(x)\{-\frac{1}{3} d_V(x)\} \ . \qquad (2.4b)
\end{aligned}
$$

with a spin–dilution factor

$$
D_f(x) = \frac{1}{H_0 N(x) + 1} \ , \qquad (2.5)
$$

where H_0 is the probability of interaction between the valence quark and gluons, and $N(x)$ denotes the density of gluons relative to the valence quarks. In the definition of $N(x)$, the sea–quark density is neglected because it is much smaller than the gluon density. It seems plausible that only in large x regions a single valence quark carries most of the proton helicity while in small x the proton helicity is carried by many partons ; valence quarks, sea quarks and gluons. Then one can consider that the polarization of partons is diluted in small x regions. The spin–dilution factor $D_f(x)$ is introduced under such considerations. By taking the effect

of nonperturbative QCD into account, $D_f(x)$ is requred to be nearly 1 at $x \sim 1$ and to be almost zero at $x \sim 0$.

Unfortunately, the spin–dependent quark distributions given by eqs.(2.4a) and (2.4b) of the CK model cannot reproduce well the EMC data. This is partly because the sea quark contributions have been neglected from the beginning in the CK model. Thus, we must modify the CK model, looking for a more realistic model to understand the EMC data.

2.1 The polarized proton wave function and the spin–dependent quark distribution functions

Let us begin by constructing a more realistic wave function of the proton [35]. In the parton model a proton is composed of three valence quarks accompanied by sea quarks and gluons, though it consists of three constituent quarks alone in the static quark model. As a realistic model of a proton which is compatible with these pictures, we here propose a new wave function of a proton. In constructing a wave function, sea quarks are separated here from gluons inside a proton, and gluons are taken as a potential source which acts on quarks. Then a proton wave function is described as a superposition of three–, five–, seven–, $\cdots$, body wave functions of quarks.

The wave function can then be written in line with the CK model by

$$\begin{aligned} |\, p\uparrow\rangle &= a_0 \left[|\, \Psi_0\rangle + |\, \Psi_1\rangle \right]_V \\ &+ a_1 \left[|\, \Psi_0'\rangle + |\, \Psi_1'\rangle + \frac{\epsilon}{\sqrt{2}} \left(|\, \Psi_0''\rangle + |\, \Psi_1''\rangle + |\, \Psi_{\frac{1}{2}}''\rangle \right) \right]_{V+S} \\ &+ \cdots , \end{aligned} \tag{2.6}$$

where the first term is due to three quarks and the second term is due to five quarks and so on. The suffix of Ψ, Ψ' and Ψ'' denotes the isospin of the core. $a_0(a_1)$ is the weight of the three–(five–) quark wave function. ϵ denotes the relative weight of an s–quark pair to light quark (u,

d) pairs. The values of these weights will be determined later. In the CK model, only the first term (V term) was taken into consideration. Here we add the second term ($V+S$ term) which includes sea quark pairs ($u\bar{u}$, $d\bar{d}$ and $s\bar{s}$). We neglect the succeeding terms of more than five quarks hereafter. This neglect can be justfied as described later. $\mid \Psi_0\rangle_V$ and $\mid \Psi_1\rangle_V$ are the same as those in the CK model and are presented in eqs.(2.2) and (2.3). Similarly, the explicit forms of the $V+S$ term in eq.(2.6) can be written down as given in Appendix A. $\mid \Psi_0'\rangle_{V+S}$ and $\mid \Psi_1'\rangle_{V+S}$ are the mixture of wave functions of five–body quarks states, $(uud\bar{u}u)$ and $(uud\bar{d}d)$. $\mid \Psi_0''\rangle_{V+S}$, $\mid \Psi_1''\rangle_{V+S}$ and $\mid \Psi_{\frac{1}{2}}''\rangle_{V+S}$ are constructed from the wave functions of $(uud\bar{s}s)$. In these cases, cores are made of four quarks such as $qqqq$ or $qqq\bar{q}$. In particular, $\mid \Psi_{\frac{1}{2}}''\rangle$ includes either s or $\bar{s}$ quark in the core. It is noted that only the spin of the leading quark (the third quark in V or the fifth quark in $V+S$) attributes to the spin of the proton. Therefore, the effect of sea quark polarizations is automatically induced via $V+S$ term. Substituting the explicit forms of eqs.(2.2), (2.3) and those presented in Appendix A into eq.(2.6) and summing over the spin–dependent probability density of any leading quark, we can obtain the spin–dependent distribution functions of individual quarks as follows [35] :

$$\begin{aligned}
\delta u(x) &= \widehat{D_f}(x)[a_0^2\{u_V(x)-\frac{2}{3}d_V(x)\}+a_1^2\{\frac{17}{12}u_V(x)-\frac{5}{4}d_V(x) \\
&+ \frac{17}{6}\bar{u}_S(x)-\frac{5}{2}\bar{d}_S(x)+\frac{\epsilon^2}{2}u_V(x)-\frac{\epsilon^2}{2}\frac{2}{3}d_V(x)\}] \,, \qquad (2.7a)\\
\delta d(x) &= \widehat{D_f}(x)[a_0^2\{-\frac{1}{3}d_V(x)\}+a_1^2\{\frac{7}{12}u_V(x)-\frac{3}{4}d_V(x) \\
&+ \frac{7}{6}\bar{u}_S(x)-\frac{3}{2}\bar{d}_S(x)-\frac{\epsilon^2}{2}\frac{1}{3}d_V(x)\}] \,, \qquad (2.7b)\\
\delta s(x) &= \widehat{D_f}(x)[a_1^2\frac{\epsilon^2}{2}\frac{1}{3}\{s_S(x)+\bar{s}_S(x)\}] \,, \qquad (2.7c)
\end{aligned}$$

where

$$\widehat{D_f}(x)=\frac{D_f(x)}{a_0^2+a_1^2+\frac{\epsilon^2}{2}a_1^2} \,. \qquad (2.8)$$

$D_f(x)$ is a spin–dilution factor in our model. The denominator in eq.(2.8) is a normalization factor. It is considered that the spin of the leading quark dilutes especially at small x because

of interactions between a leading quark and the remaining core. In this work we modify the spin–dilution factor $D_f(x)$ from that of the original CK model. The explicit form will be given in the next subsection. Note that by taking $a_0 = 1$ and $a_1 = 0$, eqs.(2.7a)–(2.7c) reduce to eqs.(2.4a)–(2.4b), that is, the model reduces to the CK model as expected.

Now, let us determine the values of a_0, a_1 and ϵ in eq.(2.6) (see Appendix B for details). The K/π production ratio in hadron collisions at high energies gives us an information on ϵ^2. The experimental value of the strangeness suppression factor λ, which is defined as the production ratio of $s\bar{s}$ pairs to $u\bar{u}$ or $d\bar{d}$ pairs, is around $0.2 \sim 0.3$[36]. We simply put $\frac{1}{2}\epsilon^2 = \lambda$ and take $\epsilon^2 = 0.5$. As is well known, the SU(6) model gives the ratio of magnetic moments of neutron to proton $\mu_n/\mu_p = -\frac{2}{3}$. In our case, we have the same ratio if only a_0 term in eqs.(B.1) and (B.2) is taken. We assume that the small difference of the experimental value $\mu_n/\mu_p = -0.68498$ from $-\frac{2}{3}$ is due to an effect of $qqqq\bar{q}$, namely a_1 terms. Then we get

$$\frac{a_1^2}{a_0^2} = 0.1425 \ . \tag{2.9}$$

This may justify our perturbative approximation under which the wave functions of more than five quarks have been neglected in eq.(2.6). Since a_1^2/a_0^2 depends weakly on ϵ^2, our analysis is not affected significantly by the experimental K/π ratio.

2.2 The spin–dilution factor

In the CK model the spin–dilution factor $D_f(x)$ was determined based on only the statistical consideration of interactions between quarks and gluons. Here, we modify the spin–dilution factor by taking the dynamics of quarks and gluons into account. First let us introduce a spin–flip probability $P_f(x)$ of a quark interacting with a gluon, as

$$P_f(x) = \frac{\sigma_{\downarrow\uparrow}(x)}{\sigma_{\uparrow\uparrow}(x) + \sigma_{\downarrow\uparrow}(x)} \ , \tag{2.10}$$

where σ is the cross section of the quark–gluon scattering. The subscripts $\downarrow\uparrow$ and $\uparrow\uparrow$ mean the spin–flip and spin–nonflip of the quark, respectively. Then, in a similar way as the CK model but by taking the function $P_f(x)$ into account, we define a modified spin–dilution factor $D_f(x,Q^2)$, as follows [35] ;

$$D_f(x,Q^2) = \frac{\{1-2P_f(x)\}H_0N(x,Q^2)+1}{H_0N(x,Q^2)+1} \ , \tag{2.11}$$

where $N(x,Q^2)$ is the density of gluons relative to the valence quarks and H_0 is treated as a constant and is fixed as $H_0 = 0.0055$ by the Bjorken sum rule[37]. The spin–dilution factor $D_f(x)$ of eq.(2.5) in the CK model is given by putting $P_f(x) = \frac{1}{2}$ into eq.(2.11). In practice, however, it is expected that $P_f(x)$ is x dependent and should be large at small x.

Here we estimate $P_f(x)$ by using the analogy of Rutherford scattering where the leading quark is scattered by a gluon source. The differential cross sections of spin–nonflip and spin–flip scatterings with a scattering angle θ, are given by

$$\begin{aligned}
\frac{d\sigma_{\uparrow\uparrow}(x)}{d\Omega} &= \frac{\frac{4}{3}\alpha_S^2 m_q^2}{4p_i^4(x)\sin^4\frac{\theta}{2}} \\
&\times \ \mathrm{Tr}\left\{\gamma_0\frac{(1+\gamma_5\ \not{s}_{i\uparrow})}{2}\frac{(\not{p}_i+m_q)}{2m_q}\gamma_0\frac{(1+\gamma_5\ \not{s}_{f\uparrow})}{2}\frac{(\not{p}_f+m_q)}{2m_q}\right\} , \qquad (2.12a) \\
\frac{d\sigma_{\downarrow\uparrow}(x)}{d\Omega} &= \frac{\frac{4}{3}\alpha_S^2 m_q^2}{4p_i^4(x)\sin^4\frac{\theta}{2}} \\
&\times \ \mathrm{Tr}\left\{\gamma_0\frac{(1+\gamma_5\ \not{s}_{i\uparrow})}{2}\frac{(\not{p}_i+m_q)}{2m_q}\gamma_0\frac{(1-\gamma_5\ \not{s}_{f\uparrow})}{2}\frac{(\not{p}_f+m_q)}{2m_q}\right\} , \qquad (2.12b)
\end{aligned}$$

where p_i and m_q are the incident momentum and mass of the quark, respectively. Integrating on Ω from a minimum of scattering angle θ_m, we get

$$\sigma_{\uparrow\uparrow}(x) = \frac{\pi\frac{4}{3}\alpha_S^2E^2(x)}{p_i^4(x)}\left\{2\log\mid\sin\frac{\theta_m}{2}\mid+(\sin\frac{\theta_m}{2})^{-2}-1\right\} , \tag{2.13a}$$

$$\sigma_{\downarrow\uparrow}(x) = \frac{2\pi\frac{4}{3}\alpha_S^2m_q^2}{p_i^4(x)}\left\{-\log\mid\sin\frac{\theta_m}{2}\mid\right\} , \tag{2.13b}$$

where θ_m is related to the largest impact parameter b as follows

$$\cot\frac{\theta_m}{2} = \frac{2E(x)b}{\frac{4}{3}\alpha_S(Q^2)} \ . \tag{2.14}$$

Since b is considered to be the interaction length between the leading quark and a gluon source, we take it to be a radius of a constituent quark as follows :

$$b = (\frac{1}{3})^{\frac{1}{3}} R_p = 0.55 \text{ [fm]} , \tag{2.15}$$

where R_p is the proton radius. The energy of a quark, $E(x)$, is simply assumed as a function of x as

$$E^2(x) = M_p^2 x^2 + (1 - x^2) m_q^2 . \tag{2.16}$$

It implies that E reduces to the mass of a quark at $x = 0$ and to the mass of a proton at $x = 1$. The argument Q^2 of α_s in eq.(2.14) is taken to be M_p^2, because the interaction region is confined within a proton. As for the quark mass in eqs.(2.13a), (2.13b) and (2.16) we prefer a current mass to a constituent mass, because the leading quark interacting with a virtual photon is identified with a parton that is almost massless. $P_f(x)$ is determined this way.

Our $D_f(x, Q^2)$ is obtained after substituting $\frac{G(x,Q^2)}{u_V(x,Q^2)+d_V(x,Q^2)}$ to $N(x, Q^2)$ in eq.(2.11), where $G(x, Q^2)$, $u_V(x, Q^2)$ and $d_V(x, Q^2)$ are the spin–independent gluon, valence–u and d quark distribution functions of Duke and Owens parametrizations [16], respectively. For $Q^2 = 10.7\text{GeV}^2$ (EMC value), the resultant $D_f(x, Q^2_{EMC})$ for the case of $m_u = m_d = 5$ MeV is compared with that for the case of $m_u = m_d = 300$ MeV and with that given by Carlitz and Kaur in Fig.2. There is a significant difference between our $D_f(x, Q^2_{EMC})$ and that of the CK model. As for the mass of s quarks, we use $m_s = 150$ MeV.

2.3 Spin–dependent structure functions of nucleons

So far we have been concerned only with the polarization of quarks. At the nonperturbative level gluons act on quarks collectively. At high Q^2, where partons become asymptotically free, gluons distinguish themselves as independent partons. Thus we should also take gluon's polarization into account in the following way. As described in Introduction, gluons affect the

first moment of $g_1^p(x)$ through the singlet axial vector current $j_5^{(0)}{}_\mu$. It can include the spin-dependent distribution function of gluons in the lowest order of α_S, because of the anomaly effects [29, 31]. Then the spin-dependent quark distribution functions should be modified from δq to $\widetilde{\delta q}$ as follows ;

$$\widetilde{\delta q_i}(x,Q^2) = \delta q_i(x,Q^2) - \frac{\alpha_S(Q^2)}{2\pi}\delta G(x,Q^2) \ , \tag{2.17}$$

where i denotes flavors(u,d,s) and

$$\delta G(x,Q^2) = G_\uparrow(x,Q^2) - G_\downarrow(x,Q^2) \ . \tag{1.32}$$

As gluons are confined in a proton, they could have a transverse component to the direction of the proton spin. However, we neglect the effect of this component since it is supposed to be small.

The evaluation of $\delta G(x,Q^2)$ is rather hard. At present we have no definite knowledge of it except for a trivial condition

$$\left|\frac{\delta G(x,Q^2)}{G(x,Q^2)}\right| \ \leq \ 1 \ .$$

Some authors have tried to determine the explicit expression of $\delta G(x,Q^2)$ from counting rules[38], Regge behavior [39] or Q^2 evolution equations of $\delta G(x,Q^2)$ [40].

In this paper, we assume simply the following form of $\delta G(x,Q^2)$ as an example of the spin-dependent gluon distributions

$$x\delta G(x,Q^2_{EMC}) = C \ x^{0.1}(1-x)^{17} \ . \tag{2.18}$$

At present we do not know the underlying physics of where the powers of x and $(1-x)$ come from. To understand it, we need further investigation on nonperturbative effects of QCD. A constant $C = 3.1$ is determined so as to fit the experimental first moment of $g_1^p(x,Q^2)$ in eq(1.17), *i.e.*, $\int_0^1 g_1^p(x,Q^2_{EMC})dx = 0.126$ (EMC data). Eq.(2.18) leads to a large value of the first moment of the spin-dependent gluon distributions, $\Delta G(Q^2_{EMC}) \equiv \int_0^1 \delta G(x,Q^2_{EMC})dx =$

6.32. In literature[39, 40], there have been discussed several examples of large $\Delta G(Q^2_{EMC})$, which also fit well to EMC $g_1^p(x)$ data. Compared with these distributions of polarized gluons, the distribution given by eq.(2.18) is quite distinct since it has a sharp peak at very small x ($x < 0.01$) and decreases rapidly with increasing x. A similar shape of $\delta G(x, Q^2)$ has been proposed by Vogelsang and Weber[41] to study the two-spin asymmetries of π^0 productions in $\overset{(-)}{p}p$ collisions, which will be discussed in the next section.

The $g_1^p(x)$ can be written in terms of eq.(2.17)

$$g_1^p(x, Q^2) = \frac{1}{2}\left[\frac{4}{9}\widetilde{\delta u}(x, Q^2) + \frac{1}{9}\widetilde{\delta d}(x, Q^2) + \frac{1}{9}\widetilde{\delta s}(x, Q^2)\right] . \tag{2.19}$$

By using the Duke–Owens parametrization for spin–independent quark and gluon distribution functions and the spin–dependent gluon distribution given by eq.(2.18) with $C = 3.1$, the modified spin–dependent distribution functions of quarks $\widetilde{\delta u}(x, Q^2)$, $\widetilde{\delta d}(x, Q^2)$ and $\widetilde{\delta s}(x, Q^2)$ can be calculated. The $x\widetilde{\delta q}$ as well as $x\delta G$ at $Q^2 = 10.7$ GeV^2 (EMC value) are shown in Fig.3. The resultant $xg_1^p(x, Q^2)$ fits well with experimental data as depicted in Fig.4.

As described above, by choosing $C = 3.1$, the first moment of $g_1^p(x, Q^2)$ at $Q^2 = 10.7$ GeV^2 is consistent with the experimental value as

$$\int_0^1 g_1^p(x, Q^2)dx = 0.126 . \tag{2.20}$$

The first moment of each $\widetilde{\delta q_i}$ is given by

$$\widetilde{\Delta q_i}(Q^2) = \int_0^1 \widetilde{\delta q_i}(x, Q^2)dx = \Delta q_i(Q^2) - \frac{\alpha_s}{2\pi}\Delta G(Q^2) , \tag{1.31}$$

where $\Delta q_i(Q^2)$ and $\Delta G(Q^2)$ are defined by eqs.(1.19) and (1.32). Then, we can get $\widetilde{\Delta u}(Q^2) = 0.752$, $\widetilde{\Delta d}(Q^2) = -0.507$ and $\widetilde{\Delta s}(Q^2) = -0.232$. We also obtain

$$\Delta u(Q^2) = 1.003 , \tag{2.21a}$$

$$\Delta d(Q^2) = -0.256 , \tag{2.21b}$$

$$\Delta s(Q^2) = 0.019 , \tag{2.21c}$$

and

$$\Delta G(Q^2) \;=\; 6.32\;, \tag{2.22}$$

at $Q^2 = 10.7$ GeV^2. Note that the first moment of the gluon distribution must be quite large in order to reproduce the EMC data.

Eqs.(2.21a)–(2.21c) lead to a result

$$\Delta u(Q^2) + \Delta d(Q^2) - 2\Delta s(Q^2) = 0.709\;, \tag{2.23}$$

which is consistent with the experimental data 0.688 ± 0.035[22] obtained from the β decays of hyperons. It is remarkable that eq.(2.23) is not an input but an outcome of our model.

Our values given in eqs.(2.21a)–(2.21c) also lead to

$$\frac{1}{2}\left\{\Delta u(Q^2) + \Delta d(Q^2) + \Delta s(Q^2)\right\} = 0.383\;, \tag{2.24}$$

which is rather near to $\frac{1}{2}$: the spin value of the proton. As seen in eq.(2.21c), Δs is uniquely determined owing to eq.(2.7c) in our model. Its value is much smaller than the absolute value of Δu or Δd. Our model has a parton–like picture in one hand because only a leading quark absorbs a virtual photon. On the other hand, it has also a static picture in the sense that the wave function given in eq.(2.6) is its starting point. Therefore, eq.(2.24) and the smallness of Δs seem to be reasonable consequences.

Recently, the spin–dependent structure function of deutron $g_1^d(x)$ has been measured by the SMC group at CERN[42] by using polarized muon beams on polarized deuteron targets. The experimental result is

$$\int_0^1 g_1^d(x)dx = 0.023 \pm 0.020(stat.) \pm 0.015(syst.)\;, \tag{2.25}$$

at $Q^2 = 4.6$ GeV^2 (hereafter, this value is cited as Q^2_{SMC}). Furthermore, the spin–dependent structure function of the neutron can be derived from $g_1^d(x, Q^2_{SMC})$ measured by using the

relation $g_1^p(x) + g_1^n(x) \simeq 2g_1^d(x)/(1 - 1.5\omega_D)$, where ω_D is the probability of the deuteron to be in a D–state. Using $\omega = 0.058$[43], the experimental value for the neutron becomes

$$\int_0^1 g_1^n(x)dx = -0.08 \pm 0.04(stat.) \pm 0.04(syst.) \ , \tag{2.26}$$

which is much less than -0.002 predicted by the Ellis–Jaffe sum rule in eq.(1.20). However, this experimental result together with the EMC data in eq(1.17) implies agreement with the Bjorken sum rule [37].

Here, to examine our model for this experiment, we calculate the x dependence of $g_1^d(x)$ by using spin–dependent parton distribution functions. When each term in eq.(2.19) is known, from the isospin symmetry $g_1^d(x, Q^2)$ is directly obtained without any additional parameter. The calculated results are shown in Fig.5, in which one can see that our distribution is consistent with the SMC data even though ΔG is large. Note that we have no free parameters in calculating $g_1^d(x)$. Also, the first moments become

$$\int_0^1 g_1^d(x, Q^2)dx = 0.019 \ , \tag{2.27}$$

and

$$\int_0^1 g_1^n(x, Q^2)dx = -0.084 \ , \tag{2.28}$$

at $Q^2 = 4.6$ GeV^2. Both of these values agree well with the experimental results already shown in eqs.(2.25) and (2.26).

Let us summarize the main points that have been done in this section. A model was presented to find a way getting out of the "proton spin crisis" brought about from the EMC experiment. The proton wave function in the model consists of uud and $uudq\bar{q}$ where $q\bar{q} = u\bar{u}$, $d\bar{d}$ and $s\bar{s}$, and hence the sea–quark effect is taken into consideration. In line with the Carlitz–Kaur approach, we consider that, among constituents of the proton, only one quark(or antiquark) interacts with the virtual photon and the remaining components which form a

"core" in an isospin eigenstate work as a spectator. The spin–dependent distribution functions $\delta q_i(x,Q^2)$ of quarks are obtained by the product of the spin–dilution factor $\widehat{D_f}(x,Q^2)$ and the linear combination of spin–independent distribution functions. The spin–dependent gluon distribution is introduced through the $U_A(1)$ anomaly. Our spin–dependent gluon distribution function $x\delta G(x,Q^2)$ given by eq.(2.18) is very special since it has a sharp peak at $x < 0.01$ and decreases rapidly with increasing x.

Our results are summarized as follows ;

(i) A value of $(\Delta u + \Delta d - 2\Delta s) = 0.709$ is consistent with that from hyperon β decays.

(ii) Not only the x dependence of $g_1^p(x,Q^2_{EMC})$ but also that of $g_1^d(x,Q^2_{SMC})$ and the first moment of $g_1^{d\ (n)}(x,Q^2_{SMC})$ agree well with the experimental data.

(iii) The value of $\frac{1}{2}\Delta\Sigma \equiv \frac{1}{2}(\Delta u + \Delta d + \Delta s)$ is 0.383, which is rather near to 1/2. It means that quarks carry a large part of the proton spin.

(iv) ΔG is large, $\Delta G = 6.32$.

Among these results, the prediction of large gluon polarizations has not yet been tested experimentaly. It is important to check the magnitude of gluon polarizations through the analyses of other reactions in order to confirm our model. The next section is devoted to this subject.

3 SPIN–ASYMMERTY PROBE OF PARTON SPIN DENSITIES

In the previous section, we saw that the polarized gluon δG and the polarized sea δq_s play an important role for solving "proton spin crisis". However, the magnitude of δG can not be directly measured by the EMC or SMC experiment for the deep inelastic scattering. Therefore, it is absolutely necessary to determine their magnitude by other processes experimentally.

In this section, we will investigate several physical processes which give us further informations of the polarized gluons δG inside a proton. Interesting processes are inclusive π^0– [41, 44], high p_T direct photon– [45] and inclusive J/ψ–productions [46] in polarized hadron–polarized hadron reactions, which will be discussed in this section.

The interesting physical parameter to be measured is the two–spin asymmetry A_{LL} as a function of transverse momenta p_T of produced particles such as π^0, γ and J/ψ. A_{LL} is defined as

$$\begin{aligned} A_{LL} &= \frac{[d\sigma_{\uparrow\uparrow} - d\sigma_{\uparrow\downarrow} + d\sigma_{\downarrow\downarrow} - d\sigma_{\downarrow\uparrow}]}{[d\sigma_{\uparrow\uparrow} + d\sigma_{\uparrow\downarrow} + d\sigma_{\downarrow\downarrow} + d\sigma_{\downarrow\uparrow}]} \\ &= \frac{Ed\Delta\sigma/d^3p}{Ed\sigma/d^3p} , \end{aligned} \tag{3.1}$$

where $d\sigma_{\uparrow\downarrow}$, for instance, denotes that the helicity of a beam particle is positive and that of a target particle is negative. How a two–spin asymmetry in the fundamental 2–2 subprocesses can be responsible for an inclusive production asymmetry, A_{LL}, is given in Appendix C and ref.[47]. In addition, a comprehensive and general review on the spin physics for high energy reactions is given by Craigie et al. [48] and Bourrely et al [49].

In order to discuss how these processes are affected by spin–dependent gluon distributions, we take the following four different types of $x\delta G(x)$:

(a) our model ;

$$x\delta G(x, Q^2 = 10.7\text{GeV}^2) = 3.1x^{0.1}(1-x)^{17} \text{ then} \tag{2.18}$$

$$\Delta G(Q^2_{EMC}) = 6.32 \ ,$$

(b) Cheng–Lai type model [50] ;

$$x\delta G(x, Q^2 = 10\text{GeV}^2) = 3.34x^{0.31}(1-x)^{5.06}(1-0.177x) \text{ then} \tag{3.2}$$

$$\Delta G(Q^2_{EMC}) = 5.64 \ ,$$

(c) BBS model [38] ;

$$x\delta G(x, Q^2 = 4\text{GeV}^2) = 0.281\left\{(1-x)^4 - (1-x)^6\right\} + 1.1739\left\{(1-x)^5 - (1-x)^7\right\}$$

$$\text{then} \quad \Delta G(Q^2_{EMC}) = 0.53 \ , \tag{3.3}$$

(d) no gluon polarization model [50] ;

$$x\delta G(x, Q^2 = 10\text{GeV}^2) = 0 \ \text{ then } \ \Delta G(Q^2_{EMC}) = 0 \ . \tag{3.4}$$

Among these models, ΔG of types (a) and (b) are large while those of types (c) and (d) are small and zero, respectively. The x dependence of $x\delta G(x, Q^2)$ and $\delta G(x, Q^2)/G(x, Q^2)$ which are evolved up to $Q^2 = 10.7$ GeV^2 by the Altarelli–Parisi equations are depicted in Fig.6 (A) and (B), respectively. As for the spin–dependent gluon distributions with large ΔG, the $x\delta G(x, Q^2)$ which is taken up so far by many authors[39, 40] has almost the same behavior as that of type (b). As shown Fig.6, the $x\delta G(x)$ of type (b) has a peak at $x \approx 0.05$ and gradually decreases with increasing x while that of (a) has a sharp peak at $x < 0.01$ and rapidly decreases. The type (c) which is derived from the requirements of the color coherence at $x \sim 0$ and the counting rule at $x \sim 1$ [38] has no sharp peak but rather broad behavior.

3.1 Two–Spin Asymmetry for π^0 Productions

So far, only the inclusive π^0–productions have been measured by the E581/704 Collaboration at Fermilab[34] by using longitudinally polarized proton (antiproton) beams and longitudinally polarized proton targets. We will compare the theoretical predictions with the E581/704 data and discuss not only the magnitude and behavior of δG but also the reliability of the hard–scattering parton model for various subprocesses.

In a hard–scattering parton model with perturbative QCD, the spin–dependent and spin–independent cross sections for π^0 productions in hadron–hadron processes, shown in Fig.7, are given as [47]

$$E\frac{d\Delta\sigma}{d^3p}(s,p_T,\theta) = \frac{1}{\pi}\sum_{ab\to cd}\int_{x_a\ min}^{1} dx_a \int_{x_b\ min}^{1} dx_b \delta f_{a/A}(x_a,Q^2)\delta f_{b/B}(x_b,Q^2) \times D_{\pi^0/c}(z_c,Q^2)\frac{1}{z_c}\frac{d\Delta\hat{\sigma}}{d\hat{t}}(ab\to cd;\hat{s},\hat{t},\hat{u}) , \tag{3.5}$$

$$E\frac{d\sigma}{d^3p}(s,p_T,\theta) = \frac{1}{\pi}\sum_{ab\to cd}\int_{x_a\ min}^{1} dx_a \int_{x_b\ min}^{1} dx_b f_{a/A}(x_a,Q^2) f_{b/B}(x_b,Q^2) \times D_{\pi^0/c}(z_c,Q^2)\frac{1}{z_c}\frac{d\hat{\sigma}}{d\hat{t}}(ab\to cd;\hat{s},\hat{t},\hat{u}) , \tag{3.6}$$

with $\hat{s},\hat{t},\hat{u}$ being the Mandelstam variables for the parton subprocess. $\delta f_{a/A}(x_a,Q^2)$ ($f_{a/A}(x_a,Q^2)$) represents the spin–dependent (spin–independent) parton distribution functions for a parton a in a hadron A with momentum fraction x_a. $D_{\pi^0/c}(z_c,Q^2)$ is the fragmentation function of an outgoing parton c decaying into a π^0 with momentum fraction z_c. $d\Delta\hat{\sigma}/d\hat{t}$ and $d\hat{\sigma}/d\hat{t}$ are the differential cross sections of subprocesses and are formulated in the framework of perturbative QCD[47]. The explicit expressions for various subprocesses are summarized in Table 1.

The kinematical parameters included in eqs.(3.5) and (3.6) are given by[47, 51]

$$\hat{s} = x_a x_b s , \qquad \hat{t} = -\frac{s}{2}\frac{x_a x_T}{z_c}\tan\frac{\theta}{2} ,$$

$$\hat{u} = -\frac{s}{2}\frac{x_b x_T}{z_c}\cot\frac{\theta}{2}, \qquad z_c = \frac{1}{2}x_T\left\{\frac{\cot\frac{\theta}{2}}{x_a}+\frac{\tan\frac{\theta}{2}}{x_b}\right\}, \tag{3.7}$$

$$x_{a\ min} = \frac{x_T\cot\frac{\theta}{2}}{2-x_T\tan\frac{\theta}{2}}, \qquad x_{b\ min} = \frac{x_a x_T\tan\frac{\theta}{2}}{2x_a - x_T\cot\frac{\theta}{2}},$$

with $x_T \equiv 2p_T/\sqrt{s}$, where θ is the production angle of π^0 in the CMS of colliding protons.

Using the fragmentation functions $D_{\pi^0/q}(z_c, Q^2)$ of quarks [52] and $D_{\pi^0/G}(z_c, Q^2)$ of gluons [53] together with one of the four types of spin-dependent gluon distribution functions presented before ((a)~(d)), we can calculate $A_{LL}^{\pi^0}(pp)$ and $A_{LL}^{\pi^0}(\overline{p}p)$. Calculated results for $A_{LL}^{\pi^0}(pp)$ and $A_{LL}^{\pi^0}(\overline{p}p)$ are shown in Figs.8 and 9 for $\sqrt{s} = 20$ GeV and $\theta = 90°$, respectively. Here we typically choose $Q^2 = 4p_T^2$ with the transverse momentum p_T of π^0. As for the definition of Q^2 for the present processes, there is no theoretical grounds. Although the best choice of Q^2 would be the one that minimizes contributions of higher order terms and thus provides us with an accurate approximation, this cannot be determined without knowing terms beyond the leading order. At present there are several guesses for a choice of Q^2 ; $Q^2 = 4p_T^2$, $(\hat{s}\hat{t}\hat{u})^{1/3}$, $-\hat{t}$ and so on[47, 51]. We examined the difference of results generated from these choices of Q^2 and found that $A_{LL}^{\pi^0}(\overset{(-)}{p}p)$ is changed only slightly.

Two-spin asymmetries $A_{LL}^{\pi^0}(\overset{(-)}{p}p)$ contain contributions of various subprocesses. The difference between $A_{LL}^{\pi^0}(pp)$ and $A_{LL}^{\pi^0}(\overline{p}p)$ for theoretical calculations is due to the magnitude and sign of contributing subprocesses to pp and $\overline{p}p$ reactions. For subprocesses concerned here, an incident $\overline{q}$ is a sea component for a proton while it is a valence component for an antiproton. Hence, $q\overline{q} \to q\overline{q}$, $q\overline{q} \to gg$ and $\overline{q}g \to \overline{q}g$ contribute more to $\overline{p}p$ than to pp reactions. On the other hand, $qq \to qq$ and $qg \to qg$ contribute more to pp than to $\overline{p}p$ reactions. Furthermore, the spin-dependent subprocess cross section $d\Delta\hat{\sigma}/d\hat{t}$ is negative for $q_i\overline{q}_i \to \overline{q}_i q_i$, $q_i\overline{q}_i \to q_j\overline{q}_j/\overline{q}_j q_j$, $q_i\overline{q}_i \to gg$ and $gg \to q_i\overline{q}_i$, while it is positive for other subprocesses. Therefore, the spin-dependent differential cross section $Ed\Delta\sigma/d^3p$ for $\overline{p}p$ reactions becomes a little smaller than the one for pp reactions. This leads to smaller $A_{LL}^{\pi^0}(\overline{p}p)$ than $A_{LL}^{\pi^0}(pp)$ as shown in Figs.8 and

9. The results suggest that the hard-scattering parton model is essentially correct.

Comparing theoretical predictions with the experimental data, we see that not only the no gluon polarization model (type (d)) but also our model (type (a)) seem to be consistent with the experimental data for both pp and $\overline{p}p$ collisions. Since the lower limit of the integral variable $x_{a\ min}$ in eqs.(3.5) and (3.6) is expected to be about 0.05 at $p_T = 1$ GeV as seen from eq.(3.7), the contributions of parton distributions for $0 < x < 0.05$ to $A_{LL}^{\pi^0}(\overset{(-)}{p}p)$ are vanishing. Also, since the momentum fraction z_c given by eq.(3.7) becomes larger than 0.5 for $x_a \lesssim 0.2$ or $x_b \lesssim 0.2$, the gluon contributions from $x \lesssim 0.2$ to $A_{LL}^{\pi^0}(\overset{(-)}{p}p)$ are significantly suppressed by the fragmentation function $D_{\pi^0/c}(z_c, Q^2)$, which sharply decreases with increasing z_c. Therefore, the dominant contributions of the spin-dependent gluon distribution to $A_{LL}^{\pi^0}(\overset{(-)}{p}p)$ come from $x > 0.2$. As can be seen in Fig.6 (A), $x\delta G(x)$ of type (a) is very small for $x > 0.2$ though $\Delta G(Q^2_{EMC})$ for this type is quite large. Therefore, $A_{LL}^{\pi^0}(\overset{(-)}{p}p)$ becomes small. However, if we take the polarized gluon distribution $x\delta G(x)$ of type (b) which is large for $x > 0.2$, we have a significant contribution from the large $x\delta G(x)$ to $A_{LL}^{\pi^0}(\overset{(-)}{p}p)$ and then the result becomes inconsistent with the E581/704 data. Furthermore, type (c), though its ΔG is small, does not completely reproduce the data because it is not quite small for $x > 0.2$. In order to reproduce the data of $A_{LL}^{\pi^0}(\overset{(-)}{p}p)$, $x\delta G(x)$ should be very small. Therefore, one can see that a large gluon polarization inside a proton is not necessarily ruled out but the shape of the spin-dependent gluon distribution function is strongly constrained by the E581/704 data.

In addition, Vogelsang and Weber[41] have studied the intrinsic k_T-smearing effects on $A_{LL}^{\pi^0}(\overset{(-)}{p}p)$ and the reliability of perturbative QCD. They found that $A_{LL}^{\pi^0}(\overset{(-)}{p}p)$ at small p_T regions ($p_T \lesssim 3$ GeV) becomes consistent with the experimental data by taking k_T-smearing effects into account even for type (b). These observations lead to the conclusion that the present data for $A_{LL}^{\pi^0}(\overset{(-)}{p}p)$ are not quite useful to discriminate the magnitude of spin-dependent gluon distribution because p_T regions measured by the E581/704 Collaboration are small.

To examine the $\sqrt{s}$ dependence of the present model, we have calculated $A_{LL}^{\pi^0}(pp)$ and $A_{LL}^{\pi^0}(\bar{p}p)$ for $\sqrt{s} = 100$ GeV and $\theta = 90°$, which are presented in Fig.10(A) and (B). High energy data will be more preferable to distinguish various models since the intrinsic k_T contribution originating from the nonperturbative QCD effects becomes smaller for large $\sqrt{s}$ and p_T. We hope our predictions can be tested in the forthcoming experiments.

3.2 Two–Spin Asymmetry for Direct Photon Productions

Another hard scattering process which attracts interest for the spin–dependent gluon distributions is the production of prompt photons at large transverse momentum [45]. A clearer test as a probe of the magnitude of the gluon polarization may be obtained from this process in polarized $\overset{(-)}{p}p$ collisions because a photon is directly produced from the fundamental subprocesses and its cross section has no fragmentation functions which possess some theoretical ambiguity. The subprocesses dominating this reaction are shown in Fig.11.

In this subsection we calculate the two–spin asymmetry $A_{LL}^{\gamma}(\overset{(-)}{p}p)$ for high p_T photon productions in $\overset{(-)}{p}p$ collisions. When $A_{LL}^{\gamma}(\overset{(-)}{p}p)$ is defined similarly to eq.(3.1), the cross sections for $\overset{(-)}{p} + p \rightarrow \gamma + X$ are given by[50, 51]

$$E\frac{d\Delta\sigma}{d^3p}(s, p_T, \theta) = \frac{1}{\pi}\sum_{ab\rightarrow\gamma d}\int_{x_{a\ min}}^{1} dx_a \delta f_{a/A}(x_a, Q^2)\delta f_{b/B}(x_b, Q^2)\left(\frac{x_a x_b}{x_a - x_1}\right) \times\frac{d\Delta\hat{\sigma}}{d\hat{t}}(ab \rightarrow \gamma d; \hat{s}, \hat{t}, \hat{u}) , \tag{3.8}$$

$$E\frac{d\sigma}{d^3p}(s, p_T, \theta) = \frac{1}{\pi}\sum_{ab\rightarrow\gamma d}\int_{x_{a\ min}}^{1} dx_a f_{a/A}(x_a, Q^2) f_{b/B}(x_b, Q^2)\left(\frac{x_a x_b}{x_a - x_1}\right) \times\frac{d\hat{\sigma}}{d\hat{t}}(ab \rightarrow \gamma d; \hat{s}, \hat{t}, \hat{u}) , \tag{3.9}$$

with

$$x_1 = \frac{1}{2}x_T \cot\frac{\theta}{2} , \quad x_b = \frac{x_a x_T \tan\frac{\theta}{2}}{2x_a - x_T\cot\frac{\theta}{2}} , \quad x_{a\ min} = \frac{x_T\cot\frac{\theta}{2}}{2 - x_T\tan\frac{\theta}{2}} ,$$

$$\hat{s} = x_a x_b s , \qquad \hat{t} = -\frac{s}{2} x_a x_T \tan\frac{\theta}{2} , \quad \hat{u} = -\frac{s}{2} x_b x_T \cot\frac{\theta}{2} ,$$

where $x_T \equiv 2p_T/\sqrt{s}$ and θ is the production angle of γ in the CMS of colliding protons. $d\Delta\hat{\sigma}/d\hat{t}$ and $d\hat{\sigma}/d\hat{t}$ included in eqs.(3.8) and (3.9) are given by

$$\frac{d\Delta\hat{\sigma}}{d\hat{t}}(q\,\bar{q} \to \gamma\, G) = -\frac{4}{9}\left(\frac{\hat{t}}{\hat{u}} + \frac{\hat{u}}{\hat{t}}\right) , \tag{3.10a}$$

$$\frac{d\Delta\hat{\sigma}}{d\hat{t}}(\overset{(-)}{q}G \to \gamma\,\overset{(-)}{q}) = -\frac{1}{6}\left(\frac{\hat{s}}{\hat{t}} - \frac{\hat{t}}{\hat{s}}\right) , \tag{3.10b}$$

$$\frac{d\Delta\hat{\sigma}}{d\hat{t}}(G\overset{(-)}{q} \to \gamma\,\overset{(-)}{q}) = -\frac{1}{6}\left(\frac{\hat{u}}{\hat{s}} - \frac{\hat{s}}{\hat{u}}\right) , \tag{3.10c}$$

and

$$\frac{d\hat{\sigma}}{d\hat{t}}(q\,\bar{q} \to \gamma\, G) = \frac{4}{9}\left(\frac{\hat{t}}{\hat{u}} + \frac{\hat{u}}{\hat{t}}\right) , \tag{3.11a}$$

$$\frac{d\hat{\sigma}}{d\hat{t}}(\overset{(-)}{q}G \to \gamma\,\overset{(-)}{q}) = -\frac{1}{6}\left(\frac{\hat{s}}{\hat{t}} + \frac{\hat{t}}{\hat{s}}\right) , \tag{3.11b}$$

$$\frac{d\hat{\sigma}}{d\hat{t}}(G\overset{(-)}{q} \to \gamma\,\overset{(-)}{q}) = -\frac{1}{6}\left(\frac{\hat{u}}{\hat{s}} + \frac{\hat{s}}{\hat{u}}\right) , \tag{3.11c}$$

where these subprocess cross sections are omitted a common factor of $2\pi\alpha\alpha_S e_q^2/\hat{s}^2$. For further details on the derivation of eqs.(3.10a)-(3.11c), see refs.[50, 51]. As mentioned before, the best choice of Q^2 would be the one that minimizes the higher order terms. We set here $Q^2 = p_T^2/2$ in order to make higher order corrections to the cross sections smaller[54] for the unpolarized differential cross section in eq.(3.9).

Shown in Fig.12(A) are $A_{LL}^{\gamma}(\overset{(-)}{p}p)$ calculated by using the spin-dependent gluon distribution functions of (a), (b), (c) and (d) together with the quark ones, as a function of transverse momenta p_T of the photon at $\sqrt{s} = 20$ GeV and $\theta = 90°$. By comparing this with the case of π^0, a similar result has been obtained : resultant $A_{LL}^{\gamma}(\overset{(-)}{p}p)$ for type (a) is again almost the same as that for no gluon polarization model (type (d)).

The different behavior between $A_{LL}^{\gamma}(pp)$ and $A_{LL}^{\gamma}(\overline{p}p)$ can be understood as follows. The dominant subprocess for $\overline{p}p$ reactions is $q\overline{q} \to \gamma G$ whose $d\Delta\hat{\sigma}/d\hat{t}$ in eq.(3.10a) is negative, while

the one for pp reactions is $qG \to \gamma q$ with positive $d\Delta\hat{\sigma}/d\hat{t}$ in eqs.(3.10b) and (3.10c). On the other hand, $d\hat{\sigma}/d\hat{t}$ in eqs.(3.11a)–(3.11c) is positive for every subprocess.

In order to examine the $\sqrt{s}$ dependence of two-spin asymmetries for $\overset{(-)}{p} + p \to \gamma + X$, we calculate $A_{LL}^{\gamma}(\overset{(-)}{p}p)$ for $\sqrt{s} = 100$ GeV and $\theta = 90°$, which are shown in Fig.12(B).

3.3 Two-Spin Asymmetry for J/ψ Productions

In order to get a more direct information of spin-dependent gluon distributions, let us discuss the inclusive J/ψ production process in polarized proton-polarized proton collisions [46]. Since the J/ψ productions come out only via gluon-gluon fusion processes at the lowest order of QCD diagrams, this quantity is strongly sensitive to the spin-dependent gluon distribution in a proton. When $A_{LL}^{J/\psi}(pp)$ is defined as in eq.(3.1), the spin-dependent (spin-independent) differential cross section in the hard-scattering parton model is given by[51]

$$E\frac{d\Delta\sigma}{d^3p}(s,p_T,y) = \frac{1}{\pi}\int_{x_{a\ min}}^{1} dx_a \delta G(x_a,Q^2)\delta G(x_b,Q^2)\left(\frac{x_a x_b}{x_a - x_1}\right)\frac{d\Delta\hat{\sigma}}{d\hat{t}}(\hat{s},\hat{t},\hat{u}) , \tag{3.12}$$

$$E\frac{d\sigma}{d^3p}(s,p_T,y) = \frac{1}{\pi}\int_{x_{a\ min}}^{1} dx_a G(x_a,Q^2)G(x_b,Q^2)\left(\frac{x_a x_b}{x_a - x_1}\right)\frac{d\hat{\sigma}}{d\hat{t}}(\hat{s},\hat{t},\hat{u}) , \tag{3.13}$$

where x_a is the momentum fraction in a proton A and the kinematic variables are written by[51]

$$\begin{aligned} x_1 &= \frac{e^{y}}{\sqrt{s}}\sqrt{m_{J/\psi}^2 + p_T^2} , \qquad x_2 = \frac{e^{-y}}{\sqrt{s}}\sqrt{m_{J/\psi}^2 + p_T^2} , \\ x_b &= \frac{x_a x_2 s - m_{J/\psi}^2}{s(x_a - x_1)} , \qquad x_{a\ min} = \frac{x_1 - \tau}{1 - x_2} . \end{aligned} \tag{3.14}$$

Here y (p_T) is the rapidity (transverse momentum) of the produced J/ψ particle and $\tau \equiv m_{J/\psi}^2/s$. As J/$\psi$ particles are produced via $GG \to J/\psi\ G$, differential cross sections of the subprocess included in eqs.(3.12) and (3.13) are formulated in the framework of perturbative

QCD[55]. Then we get

$$\frac{d\Delta\hat{\sigma}}{d\hat{t}} = \frac{5\pi\alpha_S^3(Q^2)|R(0)|^2 m_{J/\psi}}{9\ \hat{s}^2} \tag{3.15}$$
$$\times \left[\frac{\hat{s}^2}{(\hat{t}-m_{J/\psi}^2)^2(\hat{u}-m_{J/\psi}^2)^2} - \frac{\hat{t}^2}{(\hat{u}-m_{J/\psi}^2)^2(\hat{s}-m_{J/\psi}^2)^2} - \frac{\hat{u}^2}{(\hat{s}-m_{J/\psi}^2)^2(\hat{t}-m_{J/\psi}^2)^2}\right] ,$$

$$\frac{d\hat{\sigma}}{d\hat{t}} = \frac{5\pi\alpha_S^3(Q^2)|R(0)|^2 m_{J/\psi}}{9\ \hat{s}^2} \tag{3.16}$$
$$\times \left[\frac{\hat{s}^2}{(\hat{t}-m_{J/\psi}^2)^2(\hat{u}-m_{J/\psi}^2)^2} + \frac{\hat{t}^2}{(\hat{u}-m_{J/\psi}^2)^2(\hat{s}-m_{J/\psi}^2)^2} + \frac{\hat{u}^2}{(\hat{s}-m_{J/\psi}^2)^2(\hat{t}-m_{J/\psi}^2)^2}\right] ,$$

with

$$\hat{s} = x_a x_b s\ , \quad \hat{t} = -x_a x_2 s + m_{J/\psi}^2\ , \quad \hat{u} = -x_b x_1 s + m_{J/\psi}^2\ ,$$

where $R(0)$ is the value of the radial S-wave function at the origin. As for the derivation of eqs.(3.15) and (3.16), see Appendix D. In order to calculate $A_{LL}^{J/\psi}(pp)$, we take one of the spin-dependent gluon distributions (a), (b), (c) and (d) given by eqs.(2.18), (3.2), (3.3) and (3.4). As for the definition of Q^2 for the present processes, we have again several guesses for a choice of Q^2 ; $Q^2 = m_{J/\psi}^2 + p_T^2$, $4p_T^2$, $(\hat{s}\hat{t}\hat{u})^{1/3}$, $-\hat{t}$ and so on. Setting $y = 0$ and using the four types of spin-dependent gluon distribution functions ((a), (b), (c) and (d)), together with the spin-independent gluon distribution function of the DO parametrization [16] for (a), the BBS parametrizaton [38] for (c), and the DFLM parametrization [17] for (b) and (d), we have calculated $A_{LL}^{J/\psi}(pp)$ for some of these choices of Q^2. We see that $A_{LL}^{J/\psi}(pp)$ for each type of the spin-dependent gluon distributions is insensitive to the choice of Q^2. Thus, we here take $Q^2 = m_{J/\psi}^2 + p_T^2$ by taking the mass effect of the J/ψ particle into account. The results of $A_{LL}^{J/\psi}(pp)$ are shown in Fig.13 as a function of p_T of the J/ψ at (A) $\sqrt{s} = 20$ and (B) 100 GeV. At $\sqrt{s} = 20$ GeV our largely polarized gluon distribution, (a), contributes little to $A_{LL}^{J/\psi}(pp)$ in all the p_T region because the important kinematical region near the peak of $x\delta G(x)$ is truncated by $x_{a\ min}$. The $A_{LL}^{J/\psi}$ predicted with type (a) is not so significantly different from that with no gluon polarization (type (d)), and hence we cannot practically find the difference between them. However, for higher energies such as $\sqrt{s} = 100$ GeV, we can distinguish types (a) and

(d) for spin–dependent gluon distributions by choosing a moderate p_T region. In addition, one can see that the behavior of $A_{LL}^{J/\psi}$ for types (b) and (c) largely differs from that for types (a) and (d) at $\sqrt{s} = 20$ and 100 GeV. Therefore, it is expected that one can either rule out or confirm types (b) and (c) by measuring $A_{LL}^{J/\psi}$.

In the next section, we will investigate the process which is usefull to distinguish type (a) from type (d) of $x\delta G$.

4 EFFECTS OF GLUON POLARIZATIONS ON INELASTIC J/ψ LEPTOPRODUCTIONS

In this section, to see more clearly the effect of the spin-dependent gluon distributions, we study the J/ψ production processes in polarized ℓp collisions, which may serve as the most straightforward method for extracting δG [56]. For unpolarized ℓp collisions*, the J/ψ production processes in deep inelastic ℓp collisions are effective for getting informations of the spin-independent gluon distribution.

The processes for leptoproductions of J/ψ by polarized electron beams on polarized proton targets are shown in Fig.14,

$$\vec{e} + \vec{p} \rightarrow e' + J/\psi + X \ . \tag{4.1}$$

In the one-photon exchange approximation, we can describe the process (4.1) by a virtual photon reaction

$$\gamma^* + p \rightarrow J/\psi + X \ , \tag{4.2}$$

where γ^* is the virtual photon with varying invariant mass Q^2. The cross sections of this process are directly related to the distribution of polarized gluons as shown later. Since we are considering the region where the J/ψ particles are produced via photon-gluon fusion, $\gamma^* G \rightarrow J/\psi \ G$, we can conservatively take the kinematic region as[57, 58]

$$z = \frac{p_{J/\psi} \cdot p_p}{Q \cdot p_p} < 0.8 \ , \qquad \frac{p_T^2}{m_{J/\psi}^2} > 0.1 \ , \tag{4.3}$$

where p_T is the transverse momentum of the produced J/ψ. Q, $p_{J/\psi}$ and p_p represent the four-momenta of the (virtual) photon, J/ψ and the proton, respectively. In the inelastic region given by eq.(4.3), the so-called color-singlet model[58] for J/ψ productions via photon-gluon

*The J/ψ productions via photon-gluon fusion in unpolarized μp collisions have been studied by several authors[57, 58].

fusion(Fig.14) has reproduced well not only the z, p_T and Q^2 dependence but also the absolute value of the experimetal data on unpolarized μp scatterings[59] by taking $\alpha_S \cong 0.4$[57]. As described in [57], a rather large value of $\alpha_S \cong 0.4$ (in spite of $\alpha_S(Q^2 = m^2_{J/\psi}) \cong 0.28$) includes the uncertainties in the color–singlet model, coming from the neglect of the higher order QCD corrections, the use of the nonrelativistic treatment of charmonium and the neglect of the J/ψ binding energy. Accordingly, $\alpha_S \cong 0.4$ is interpreted as an "effective" coupling constant. In the polarized lepton–proton scatterings discussed here, we assume that the same model with $\alpha_S \cong 0.4$ would also work well since we are considering the same kinematical region as that in the unpolarized case. Although the value of α_S is important, the reader should not take the rather large value $\alpha_S \cong 0.4$ at face value, since it is taken as a representative in the present analysis. $z \to 1$ is in the elastic domain and for $p_T \to 0$ the multiple soft gluon emission must be considered. The spin–dependent differential cross section for the subprocess $\gamma^* G \to J/\psi\, G$ is given by

$$\begin{aligned} \frac{d\Delta\hat{\sigma}}{d\hat{t}} &\equiv \frac{1}{4}\left[\frac{d\hat{\sigma}_{\uparrow\uparrow}}{d\hat{t}} - \frac{d\hat{\sigma}_{\uparrow\downarrow}}{d\hat{t}} + \frac{d\hat{\sigma}_{\downarrow\downarrow}}{d\hat{t}} - \frac{d\hat{\sigma}_{\downarrow\uparrow}}{d\hat{t}}\right] \\ &= \frac{8\pi m^3_{J/\psi}\alpha_S^2\Gamma_{ee}}{3\alpha\ \hat{s}^2}\frac{\hat{s}^2(\hat{s}-m^2_{J/\psi})^2 - \hat{t}^2(\hat{t}-m^2_{J/\psi})^2 - \hat{u}^2(\hat{u}-m^2_{J/\psi})^2}{(\hat{s}-m^2_{J/\psi})^2(\hat{t}-m^2_{J/\psi})^2(\hat{u}-m^2_{J/\psi})^2}\ , \end{aligned} \tag{4.4}$$

where $\frac{d\hat{\sigma}_{\uparrow\downarrow}}{d\hat{t}}$, for instance, denotes the differential cross section in which the helicity of the virtual photon is positive and that of the gluon negative, and Γ_{ee} is the leptonic decay width of J/ψ, $\Gamma_{ee} = 5.36$keV. $\hat{s}$,$\hat{t}$ and $\hat{u}$ are Mandelstam variables. Eq.(4.4) can be easily obtained by replacing the color factors and coupling constants for $GG \to J/\psi\ G$ in eq.(3.15) by the ones for $\gamma G \to J/\psi\ G$. At the hadron level $\gamma^* p \to J/\psi\ X$, we can calculate the differential cross section as

$$\frac{d\Delta\sigma}{d\hat{t}} = \int \delta G(x,Q^2)\frac{d\Delta\hat{\sigma}}{d\hat{t}}dx\ , \tag{4.5}$$

where $\delta G(x,Q^2)$ is the spin–dependent gluon distribution function. x is the fraction of the

proton momentum carried by the initial state gluon, and is given as[57, 58]

$$x = \frac{1}{s_T}\left(\frac{m_{J/\psi}^2}{z} + \frac{p_T^2}{z(1-z)}\right) , \tag{4.6}$$

where $\sqrt{s_T}$ is the total energy in photon–proton collisions. We express eq.(4.5) in terms of observable variables as

$$\begin{aligned}\frac{d^2\Delta\sigma}{dzdp_T^2} &= \frac{8\pi\alpha_S^2 m_{J/\psi}^3 \Gamma_{ee} z(1-z) x\delta G(x,Q^2)}{3\alpha\{m_{J/\psi}^2(1-z)+p_T^2\}^2} \\ &\times \left[\frac{1}{(m_{J/\psi}^2+p_T^2)^2} - \frac{(1-z)^4}{\{m_{J/\psi}^2(1-z)^2+p_T^2\}^2} - \frac{z^4 p_T^4}{(m_{J/\psi}^2+p_T^2)^2\{m_{J/\psi}^2(1-z)^2+p_T^2\}^2}\right] .\end{aligned} \tag{4.7}$$

Using $\alpha_S = 0.4$ together with $x\delta G(x,Q^2)$ presented in eq.(2.18), we can estimate the spin–dependent differential cross section eq.(4.7). At HERA energy $\sqrt{s_T} = 185$ GeV, $d^2\Delta\sigma/dzdp_T^2$ versus p_T^2 is shown in Fig.15 for various values of z. As shown in eq.(4.7), this distribution is directly proportional to the magnitude of the spin–dependent gluon distribution. Therefore, by detecting it with high precision, one can get to know how large the gluon polarization is. We hope that our present predictions will be tested in the forthcoming HERA experiments for polarized electron–polarized proton collisions.

Another interesting quantity is the x dependence of the spin–dependent differential cross section, which will also be measured in the forthcoming experiments. By rewriting eq.(4.7), one can get

$$\frac{d\Delta\sigma}{dx} = x\delta G(x,Q^2)\delta f(x,x_{min}) , \tag{4.8}$$

with

$$\begin{aligned}\delta f(x,x_{min}) &= \frac{16\pi\alpha_S^2\Gamma_{ee}}{3\alpha m_{J/\psi}^3}\frac{x_{min}^2}{x^2} \\ &\times \left[\frac{x-x_{min}}{(x+x_{min})^2} + \frac{2x_{min}x\ln\frac{x}{x_{min}}}{(x+x_{min})^3} - \frac{x+x_{min}}{x(x-x_{min})} + \frac{2x_{min}\ln\frac{x}{x_{min}}}{(x-x_{min})^2}\right] ,\end{aligned} \tag{4.9}$$

where $x_{min} \equiv m_{J/\psi}^2/s_T$. Eq.(4.9) can be derived easily from eq.(4.7) by the same manner as in the unpolarized case given by ref.[58]. δf is a function which is sharply peaked at x just above

x_{min}. A numerical calculation derives $x_{peak} = 1.53x_{min}$. Fig.16 shows the x dependence of $d\Delta\sigma/dx$ calculated by using the large gluon polarizations ((a) and (b)) of eqs.(2.18) and (3.2) at various energies including relevant HERA energies. As δf has a sharp peak, the observed cross section $d\Delta\sigma/dx$ directly reflects the spin-dependent gluon distribution near x_{peak}. As is seen from eq.(4.8), $d\Delta\sigma/dx$ is linearly dependent on the spin-dependent gluon distribution. Thus, if $\delta G(x)$ is small or vanishing, $d\Delta\sigma/dx$ ought to be necessarily small. We are eager for experimental check of the result in Fig.16. According to these observations, we can obviously distinguish type (a) from type (d) of the spin-dependent gluon distributions.

5 CONCLUSION AND DISCUSSION

The measurement of the spin–dependent proton structure function $g_1^p(x)$ by the EMC Collaboration in 1988 suggested that very little of the proton spin was carried by quarks. This result was very exciting because it was inconsistent with the conventional understanding of a proton spin structure that the proton spin should be almost constructed by the quark spins, and it has been called "proton spin crisis". So far, many interesting ideas have been presented in order to get out of this crisis. But the situation is still controversial and people have no clear understandings yet.

In the present paper, we have proposed a different approach in order to explain the stimulating EMC data and aimed to get a deep understanding of hadron dynamics. More than ten years ago, Carlitz and Kaur (CK) proposed a simple model which in some sense incorporated both the nonrelativistic quark model and the parton model, and explained the SLAC $g_1^p(x)$ data rather well. However, the CK model could not succeed in explaining the EMC $g_1^p(x)$ data. In this work, from a rather conservative point of view we have modified the CK model : (i) a proton wave function has been improved by taking account of not only the three–body quarks states but also the five–body states, so that the strange quark component has been taken up accordingly, (ii) based on the analogy of Rutherford scattering, where the leading quark is scattered by a gluon source, the spin–dilution factor has been modified by taking account of the dynamics of quarks and gluons, (iii) the effect of the polarized gluon density on the spin–dependent quark distribution functions has been taken into account via the $U_A(1)$ anomaly of QCD. In our model a gluon plays two roles. One is the source interacting with a quark as mentioned in (ii). The other is the free polarized gluon introduced through the $U_A(1)$ anomaly. At the nonperturbative level with low Q^2, gluons act on quarks collectively. On the other hand, at high Q^2 gluons distinguish themselves as independent partons, since they are in the asymptotically free region. Then, we expect that even if there exists no gluon polar-

ization at the nonperturbative stage, a gluon polarization can be generated at higher Q^2 from polarized quarks by the Altarelli–Parisi equations. Such considerations lead us to realize the important role of the spin–dependent gluon distribution function $\delta G(x)$. The $x\delta G(x)$ which we have proposed in the present work has a sharp peak at $x < 0.01$ and rapidly decreases with increasing x.

By using our spin–dependent parton distribution functions, we have reproduced well the x dependence of not only the EMC $g_1^p(x)$ data but also the recent SMC $g_1^d(x)$ data. The amount of the proton spin carried by quarks is not necessarily small : it is almost 3/4 and not so far the value of proton spin, 1/2. However, the model has a large value of the first moment of the polarized gluon distribution inside a proton, $\Delta G(Q^2) = 6.32$ at $Q^2 = 10.7$ GeV^2(EMC value). To confirm these results, it is necessary to examine the effect of the polarized gluons on other processes. There are several physical processes such as the inclusive π^0–, high–p_T direct photon and J/ψ–productions, which are affected by a polarized gluon content inside a proton. We have calculated two–spin asymmetries A_{LL} for these processes by using our large gluon polarization $x\delta G(x)$. In addition, we have examined the cases of additional three different spin–dependent distributions : one is the conventional one where $x\delta G(x)$ has rather broad behavior of x given by (b), the other is a small gluon polarization ((c)) and the third is $x\delta G(x, Q^2_{EMC}) = 0$ ((d)). From these analyses, we can see that even for large gluon polarization, $\Delta G(Q^2_{EMC}) \simeq 5 \sim 6$, if $x\delta G(x)$ has a sharp peak at $x < 0.01$ and decreases rapidly with increasing x, then A_{LL} becomes almost the same as that calculated by using no gluon polarization ((d)) and is consistent with the E581/704 data. The type (b) which has also large $\Delta G(Q^2_{EMC})$ could not reproduce the E581/704 data on $A_{LL}^{\pi^0}(\vec{p}^{(-)}p)$. In addition, type (c) is not completely consistent with the data. Therefore, one can say that a large gluon polarization inside a proton is not necessarily ruled out but the shape of $x\delta G(x)$ is strongly constrained by the E581/704 data. Furthermore, in order to analyze more directly the magnitude and behavior of the spin–dependent gluon distribution, we have studied the J/ψ leptoproduction in polarized electron–polarized proton

collisions. Since the differential cross sections of the J/ψ leptoproductions in polarized ep collisions are directly proportional to the spin–dependent gluon distribution, one can easily check the magnitude and behavior of the polarized gluon. The HERA collider which is now running, will do a good job for extracting the knowledge of $x\delta G(x)$ and test our predictions in the forthcoming experiments on the J/ψ production in polarized ep collisions. Although our model has a large gluon polarization in a proton, the results calculated with our spin–dependent gluon distribution ((a)) are consistent with the EMC, SMC and E581/704 data. We believe that the polarized gluons would give us a clue getting out of the proton spin crisis.

Before closing the final section, some comments are in order on the remaining subjects and perspect on the spin problems of hadrons. One comment is on the proton spin sum rule. The consideration of the $U_A(1)$ anomaly presents an attractive view that if ΔG is large (~ 5), the most part of the proton spin ($\simeq 70\%$) is to be carried by quarks. If this is indeed the case, then we are to have an approximate relation $\langle L_Z\rangle_{q+G} \sim -\Delta G$ from the proton spin sum rule

$$\frac{1}{2} = \frac{1}{2}\Delta\Sigma + \Delta G + \langle L_Z\rangle_{q+G} \ .$$

However, at present nobody knows the underlying physics of what it means. It remains to be a problem, though the idea that the $U_A(1)$ anomaly affects largely the polarized quark density is attractive.

Another comment is on the polarized sea quarks, in particular the polarized strange quarks[60]. The EMC data suggest a large and negative contribution of strange quarks to the proton spin, -0.19, as shown in eq.(1.23). However, contrary to such a large Δs extracted from the EMC experiment, the experimental data on charm productions in neutrino DIS, which provide a more direct knowledge of the strange quark content in a proton, gave a restrictive bound as follows [61] ;

$$|\Delta s| \leq |s| = 0.057^{+0.023}_{-0.057} \ ,$$

which is in little agreement with the EMC results : A way to get rid of this inconsistency might come from the $U_A(1)$ anomaly. If the $U_A(1)$ anomaly is taken into account and Δs is replaced by $\widetilde{\Delta s}$ as shown in eq.(2.17), then these data might be reconciled with each other by taking rather large ΔG. (See eqs.(2.21c) and (2.22).) To confirm this interpretation, one need to measure independently both the magnitude of the polarized gluons and strange quarks.

Further comment is on the $g_2(x)$ and higher twists of QCD. If the experiments are carried out by using longitudinally polarized lepton beams on transversely polarized nucleon targets, one can get the "transverse" spin–dependent structure function, so–called g_2. While $g_1(x)$ is due to only the leading twist (twist–2) in the operator product expansion, $g_2(x)$ contains the contribution of more complicated terms of higher twists. The contribution of the twist–2 to $g_2(x)$ can be related to $g_1(x)$ by the Wandzura–Wilczek sum rule[62] and satisfies the Burkhardt–Cottingham sum rule[63]. On the other hand, the contribution of the twist–3 depends on the quark–gluon interaction, the parton mass and so on, which are not negligible. The contribution estimated by using the bag model is large and of opposite sign to that from the twist–2 [64]. In order to understand the effect of higher twist of QCD, we have to analyze $g_2(x)$ carefully. Recently, there are several interesting experiments to examine the hadron structure. The measurements of the single transverse asymmetry A_N for π^0 productions have been carried out by using transversely polarized proton (antiproton) beams on unpolarized proton targets at large p_T. Contrary to the prediction of the parton model, in which partons hardly polarize transversely at the leading twist because they are massless and hence A_N is almost zero, the experimental result has shown us a large value of A_N for π^0 productions at $p_T = 4 \sim 5$ GeV[65]. This fact suggests the existence of transversely polarized partons and gives us an informations of higher twists.

Our final comment is devoted to the activity under going and a prospect. At HERA,

in order to research the hadron dynamics at very small x, the new measurements of the spin–independent structure function $F_2^p(x)$ have been carried out by the use of unpolarized electron–proton collisions. Since $x = Q^2/2M_N\nu$, the small x region, *i.e.* small Q^2, describes the transition from perturbative QCD to nonperturbative QCD [66]. If the data of the proton structure function $F_2^p(x)$ are collected for extremely small x regions, it would be very helpful to understand the dynamics of the hadron structure in nonperturbative regions. Furthermore, the precise measurement of $g_1^p(x)$ and $g_1^d(x)$ by the SMC Collaboration is in progress. In the near future, one will obtain a lot of interesting data from the HERA, the SMC Collaboration and so on, and we need further theoretical investigation to go beyond the present understanding on the hadron structure.

A The wave function of a polarized nucleon

In order to derive the spin-dependent sea-quark distribution function, we have to construct a polarized wave function composed of $u_V u_V d_V + (q\bar{q})$ pairs. We restrict ourselves to five-body quark states, $u_V u_V d_V + (q\bar{q})$. Then the wave function of the polarized proton is written by

$$\begin{aligned} |\, p\uparrow\rangle &= a_0\Big[\,|\,\Psi_0\rangle + |\,\Psi_1\rangle\Big]_V \\ &+ a_1\Big[\,|\,\Psi_0'\rangle + |\,\Psi_1'\rangle + \tfrac{\epsilon}{\sqrt{2}}(|\,\Psi_0''\rangle + |\,\Psi_1''\rangle + |\,\Psi_{\frac{1}{2}}''\rangle)\Big]_{V+S}\ , \end{aligned} \tag{A.1}$$

where the suffix $V+S$ means $u_V u_V d_V + (q_S\bar{q}_S)$ and the suffix of Ψ' and Ψ'' represents the isospin of the core, which consists of $qqqq$ or $qqq\bar{q}$. $|\,\Psi_0'\rangle$ and $|\,\Psi_1'\rangle$ are constructed by $(uudu\bar{u})$ and $(uuddd\bar{d})$. Each $|\,\Psi_i''\rangle$ in the ϵ term comes from $(uuds\bar{s})$.

$|\,\Psi_0'\rangle$, $|\,\Psi_1'\rangle$ and $|\,\Psi_i''\rangle$ are written in factorized forms of isospin, spin and space parts as follows :

$$\begin{aligned} |\,\Psi_0'\rangle &= \frac{1}{2}\Big\{|\,\psi_1\rangle + \frac{1}{\sqrt{2}}(|\,\psi_1'\rangle + |\,\psi_2'\rangle)\Big\} \otimes |\,s=0, s_3=0\,|\uparrow\rangle f_0'(x)\ , \\ |\,\Psi_1'\rangle &= \Big[\frac{1}{\sqrt{6}}\{\frac{1}{\sqrt{2}}(|\,\psi_2\rangle + |\,\psi_3\rangle) + |\,\psi_3'\rangle\} - \frac{1}{\sqrt{12}}\{|\,\psi_4\rangle + \frac{1}{\sqrt{2}}(|\,\psi_4'\rangle + |\,\psi_5'\rangle)\}\Big] \\ &\otimes \Big[\sqrt{\frac{2}{3}}\,|\,s=1, s_3=1\,|\downarrow\rangle - \frac{1}{\sqrt{3}}\,|\,s=1, s_3=0\,|\uparrow\rangle\Big] f_1'(x)\ . \\ |\,\Psi_0''\rangle &= \frac{1}{2}|\,\psi_1''\rangle \otimes |s=0, s_3=0\,|\uparrow\rangle f_0''(x)\ , \\ |\,\Psi_1''\rangle &= \frac{1}{2}\Big[\sqrt{\frac{2}{3}}|\,\psi_2''\rangle - \frac{1}{\sqrt{3}}|\,\psi_3''\rangle\Big] \\ &\otimes \Big[\sqrt{\frac{2}{3}}\,|\,s=1, s_3=1\,|\downarrow\rangle - \frac{1}{\sqrt{3}}\,|\,s=1, s_3=0\,|\uparrow\rangle\Big] f_1''(x)\ , \\ |\,\Psi_{\frac{1}{2}}''\rangle &= \frac{1}{2}\Big[|\,\psi_4''\rangle + |\,\psi_5''\rangle\Big] \\ &\otimes \frac{1}{\sqrt{2}}\Big[|\,s=0, s_3=0\,|\uparrow\rangle + (\sqrt{\frac{2}{3}}\,|\,s=1, s_3=1\,|\downarrow\rangle \\ &- \frac{1}{\sqrt{3}}\,|\,s=1, s_3=0\,|\uparrow\rangle)\Big] f_{\frac{1}{2}}(x)\ , \end{aligned} \tag{A.2}$$

where s and s_3 are the spin of the core and its third component, respectively, and $\mid \psi_i\rangle$, $\mid \psi_i'\rangle$ and $\mid \psi_2''\rangle$ are given in eqs.(A.4).

The spin parts are

$$\mid s=0, s_3=0 \mid \uparrow\rangle = \frac{1}{2}(\uparrow\downarrow\uparrow\downarrow - \downarrow\uparrow\uparrow\downarrow - \uparrow\downarrow\downarrow\uparrow + \downarrow\uparrow\downarrow\uparrow) \mid\uparrow\rangle \ ,$$

and

$$\begin{aligned} &\sqrt{\frac{2}{3}} \mid s=1, s_3=1 \mid\downarrow\rangle - \frac{1}{\sqrt{3}} \mid s=1, s_3=0 \mid\uparrow\rangle \\ &= \frac{1}{3}(2\uparrow\uparrow\downarrow\uparrow - \uparrow\downarrow\uparrow\uparrow - \downarrow\uparrow\uparrow\uparrow) \mid\downarrow\rangle \\ &-\frac{1}{6}(2\uparrow\uparrow\downarrow\downarrow - \uparrow\downarrow\uparrow\downarrow - \downarrow\uparrow\uparrow\downarrow + \uparrow\downarrow\downarrow\uparrow + \downarrow\uparrow\downarrow\uparrow - 2\downarrow\downarrow\uparrow\uparrow) \mid\uparrow\rangle \ . \end{aligned} \tag{A.3}$$

The momentum–dependent functions $f_0'(x)$, $f_1'(x)$, $f_0''(x)$, $f_1''(x)$ and $f_{\frac{1}{2}}(x)$ are equal to one another in the SU(6) limit.

The isospin parts $\mid \psi_i\rangle$, $\mid \psi_i'\rangle$ and $\mid \psi_i''\rangle$ in eq.(A.2) can be represented in the form of $\mid I, I_3$; quark contents of the core $\mid$ the 5th quark (or antiquark)$\rangle$ and their explicit forms are as follows :

$$\begin{aligned} \mid \psi_1\rangle &= \mid I=0, I_3=0; uud\bar{u}\mid u\rangle \\ &= \frac{1}{2}(u\bar{u}ud - \bar{u}uud - u\bar{u}du + \bar{u}udu) \mid u\rangle \ , \\ \mid \psi_2\rangle &= \mid I=1, I_3=1; uudu \mid \bar{u}\rangle \\ &= \frac{1}{\sqrt{6}}(2uudu - uduu - duuu) \mid \bar{u}\rangle \ , \\ \mid \psi_3\rangle &= \mid I=1, I_3=1; uuu\bar{u} \mid d\rangle \\ &= \frac{1}{\sqrt{6}}(2uu\bar{u}u - u\bar{u}uu - \bar{u}uuu) \mid d\rangle \ , \\ \mid \psi_4\rangle &= \mid I=1, I_3=0; uud\bar{u} \mid u\rangle \\ &= \frac{1}{\sqrt{12}}(2uud\bar{u} - udu\bar{u} - duu\bar{u} + u\bar{u}du + \bar{u}udu - 2d\bar{u}uu) \mid u\rangle \ ; \end{aligned}$$

(A.4a)

$$
\begin{aligned}
|\,\psi_1'\rangle &= |\,I=0, I_3=0; uddd\bar{d}\,|\,u\rangle \\
&= \frac{1}{2}(dd\bar{d}ud - \bar{d}ddud - dd\bar{d}du + \bar{d}uddu)\,|\,u\rangle\ , \\
|\,\psi_2'\rangle &= |\,I=0, I_3=0; uudd\,|\,\bar{d}\rangle \\
&= \frac{1}{2}(udud - duud - uddu + dudu)\,|\,\bar{d}\rangle\ , \\
|\,\psi_3'\rangle &= |\,I=1, I_3=1; uudd\bar{d}\,|\,d\rangle \\
&= \frac{1}{\sqrt{6}}(-2uudd\bar{d} + udud\bar{d} + duud\bar{d})|d\rangle\ , \\
|\,\psi_4'\rangle &= |\,I=1, I_3=0; uddd\bar{d}\,|\,u\rangle \\
&= \frac{1}{\sqrt{12}}(2ddud\bar{d} - uddd\bar{d} - dudd\bar{d} + dd\bar{d}ud + \bar{d}dud - 2ud\bar{d}dd)\,|\,u\rangle\ , \\
|\,\psi_5'\rangle &= |\,I=1, I_3=0; uudd\,|\,\bar{d}\rangle \\
&= \frac{1}{\sqrt{12}}(2uudd - udud - duud + uddu + dudu - 2dduu)\,|\,\bar{d}\rangle\ ;
\end{aligned}
$$

(A.4b)

and

$$
\begin{aligned}
|\,\psi_1''\rangle &= |\,I=0, I_3=0; uds\bar{s}\,|\,u\rangle \\
&= \frac{1}{2}(uds\bar{s} - dus\bar{s} + ud\bar{s}s - du\bar{s}s)\,|\,u\rangle\ , \\
|\,\psi_2''\rangle &= |\,I=1, I_3=1; uus\bar{s}\,|\,d\rangle \\
&= \frac{1}{\sqrt{2}}(uus\bar{s} + uu\bar{s}s)\,|\,d\rangle\ , \\
|\,\psi_3''\rangle &= |\,I=1, I_3=0; uds\bar{s}\,|\,u\rangle \\
&= \frac{1}{2}(uds\bar{s} + dus\bar{s} + ud\bar{s}s + du\bar{s}s)\,|\,u\rangle\ , \\
|\,\psi_4''\rangle &= |\,I=\frac{1}{2}, I_3=\frac{1}{2}; uud\bar{s}\,|\,s\rangle \\
&= \{\frac{1}{\sqrt{12}}(2uud\bar{s} - ud u\bar{s} - duu\bar{s}) + \frac{1}{\sqrt{8}}(udu\bar{s} - duu\bar{s})\}\,|\,s\rangle\ , \\
|\,\psi_5''\rangle &= |I=\frac{1}{2}, I_3=\frac{1}{2}; uuds\,|\,\bar{s}\rangle
\end{aligned}
$$

$$= \{\frac{1}{\sqrt{12}}(2uuds - udus - duus) + \frac{1}{\sqrt{8}}(udus - duus)\} \mid \bar{s}\rangle \ . \tag{A.4c}$$

We also formulate the neutron wave function in the same way. In the following eqs.(A.5), (A.6) and (A.7), the same notations $\mid \Psi_i\rangle$, $\mid \Psi_i'\rangle$, $\mid \psi_i\rangle$ etc. are used but their contents are different from those in the case of the proton.

$$\begin{aligned} \mid n\uparrow\rangle &= a_0\Big[\mid \Psi_0\rangle + \mid \Psi_1\rangle\Big]_V \\ &+ a_1\Big[\mid \Psi_0'\rangle + \mid \Psi_1'\rangle + \tfrac{\epsilon}{\sqrt{2}}(\mid \Psi_0''\rangle + \mid \Psi_1''\rangle + \mid \Psi_{\frac{1}{2}}''\rangle)\Big]_{V+S} \ , \end{aligned} \tag{A.5}$$

where

$$\begin{aligned} \mid \Psi_0'\rangle &= \frac{1}{2}\Big\{\frac{1}{\sqrt{2}}(\mid \psi_1\rangle + \mid \psi_2\rangle) + \mid \psi_1'\rangle\Big\} \otimes \mid s=0, s_3=0\mid\uparrow\rangle f_0'(x) \ , \\ \mid \Psi_1'\rangle &= \Big[\frac{1}{\sqrt{12}}\{\frac{1}{\sqrt{2}}(\mid \psi_3\rangle + \mid \psi_4\rangle) + \mid \psi_2'\rangle\} \\ &- \frac{1}{\sqrt{6}}\{\mid \psi_5\rangle + \frac{1}{\sqrt{2}}(\mid \psi_3'\rangle + \mid \psi_4'\rangle)\}\Big] \\ &\otimes \Big[\sqrt{\frac{2}{3}} \mid s=1, s_3=1\mid\downarrow\rangle - \frac{1}{\sqrt{3}} \mid s=1, s_3=0\mid\uparrow\rangle\Big] f_1'(x) \ , \\ \mid \Psi_0''\rangle &= \frac{1}{2}\mid \psi_1''\rangle \otimes \mid s=0, s_3=0\mid\uparrow\rangle f_0(x) \ , \\ \mid \Psi_1''\rangle &= \frac{1}{2}\Big[\frac{1}{\sqrt{3}}\mid \psi_2''\rangle - \sqrt{\frac{2}{3}}\mid \psi_3''\rangle\Big] \\ &\otimes \Big[\sqrt{\frac{2}{3}} \mid s=1, s_3=1\mid\downarrow\rangle - \frac{1}{\sqrt{3}} \mid s=1, s_3=0\mid\uparrow\rangle\Big] f_1(x) \ , \\ \mid \Psi_{\frac{1}{2}}''\rangle &= \frac{1}{2}\Big[\mid \psi_4''\rangle + \mid \psi_5''\rangle\Big] \\ &\otimes \frac{1}{\sqrt{2}}\Big[\mid s=0, s_3=0\mid\uparrow\rangle + (\sqrt{\frac{2}{3}} \mid s=1, s_3=1\mid\downarrow\rangle \\ &- \frac{1}{\sqrt{3}} \mid s=1, s_3=0\mid\uparrow\rangle)\Big] f_{\frac{1}{2}}(x) \ . \end{aligned} \tag{A.6}$$

$\mid \psi_i\rangle$, $\mid \psi_i'\rangle$ and $\mid \psi_i''\rangle$ in the above equations are given by

$$\mid \psi_1\rangle = \mid I=0, I_3=0; uud\bar{u} \mid d\rangle$$

$$
\begin{aligned}
&= \frac{1}{2}(u\bar{u}ud - \bar{u}uud - u\bar{u}du + \bar{u}udu) \mid d\rangle \ , \\
\mid \psi_2\rangle &= \mid I = 0, I_3 = 0; uudd \mid \bar{u}\rangle \\
&= \frac{1}{2}(udud - duud - uddu + dudu) \mid \bar{u}\rangle \ , \\
\mid \psi_3\rangle &= \mid I = 1, I_3 = 0; uud\bar{u} \mid d\rangle \\
&= \frac{1}{\sqrt{12}}(2uud\bar{u} - udu\bar{u} - duu\bar{u} + u\bar{u}du + \bar{u}udu - 2d\bar{u}uu) \mid d\rangle \ , \\
\mid \psi_4\rangle &= \mid I = 1, I_3 = 0; uudd \mid \bar{u}\rangle \\
&= \frac{1}{\sqrt{12}}(2uudd - udud - duud + uddu + dudu - 2dduu) \mid \bar{u}\rangle \ , \\
\mid \psi_5\rangle &= \mid I = 1, I_3 = -1; udd\bar{u} \mid u\rangle \\
&= \frac{1}{\sqrt{6}}(udd\bar{u} + dud\bar{u} - 2ddu\bar{u}) \mid u\rangle \ ; \qquad \text{(A.7a)} \\
\mid \psi_1'\rangle &= \mid I = 0, I_3 = 0; udd\bar{d} \mid d\rangle \\
&= \frac{1}{2}(d\bar{d}ud - \bar{d}dud - d\bar{d}du + \bar{d}ddu) \mid d\rangle \ , \\
\mid \psi_2'\rangle &= \mid I = 1, I_3 = 0; udd\bar{d}|d\rangle \\
&= \frac{1}{\sqrt{12}}(2ddu\bar{d} - udd\bar{d} - dud\bar{d} + d\bar{d}ud + \bar{d}dud - 2ud\bar{d}d) \mid d\rangle \ , \\
\mid \psi_3'\rangle &= \mid I = 1, I_3 = -1; ddd\bar{d} \mid u\rangle \\
&= \frac{1}{\sqrt{6}}(2ddd\bar{d} - dd\bar{d}d - \bar{d}ddd) \mid u\rangle \ , \\
\mid \psi_4'\rangle &= \mid I = 1, I_3 = -1; uddd \mid \bar{d}\rangle \\
&= \frac{1}{\sqrt{6}}(-2ddud + dudd + uddd) \mid \bar{d}\rangle \ ; \qquad \text{(A.7b)}
\end{aligned}
$$

and

$$
\begin{aligned}
\mid \psi_1''\rangle &= \mid I = 0, I_3 = 0; uds\bar{s} \mid d\rangle \\
&= \frac{1}{2}(uds\bar{s} - dus\bar{s} + ud\bar{s}s - du\bar{s}s) \mid d\rangle \ , \\
\mid \psi_2''\rangle &= \mid I = 1, I_3 = 0; uds\bar{s} \mid d\rangle \\
&= \frac{1}{2}(uds\bar{s} + dus\bar{s} + ud\bar{s}s + du\bar{s}s) \mid d\rangle \ , \\
\mid \psi_3''\rangle &= \mid I = 1, I_3 = -1; dds\bar{s} \mid u\rangle
\end{aligned}
$$

$$
\begin{aligned}
&= \frac{1}{\sqrt{2}}(dds\bar{s} + dd\bar{s}s) \mid u\rangle \ , \\
\mid \psi_4''\rangle &= \mid I = \frac{1}{2}, I_3 = \frac{1}{2}; uud\bar{s} \mid s\rangle \\
&= \{\frac{1}{\sqrt{12}}(udd\bar{s} + dud\bar{s} - 2ddu\bar{s}) + \frac{1}{\sqrt{8}}(udd\bar{s} - dud\bar{s})\} \mid s\rangle \ , \\
\mid \psi_5''\rangle &= |I = \frac{1}{2}, I_3 = \frac{1}{2}; uuds \mid \bar{s}\rangle \\
&= \{\frac{1}{\sqrt{12}}(udds + duds - 2ddus) + \frac{1}{\sqrt{8}}(udds - duds)\} \mid \bar{s}\rangle \ .
\end{aligned}
\tag{A.7c}
$$

B The mixing rate of the five–body wave function with the three–body wave function

In this appendix we determine the ratio of a_1^2 to a_0^2. As seen in eqs.(2.6), (A.1) and (A.5), a_1 and a_0 are amplitudes of $(qqqq\bar{q})$ and (qqq), respectively. The ratio is given by fitting the expectation value for the magnetic moment ratio of a neutron to a proton with experimental data.

The expectation value of the proton magnetic moment in our model becomes

$$\begin{aligned}
&\langle p\uparrow|\, e_i\sigma_i \mid p\uparrow\rangle = a_0^2\Big[\langle\Psi_0 \mid e_i\sigma_i \mid \Psi_0\rangle + \langle\Psi_1 \mid e_i\sigma_i \mid \Psi_1\rangle\Big] \\
&+a_1^2\Big[\langle\Psi_0' \mid e_i\sigma_i \mid \Psi_0'\rangle + \langle\Psi_1' \mid e_i\sigma_i \mid \Psi_1'\rangle + \frac{\epsilon^2}{2}(\langle\Psi_0'' \mid e_i\sigma_i \mid \Psi_0''\rangle \\
&+\langle\Psi_1'' \mid e_i\sigma_i \mid \Psi_1''\rangle + \langle\Psi_{\frac{1}{2}}'' \mid e_i\sigma_i \mid \Psi_{\frac{1}{2}}''\rangle)\Big] \\
&= a_0^2\Big[\frac{1}{6} + 0\Big] + a_1^2\Big[\frac{7}{24} + \frac{3}{216} + \frac{\epsilon^2}{2}(\frac{1}{6} + 0 + 0)\Big] \\
&= a_0^2(\frac{1}{6}) + a_1^2(\frac{33}{108} + \frac{\epsilon^2}{2}\frac{1}{6}) \,,
\end{aligned} \tag{B.1}$$

where we consider only the third quark in the a_0 term and only the fifth quark in the a_1 term. ϵ denotes the weight of the s–quark distribution.

Similary, for the expectation value of the neutron magnetic moment we have

$$\begin{aligned}
&\langle n\uparrow|\, e_i\sigma_i \mid n\uparrow\rangle = a_0^2\Big[\langle\Psi_0 \mid e_i\sigma_i \mid \Psi_0\rangle + \langle\Psi_1 \mid e_i\sigma_i \mid \Psi_1\rangle\Big] \\
&+a_1^2\Big[\langle\Psi_0' \mid e_i\sigma_i \mid \Psi_0'\rangle + \langle\Psi_1' \mid e_i\sigma_i \mid \Psi_1'\rangle + \frac{\epsilon^2}{2}(\langle\Psi_0'' \mid e_i\sigma_i \mid \Psi_0''\rangle \\
&+\langle\Psi_1'' \mid e_i\sigma_i \mid \Psi_1''\rangle + \langle\Psi_{\frac{1}{2}}'' \mid e_i\sigma_i \mid \Psi_{\frac{1}{2}}''\rangle)\Big] \\
&= a_0^2\Big[-\frac{1}{12} - \frac{1}{36}\Big] + a_1^2\Big[-\frac{5}{24} - \frac{5}{216} + \frac{\epsilon^2}{2}(-\frac{1}{12} - \frac{1}{36} + 0)\Big] \\
&= a_0^2(-\frac{1}{9}) + a_1^2(-\frac{25}{108} - \frac{\epsilon^2}{2}\frac{1}{9}) \,.
\end{aligned} \tag{B.2}$$

Then the ratio of the magnetic moment μ_n/μ_p is given by

$$\frac{\mu_n}{\mu_p} = \frac{\langle n\uparrow|\, e_i\sigma_i \,|\, n\uparrow\rangle}{\langle p\uparrow|\, e_i\sigma_i \,|\, p\uparrow\rangle} = -\frac{\frac{1}{9}a_0^2 + (\frac{25}{108} + \frac{\epsilon^2}{2}\frac{1}{9})a_1^2}{\frac{1}{6}a_0^2 + (\frac{33}{108} + \frac{\epsilon^2}{2}\frac{1}{6})a_1^2} \ . \tag{B.3}$$

If $a_1^2 = 0$, $\mu_n/\mu_p = -\frac{2}{3}$, which is the same value as given in SU(6) model. After putting the experimental value $\mu_n/\mu_p = -0.68498$, the ratio of a_1^2/a_0^2 is determined but it depends on ϵ^2. The dependence, however, is very slight, namely a_1^2/a_0^2 changes from 0.138 to 0.148 as ϵ^2 varies from 0 to 1. Experimental analyses of the K/π production ratio at high energies show that the production ratio λ of $s\bar{s}$ pairs to $u\bar{u}$ or $d\bar{d}$ pairs is $0.2 \sim 0.3$[36]. Our choice consistent with λ is $\epsilon^2 = 0.5$. The corresponding ratio of a_1^2/a_0^2 is given by

$$a_1^2/a_0^2 = 0.1425 \ . \tag{B.4}$$

C How to calculate A_{LL}

When we calculate the observable A_{LL} defined by eq.(3.1) for the hard scattering of polarized protons, the parton distributions must be generalized to allow for the transmission of spin informations from the proton to its constituent. Let us start with the definition of the parton distribution for the hadron A,

$$f_{a(h_a)/A(\lambda_A)}(x_a, Q^2) \ ,$$

which is the probability of finding a parton a with helicity h_a and momentum fraction x_a in the parent hadron A with helicity λ_A at some Q^2, and similarly for the hadron B,

$$f_{b(h_b)/B(\lambda_B)}(x_b, Q^2) \ .$$

To find an expression for the differential cross section of hadron, $Ed\sigma_{\lambda_A\lambda_B}/d^3p$, we represent the spin–dependent part of the integrand of $Ed\sigma_{\lambda_A\lambda_B}/d^3p$ by $d\sigma_{A(\lambda_A)B(\lambda_B)}$ and the subprocess cross sections for partons a with helicity h_a and b with h_b by $(d\hat{\sigma}/d\hat{t})_{h_a h_b}$. Then we can schematically write down the following equations ;

$$\begin{aligned} d\sigma_{A(\uparrow)B(\uparrow)} &= f_{a(\uparrow)/A(\uparrow)} f_{b(\uparrow)/B(\uparrow)} \frac{d\hat{\sigma}_{\uparrow\uparrow}}{d\hat{t}} + f_{a(\uparrow)/A(\uparrow)} f_{b(\downarrow)/B(\uparrow)} \frac{d\hat{\sigma}_{\uparrow\downarrow}}{d\hat{t}} \\ &+ f_{a(\downarrow)/A(\uparrow)} f_{b(\uparrow)/B(\uparrow)} \frac{d\hat{\sigma}_{\downarrow\uparrow}}{d\hat{t}} + f_{a(\downarrow)/A(\uparrow)} f_{b(\downarrow)/B(\uparrow)} \frac{d\hat{\sigma}_{\downarrow\downarrow}}{d\hat{t}} \ , \qquad \text{(C.1)} \\ d\sigma_{A(\uparrow)B(\downarrow)} &= f_{a(\uparrow)/A(\uparrow)} f_{b(\uparrow)/B(\downarrow)} \frac{d\hat{\sigma}_{\uparrow\uparrow}}{d\hat{t}} + f_{a(\uparrow)/A(\uparrow)} f_{b(\downarrow)/B(\downarrow)} \frac{d\hat{\sigma}_{\uparrow\downarrow}}{d\hat{t}} \\ &+ f_{a(\downarrow)/A(\uparrow)} f_{b(\uparrow)/B(\downarrow)} \frac{d\hat{\sigma}_{\downarrow\uparrow}}{d\hat{t}} + f_{a(\downarrow)/A(\uparrow)} f_{b(\downarrow)/B(\downarrow)} \frac{d\hat{\sigma}_{\downarrow\downarrow}}{d\hat{t}} \ . \qquad \text{(C.2)} \end{aligned}$$

Here we are suppressing the integration and kinematic variables. Let us define the spin–dependent and spin–independent parton distribution functions for a and b as

$$\delta f_{a/A} = f_{a(\uparrow)/A(\uparrow)} - f_{a(\downarrow)/A(\uparrow)} \ , \quad f_{a/A} = f_{a(\uparrow)/A(\uparrow)} + f_{a(\downarrow)/A(\uparrow)} \ , \qquad \text{(C.3a)}$$

$$\delta f_{b/B} = f_{b(\uparrow)/B(\uparrow)} - f_{b(\downarrow)/B(\uparrow)} \ , \quad f_{b/B} = f_{b(\uparrow)/B(\uparrow)} + f_{b(\downarrow)/B(\uparrow)} \ , \qquad \text{(C.3b)}$$

and the cross sections for spin–dependent and spin–independent parton subprocesses as

$$\frac{d\Delta\hat{\sigma}}{d\hat{t}} = \frac{1}{4}\left(\frac{d\hat{\sigma}_{\uparrow\uparrow}}{d\hat{t}} - \frac{d\hat{\sigma}_{\uparrow\downarrow}}{d\hat{t}} + \frac{d\hat{\sigma}_{\downarrow\downarrow}}{d\hat{t}} - \frac{d\hat{\sigma}_{\downarrow\uparrow}}{d\hat{t}}\right) , \tag{C.4a}$$

$$\frac{d\hat{\sigma}}{d\hat{t}} = \frac{1}{4}\left(\frac{d\hat{\sigma}_{\uparrow\uparrow}}{d\hat{t}} + \frac{d\hat{\sigma}_{\uparrow\downarrow}}{d\hat{t}} + \frac{d\hat{\sigma}_{\downarrow\downarrow}}{d\hat{t}} + \frac{d\hat{\sigma}_{\downarrow\uparrow}}{d\hat{t}}\right) . \tag{C.4b}$$

Then, the parity invariance of the strong interaction results in

$$\begin{aligned} f_{a(\downarrow)/A(\uparrow)} &= f_{a(\uparrow)/A(\downarrow)} , \qquad f_{a(\downarrow)/A(\downarrow)} = f_{a(\uparrow)/A(\uparrow)} , \\ \frac{d\hat{\sigma}_{\downarrow\uparrow}}{d\hat{t}} &= \frac{d\hat{\sigma}_{\uparrow\downarrow}}{d\hat{t}} , \qquad \frac{d\hat{\sigma}_{\downarrow\downarrow}}{d\hat{t}} = \frac{d\hat{\sigma}_{\uparrow\uparrow}}{d\hat{t}} . \end{aligned} \tag{C.5}$$

By using eqs.(C.3a)–(C.4b) and eq.(C.5), we can write

$$\begin{aligned} &\frac{1}{4}\left(d\sigma_{\uparrow\uparrow} - d\sigma_{\uparrow\downarrow} + d\sigma_{\downarrow\downarrow} - d\sigma_{\downarrow\uparrow}\right) = \frac{1}{4}\left(\frac{d\hat{\sigma}_{\uparrow\uparrow}}{d\hat{t}} - \frac{d\hat{\sigma}_{\uparrow\downarrow}}{d\hat{t}} + \frac{d\hat{\sigma}_{\downarrow\downarrow}}{d\hat{t}} - \frac{d\hat{\sigma}_{\downarrow\uparrow}}{d\hat{t}}\right) \\ &\times \left(f_{a(\uparrow)/A(\uparrow)}f_{b(\uparrow)/B(\uparrow)} - f_{a(\uparrow)/A(\uparrow)}f_{b(\downarrow)/B(\uparrow)} - f_{a(\downarrow)/A(\uparrow)}f_{b(\uparrow)/B(\uparrow)} + f_{a(\downarrow)/A(\uparrow)}f_{b(\downarrow)/B(\uparrow)}\right) \\ &= \frac{d\Delta\hat{\sigma}}{d\hat{t}}\delta f_{a/A}\delta f_{b/B} , \end{aligned} \tag{C.6}$$

$$\begin{aligned} &\frac{1}{4}\left(d\sigma_{\uparrow\uparrow} + d\sigma_{\uparrow\downarrow} + d\sigma_{\downarrow\downarrow} + d\sigma_{\downarrow\uparrow}\right) = \frac{1}{4}\left(\frac{d\hat{\sigma}_{\uparrow\uparrow}}{d\hat{t}} + \frac{d\hat{\sigma}_{\uparrow\downarrow}}{d\hat{t}} + \frac{d\hat{\sigma}_{\downarrow\downarrow}}{d\hat{t}} + \frac{d\hat{\sigma}_{\downarrow\uparrow}}{d\hat{t}}\right) \\ &\times \left(f_{a(\uparrow)/A(\uparrow)}f_{b(\uparrow)/B(\uparrow)} + f_{a(\uparrow)/A(\uparrow)}f_{b(\downarrow)/B(\uparrow)} + f_{a(\downarrow)/A(\uparrow)}f_{b(\uparrow)/B(\uparrow)} + f_{a(\downarrow)/A(\uparrow)}f_{b(\downarrow)/B(\uparrow)}\right) \\ &= \frac{d\hat{\sigma}}{d\hat{t}}f_{a/A}f_{b/B} . \end{aligned} \tag{C.7}$$

If the two–spin asymmetry A_{LL} is defined by eq.(3.1),

$$A_{LL} = \frac{\left[d\sigma_{\uparrow\uparrow} - d\sigma_{\uparrow\downarrow} + d\sigma_{\downarrow\downarrow} - d\sigma_{\downarrow\uparrow}\right]}{\left[d\sigma_{\uparrow\uparrow} + d\sigma_{\uparrow\downarrow} + d\sigma_{\downarrow\downarrow} + d\sigma_{\downarrow\uparrow}\right]} , \tag{C.8}$$

the numerator and denominator of eq.(C.8) are given by eq.(C.6) and eq.(C.7), respectively. Therefore, the measurements of A_{LL} give us the informations of parton distributions.

D The differential subprocess cross sections for J/ψ productions

Let us consider the differential subprocess cross sections for the J/ψ hadroproductions. Because of the symmetry, it is useful to regard $GG \to J/\psi\ G$, where the J/ψ productions come out only via gluon-gluon fusion at the lowest order of QCD diagrams, as $GGG \to J/\psi$. Then we consider the following process ;

$$G(k_1,\lambda_1) + G(k_2,\lambda_2) + G(k_3,\lambda_3) \to q(\frac{1}{2}p+q) + \bar{q}(\frac{1}{2}p-q)\ ,$$

where k_1, k_2 and k_3 are the 4-momenta of the gluons, and λ_1, λ_2 and λ_3 are their helicities. $\frac{1}{2}p+q$ and $\frac{1}{2}p-q$ denote the 4-momenta of the quark and antiquark. The Mandelstam variables for its subprocess are given by

$$\hat{s} \ = \ (k_1+k_2)^2\ , \quad \hat{t} \ = \ (k_2+k_3)^2\ , \quad \hat{u} \ = \ (k_3+k_1)^2\ . \tag{D.1}$$

Let us denote the helicity amplitude by $\mathcal{M}(\lambda_1,\lambda_2,\lambda_3)$. The angular momentum conservation results in

$$\mathcal{M}(+,+,+) \ = \ 0\ . \tag{D.2}$$

The remaining amplitudes can be calculated by summing over the polarization state of J/ψ and the color degree of freedom of gluons in the initial and final states. For example, we have

$$|\mathcal{M}(+,+,-)|^2 \ = \ \frac{10240\pi^2\alpha_S^3|R(0)|^2 m_{J/\psi}\hat{s}^2}{9(\hat{t}-m_{J/\psi}^2)^2(\hat{u}-m_{J/\psi}^2)^2}\ . \tag{D.3}$$

For further details on the derivation of eqs.(D.2) and (D.3), see Gastmans and Wu[55]. Obviously, the helicity amplitude $\mathcal{M}(+,-,+)$ is derived from the above one by replacing $\hat{s} \leftrightarrow \hat{u}$, and $\mathcal{M}(-,+,+)$ by $\hat{s} \leftrightarrow \hat{t}$. Thus, by averaging over the initial spin and the color degrees of freedom of gluons, the spin-dependent and spin-independent differential cross sections can be

obtained as

$$\begin{aligned}
\frac{d\Delta\hat{\sigma}}{d\hat{t}} &= \frac{1}{\pi\hat{s}^2}\frac{1}{4}\frac{1}{8^3}\left\{|\mathcal{M}(+,+,+)|^2+|\mathcal{M}(+,+,-)|^2-|\mathcal{M}(+,-,+)|^2-|\mathcal{M}(+,-,-)|^2\right\} \\
&= \frac{5\pi\alpha_S^3(Q^2)|R(0)|^2 m_{J/\psi}}{9\ \hat{s}^2} \qquad \text{(D.4)} \\
&\times \left[\frac{\hat{s}^2}{(\hat{t}-m_{J/\psi}^2)^2(\hat{u}-m_{J/\psi}^2)^2}-\frac{\hat{t}^2}{(\hat{u}-m_{J/\psi}^2)^2(\hat{s}-m_{J/\psi}^2)^2}-\frac{\hat{u}^2}{(\hat{s}-m_{J/\psi}^2)^2(\hat{t}-m_{J/\psi}^2)^2}\right],
\end{aligned}$$

and

$$\begin{aligned}
\frac{d\hat{\sigma}}{d\hat{t}} &= \frac{1}{\pi\hat{s}^2}\frac{1}{4}\frac{1}{8^3}\left\{|\mathcal{M}(+,+,+)|^2+|\mathcal{M}(+,+,-)|^2+|\mathcal{M}(+,-,+)|^2+|\mathcal{M}(+,-,-)|^2\right\} \\
&= \frac{5\pi\alpha_S^3(Q^2)|R(0)|^2 m_{J/\psi}}{9\ \hat{s}^2} \qquad \text{(D.5)} \\
&\times \left[\frac{\hat{s}^2}{(\hat{t}-m_{J/\psi}^2)^2(\hat{u}-m_{J/\psi}^2)^2}+\frac{\hat{t}^2}{(\hat{u}-m_{J/\psi}^2)^2(\hat{s}-m_{J/\psi}^2)^2}+\frac{\hat{u}^2}{(\hat{s}-m_{J/\psi}^2)^2(\hat{t}-m_{J/\psi}^2)^2}\right],
\end{aligned}$$

respectively.

References

[1] M. Gell-Mann, Phys. Lett. **8**, 214 (1964).

[2] G. Zweig, Preprints CERN-TH. 401 and 412 (1964).

[3] For example, F. E. Close, "An Introduction to Quarks and Partons", (Academic Press 1979).

[4] W. Panofsky, in *Proc. 14th Int. Conf. on High Energy Physics (Vienna)*, 1968, CERN, Geneva, edited by J. Prentki and J. Steinberger.

[5] R. P. Feynman, Phys. Rev. Lett. **23**, 1415 (1969).

[6] R. D. Bjroken, Phys. Rev. **179**, 1547 (1969); R. D. Bjroken and E. A. Paschos, Phys. Rev. **185**, 1975 (1969).

[7] D. J. Gross and F. Wilczek, Phys. Rev. Lett. **30**, 1343 (1973); H. D. Politzer, Phys. Rev. Lett. **30**, 1346 (1973); G. t' Hooft, in *Proceedings of Colloquium on Renormalization of Yang-Mills Field and Application to Particle Physics*, 1972, Marseilles, edited by C. P. Korthals-Altes.

[8] H. J. Rothe, "Lattice Gauge Theories An Inroduction", World Scientific Lecture Notes in Physics, vol. 43 (World Scientific 1992).

[9] M. A. Shifman, A. I. Vainshtein and V. I. Zakharov, Nucl. Phys. **B147**, 385, 448 (1979); L. J. Reinders, H. Rubinstein and S. Yazaki, Phys. Rep. **127**, 1 (1985); S. Narison, "QCD Spectral Sum Rules", World Scientific Lecture Notes in Physics, vol. 26 (World Scientific 1989).

[10] M. J. Alguard et al., Phys. Rev. Lett. **37**, 1261 (1976), ibid **41**, 70 (1978); G. Baum et al., Phys. Rev. Lett. **51**, 1135 (1983).

[11] J. Ellis and R. L. Jaffe, Phys. Rev. **D9**, 1444 (1974); **D10**, 1669 (1974).

[12] J. Ashman et al., Phys. Lett. **B206**, 364 (1988); Nucl. Phys. **B328**, 1 (1989).

[13] R. P. Feynman, "Photon–Hadron Interactions", (Benjamin–Coummings Publishing Company 1972).

[14] T. Muta, "Foundations of Quantum Chromodynamics", World Scientific Lecture Notes in Physics, vol. 5 (World Scientific 1987).

[15] G. Altarelli and G. Parisi, Nucl. Phys. **B126**, 298 (1977).

[16] D. W. Duke and J. F. Owens, Phys. Rev. **D30**, 49 (1984).

[17] M. Diemoz, F. Ferroni, E. Longo and G. Martinelli, Z. Phys. **C39**, 21 (1988).

[18] E. Eichten, I. Hinchliffe, K. Lane and C. Quigg, Rev. Mod. Phys. **56**, 574 (1984); **58**, 1065(E) (1986).

[19] J. Kwiecinski, A. D. Martin, W. J. Stirling and R. G. Roberts, Phys. Rev. **D42**, 3645 (1990).

[20] J. Kodaira, S. Matsuda, T. Muta, K. Sasaki and T. Uematsu, Phys. Rev. **D20**, 627 (1979); J. Kodaira, S. Matsuda, K. Sasaki and T. Uematsu, Nucl. Phys. **B159**, 99 (1979); J. Kodaira, Nucl. Phys. **B165**, 129 (1980).

[21] J. J. de Swart, Rev. Mod. Phys. **35**, 916 (1963).

[22] M. Bourquin et al., Z. Phys. **C21**, 27 (1983).

[23] R. L. Jaffe and A. Manohar, Nucl. Phys. **B337**, 347 (1990).

[24] F. E. Close and R. G. Roberts, Phys. Rev. Lett. **60**, 1471 (1988).

[25] H. J. Lipkin, Phys. Lett. **B214**, 429 (1988), ibid **B230**, 135 (1989).

[26] S. J. Brodsky, J. Ellis and M. Karliner, Phys. Lett. **B206**, 309 (1988).

[27] T. P. Cheng and L. F. Li, Phys. Rev. Lett. **62**, 1441 (1989); H. Fritzsch, Phys. Lett. **B229**, 122 (1989); J. Soffer, CPT-90/P.2445 (1990); G. Veneziano, Mod. Phys. Lett. **A4**, 1605 (1989); CERN-TH.5840/90(1990).

[28] H. Y. Cheng and S. N. Lai, Phys. Rev. **D41**, 91 (1990); J. D. Jackson, G. G. Ross and R. G. Roberts, Phys. Lett. **B226**, 159(1989); J. Qiu, G. P. Ramsey, D. Richards and D. Sivers, Phys. Rev. **D41**, 65 (1990).

[29] G. Altarelli and G. G. Ross, Phys. Lett. **B212**, 391 (1988); R. D. Carlitz, J. C. Collins and A. H. Mueller, Phys. Lett. **B214**, 229 (1988); A. V. Efremov and O. V. Teryaev, in *Proceedings of the International Hadron Symposium*, 1988, Bechyně, Czechoslovakia, edited by Fischer et al., (Czechoslovakian Academy of Scinece, Prague, 1989).

[30] S. Forte, Phys. Lett. **B224**, 189 (1989); Nucl. Phys. **B331**, 1 (1990).

[31] R. L. Jaffe, Phys. Lett. **B193**, 101 (1987).

[32] G. Altarelli and G. G. Ross, Phys. Lett. **B212**, 391 (1988); see also, H. Y. Cheng, *Invited talk in the 1991 Annual Meeting of the Chinese Physical Society*, 1991, China, IP–ASTP –01–91, to be published in the Chinese Journal of Physics.

[33] R. D. Carlitz and J. Kaur, Phys. Rev. Lett. **38**, 673 (1977); J. Kaur, Nucl. Phys. **B128**, 219 (1977).

[34] D. L. Adams et al., FNAL E581/704 Collab., Phys. Lett. **B261**, 197 (1991).

[35] K. Kobayakawa, T. Morii, S. Tanaka and T. Yamanishi, Phys. Rev. **D46**, 2854 (1992).

[36] R. E. Ansorge et al., Z. Phys. **C41**, 179 (1988).

[37] J. D. Bjorken, Phys. Rev. **148**, 1467 (1966); **D1**, 1376 (1970).

[38] S. J. Brodsky, M. Burkardt and I. Schmidt, "PERTURBATIVE QCD CONSTRAINTS ON THE SHAPE OF POLARIZED QUARK AND GLUON DISTRIBUTIONS", preprint 6087 (1994).

[39] G.Altarelli and W.J.Stirling, Part. World **1**, 40 (1989); J. Soffer, CPT-89/P.2264 (1989); Z. Kunszt, Phys. Lett. **B218**, 243 (1989); H. Y. Cheng and S. N. Lai, Phys. Rev. **D41**, 91 (1990).

[40] F. E. Close and D. Sivers, Phys. Rev. Lett. **39**, 1116 (1977); M. Glück, E.Reya and W. Vogelsang, Nucl. Phys. **B329**, 347 (1990); Phys. Rev. **D45** 2552, (1992).

[41] W. Vogelsang and A. Weber, Phys. Rev. **D45**, 4069 (1992).

[42] B. Adeva et al., SMC Collab., Phys. Lett. **B302**, 533 (1993).

[43] M. Lacombe et al., Phys. Lett. **B101**, 139 (1981).

[44] G. Ramsey and D. Sivers, Phys. Rev. **D43**, 2861 (1991); K. Kobayakawa, T. Morii and T. Yamanishi, Z. Phys. **C59**, 251 (1993).

[45] H. Y. Cheng and S. N. Lai, Phys. Rev. **D41**, 91 (1990); G. Ramsey and D. Sivers, Phys. Rev. **D43**, 2861 (1991); K. Kobayakawa, T. Morii and T. Yamanishi, Z. Phys. **C59**, 251 (1993).

[46] M. A. Doncheski and R. W. Robinett, Phys. Lett. **B248**, 188 (1990); R. W. Robinett, Phys. Rev. **D43**, 113 (1991); T. Morii, S. Tanaka and T. Yamanishi, "Effects of the large gluon polarization on $xg_1^d(x)$ and J/ψ productions at polarized ep and pp collisions", KOBE–FHD–93–08, to be published in Phys. Lett. B.

[47] J. Babcock, E. Monsay and D. Sivers, Phys. Rev. **D19**, 1483 (1979).

[48] N. S. Craigie, K. Hidaka, M. Jacob and F. M. Renard, Phys. Rep. **99**, 69 (1983).

[49] C. Bourrely, J. Soffer, F. M. Renard and P. Taxil, Phys. Rep. **177**, 319 (1989).

[50] H. Y. Cheng and S. N. Lai, Phys. Rev. **D41**, 91 (1990).

[51] R. D. Field, "Applications of Perturbative QCD", (Addison–Wesley 1989).

[52] R. D. Field and R. P. Feynman, Nucl. Phys. **B136**, 1 (1978).

[53] R. P. Feynman, R. D. Field and G. C. Fox, Phys. Rev. **D18**, 3320 (1978).

[54] E. L. Berger and J. W. Qiu, Phys. Rev. **D40**, 778 (1989).

[55] R. Gastmans, W. Troost and T. T. Wu, Nucl. Phys. **B291**, 731 (1987); R. Gastmans and T. T. Wu, "The Ubiquitous Photon Helicity Method for QED and QCD", (Oxford 1990).

[56] J. Ph. Guillet, Z. Phys. **C39**, 75 (1988); R. M. Godbole, S. Gupta and K. Sridhar, Phys. Lett. **B255**, 120 (1991); K. Sridhar and E. Leader, Phys. Lett. **B295**, 283 (1992); T. Morii, S. Tanaka and T. Yamanishi, "Effects of the large gluon polarization on $xg_1^d(x)$ and J/ψ productions at polarized ep and pp collisions", KOBE–FHD–93–08, to be published in Phys. Lett. B.

[57] A. D. Martin, C. -K. Ng and W. J. Stirling, Phys. Lett. **B191**, 200 (1987); R. Baier and R. Rückl, Nucl. Phys. **B218**, 289 (1983); S. M. Tkaczyk, W. J. Stirling and D. H. Saxon, DESY HERA Workshop (1987), preprint RAL–88–041.

[58] E. L. Berger and D. Jones, Phys. Rev. **D23**, 1521 (1981).

[59] J. J. Aubert et al., Nucl. Phys. **B213**, 1 (1983).

[60] J. Soffer, *Lectures in the RCNP–Kikuchi School on Spin Physics at Intermediate Energies*, 1992, Osaka, CPT–92/P.2816.

[61] H. Abramowicz et al., Z. Phys. **C25**, 29 (1984); D. Allasia et al., Z. Phys. **C28**, 321 (1985).

[62] W. Wandzura and F. Wilczek, Phys. Lett. **B172**, 195 (1977).

[63] H. Burkhardt and W. N. Cottingham, Ann. Phys. (N. Y.) **56**, 453 (1970).

[64] R. L. Jaffe and X. Ji, Phys. Rev. **D43**, 724 (1991).

[65] D. L. Adams et al., FNAL E581/704 Collab., Phys. Lett. **B261**, 201 (1991); Phys. Lett. **B264**, 462 (1991).

[66] J. Bartels, Part. World **2**, 46 (1991).

Table 1 The subprocess cross sections for hard parton scatterings with definite helicity states of partons. All the cross sections down to the 6th column from the top contain a common factor $\pi\alpha_S^2/\hat{s}^2$, and the others a common factor $2\pi\alpha\alpha_S e_q^2/\hat{s}^2$ which are omitted in the table.

	$d\Delta\hat{\sigma}/d\hat{t}$	$d\hat{\sigma}/d\hat{t}$
$q_\alpha q_\beta \to q_\alpha q_\beta$	$\frac{4}{9}\left[\frac{\hat{s}^2-\hat{u}^2}{\hat{t}^2}+\delta_{\alpha\beta}\left(\frac{\hat{s}^2-\hat{t}^2}{\hat{u}^2}-\frac{2\hat{s}^2}{3\hat{t}\hat{u}}\right)\right]$	$\frac{4}{9}\left[\frac{\hat{s}^2+\hat{u}^2}{\hat{t}^2}+\delta_{\alpha\beta}\left(\frac{\hat{s}^2+\hat{t}^2}{\hat{u}^2}-\frac{2\hat{s}^2}{3\hat{t}\hat{u}}\right)\right]$
$q_\alpha \bar{q}_\beta \to q_\gamma \bar{q}_\delta$	$\frac{4}{9}[\delta_{\alpha\gamma}\delta_{\beta\delta}\frac{\hat{s}^2-\hat{u}^2}{\hat{t}^2}-\delta_{\alpha\beta}\delta_{\gamma\delta}\frac{\hat{t}^2+\hat{u}^2}{\hat{s}^2}$ $-\frac{2}{3}\delta_{\alpha\gamma}\delta_{\beta\delta}\delta_{\gamma\delta}\frac{\hat{u}^2}{\hat{s}\hat{t}}]$	$\frac{4}{9}[\delta_{\alpha\gamma}\delta_{\beta\delta}\frac{\hat{s}^2+\hat{u}^2}{\hat{t}^2}+\delta_{\alpha\beta}\delta_{\gamma\delta}\frac{\hat{t}^2+\hat{u}^2}{\hat{s}^2}$ $-\frac{2}{3}\delta_{\alpha\gamma}\delta_{\beta\delta}\delta_{\gamma\delta}\frac{\hat{u}^2}{\hat{s}\hat{t}}]$
$\overset{(-)}{q}G \to \overset{(-)}{q}G$	$\left[\frac{\hat{s}^2-\hat{u}^2}{\hat{t}^2}-\frac{4}{9}\left(\frac{\hat{s}^2-\hat{u}^2}{\hat{u}\hat{s}}\right)\right]$	$\left[\frac{\hat{s}^2+\hat{u}^2}{\hat{t}^2}-\frac{4}{9}\left(\frac{\hat{s}^2+\hat{u}^2}{\hat{u}\hat{s}}\right)\right]$
$GG \to q\bar{q}$	$-\frac{1}{2}\left[\frac{1}{3}\left(\frac{\hat{t}^2+\hat{u}^2}{\hat{t}\hat{u}}\right)-\frac{3}{4}\left(\frac{\hat{t}^2+\hat{u}^2}{\hat{s}^2}\right)\right]$	$\frac{1}{2}\left[\frac{1}{3}\left(\frac{\hat{t}^2+\hat{u}^2}{\hat{t}\hat{u}}\right)-\frac{3}{4}\left(\frac{\hat{t}^2+\hat{u}^2}{\hat{s}^2}\right)\right]$
$q\bar{q} \to GG$	$-\left[\frac{32}{27}\left(\frac{\hat{t}^2+\hat{u}^2}{\hat{t}\hat{u}}\right)-\frac{8}{3}\left(\frac{\hat{t}^2+\hat{u}^2}{\hat{s}^2}\right)\right]$	$\left[\frac{32}{27}\left(\frac{\hat{t}^2+\hat{u}^2}{\hat{t}\hat{u}}\right)-\frac{8}{3}\left(\frac{\hat{t}^2+\hat{u}^2}{\hat{s}^2}\right)\right]$
$GG \to GG$	$\frac{9}{2}\left[-3+\frac{2\hat{s}^2}{\hat{t}\hat{u}}+\frac{\hat{t}\hat{u}}{\hat{s}^2}\right]$	$\frac{9}{2}\left[3-\frac{\hat{s}\hat{t}}{\hat{u}^2}-\frac{\hat{t}\hat{u}}{\hat{s}^2}-\frac{\hat{u}\hat{s}}{\hat{t}^2}\right]$
$q\bar{q} \to G\gamma$	$-\frac{4}{9}\left[\frac{\hat{t}}{\hat{u}}+\frac{\hat{u}}{\hat{t}}\right]$	$\frac{4}{9}\left[\frac{\hat{t}}{\hat{u}}+\frac{\hat{u}}{\hat{t}}\right]$
$\overset{(-)}{q}G \to \overset{(-)}{q}\gamma$	$-\frac{1}{6}\left[\frac{\hat{s}}{\hat{t}}-\frac{\hat{t}}{\hat{s}}\right]$	$-\frac{1}{6}\left[\frac{\hat{s}}{\hat{t}}+\frac{\hat{t}}{\hat{s}}\right]$
$G\overset{(-)}{q} \to \overset{(-)}{q}\gamma$	$-\frac{1}{6}\left[\frac{\hat{u}}{\hat{s}}-\frac{\hat{s}}{\hat{u}}\right]$	$-\frac{1}{6}\left[\frac{\hat{u}}{\hat{s}}+\frac{\hat{s}}{\hat{u}}\right]$

Figure captions

Fig. 1: The one–photon exchange diagrman for deep inelasitc lepton–hadron scattering.

Fig. 2: Spin–dilution factors at $Q^2 = 10.7$ GeV^2 for $x \leq 0.5$. The solid and dashed curves represent the present model with $m_q = 5$ MeV and 300 MeV, respectively. The dash–dotted one is given by Carlitz and Kaur[33].

Fig. 3: Modified spin–dependent distribution functions of quarks and the spin–dependent distribution function of gluons at $Q^2 = 10.7$ GeV^2.

Fig. 4: Comparison of the spin–dependent structure function $xg_1^p(x, Q^2 = 10.7 \text{ GeV}^2)$ with expermental data. The solid and the dashed lines denote the result of the present model and the EMC fit, respectively. The full circle, open triangle and square points show the EMC, SLAC (E80) and SLAC(E130) data, respectively. Inner and outer error bars mean the statistical and total errors, respectively

Fig. 5: The x dependence of the spin–dependent deuteron structure function $xg_1^d(x, Q^2)$ at $Q^2 = 4.6$ GeV^2. Experimental data are taken from [42].

Fig. 6: The x dependence of (A) $x\delta G(x, Q^2)$ and (B) $\delta G(x, Q^2)/G(x, Q^2)$ for various types (a)–(d) given by eqs.(2.18), (3.2), (3.3) and (3.4) at $Q^2 = 10.7$ GeV^2.

Fig. 7: The hard–scattering diagram for two protons both longitudinally polarized.

Fig. 8: Two–spin asymmetry $A_{LL}^{\pi^0}(pp)$ for $\sqrt{s} = 20$ GeV and $\theta = 90°$, calculated with various types of $x\delta G(x)$, as a function of transverse momenta p_T of π^0. The solid, dashed, small–dashed and dash–dotted lines indicate the results using types (a), (b), (c) and (d) in eqs.(2.18), (3.2), (3.3) and (3.4), respectively. Experimental data are taken from [34].

Fig. 9: Two-spin asymmetry $A_{LL}^{\pi^0}(\overline{p}p)$ for $\sqrt{s} = 20$ GeV and $\theta = 90°$, calculated with types (a), (b), (c) and (d) for $x\delta G(x)$, as a function of transverse momenta p_T of π^0. Data are taken from [34].

Fig. 10: Two-spin asymmetries (A) $A_{LL}^{\pi^0}(pp)$ and (B) $A_{LL}^{\pi^0}(\overline{p}p)$ for $\sqrt{s} = 100$ GeV and $\theta = 90°$. The solid, dashed, small-dashed and dash-dotted lines represent types (a), (b), (c) and (d), respectively.

Fig. 11: The diagrams of subprocesses for $\overset{(-)}{p}p \rightarrow \gamma X$. (A) Annihilation diagrams for prompt photons, (B) Compton scattering diagrams.

Fig. 12: Two-spin asymmetries $A_{LL}^{\gamma}(pp)$ and $A_{LL}^{\gamma}(\overline{p}p)$ for $\theta = 90°$ as a function of transverse momenta p_T of γ at (A) $\sqrt{s} = 20$ GeV, and (B) $\sqrt{s} = 100$ GeV. The solid, dashed, small-dashed and dash-dotted curves correspond to types (a), (b), (c) and (d) for $x\delta G(x)$, respectively.

Fig. 13: The two-spin asymmetries $A_{LL}^{J/\psi}(pp)$ for $y = 0$ (namely, $\theta = 90°$, where θ is the production angle of J/ψ in the CMS of a colliding proton) calculated with using types (a), (b), (c) and (d) for $x\delta G$, as a function of transverse momenta p_T of J/ψ at (A) $\sqrt{s} = 20$ GeV, and (B) $\sqrt{s} = 100$ GeV. The solid, dashed, small-dashed and dash-dotted curves correspond to types (a), (b), (c) and (d), respectively. Q^2 is taken to be $m_{J/\psi}^2 + p_T^2$.

Fig. 14: The lowest order QCD diagram for the inelastic J/ψ leptoproduction in polarized electron-polarized proton collisions.

Fig. 15: The differential cross section $d^2\Delta\sigma/dzdp_T^2$ versus p_T^2 at $\sqrt{s_T} = 185$ GeV for various values of z. The solid (dashed) curves correspond to the predictions by using the spin-

dependent gluon distribution functions of type (a) (type (b)) for the inelastic region $p_T^2/m_{J/\psi}^2 > 0.1$. Q^2 is taken to be $m_{J/\psi}^2$.

Fig. 16: The distribution $d\Delta\sigma/dx$ predicted by using types (a) and (b) of $x\delta G(x,Q^2)$, as a function of x for different values of $\sqrt{s_T}$. The solid (dashed) curve corresponds to type (a) (type (b)).

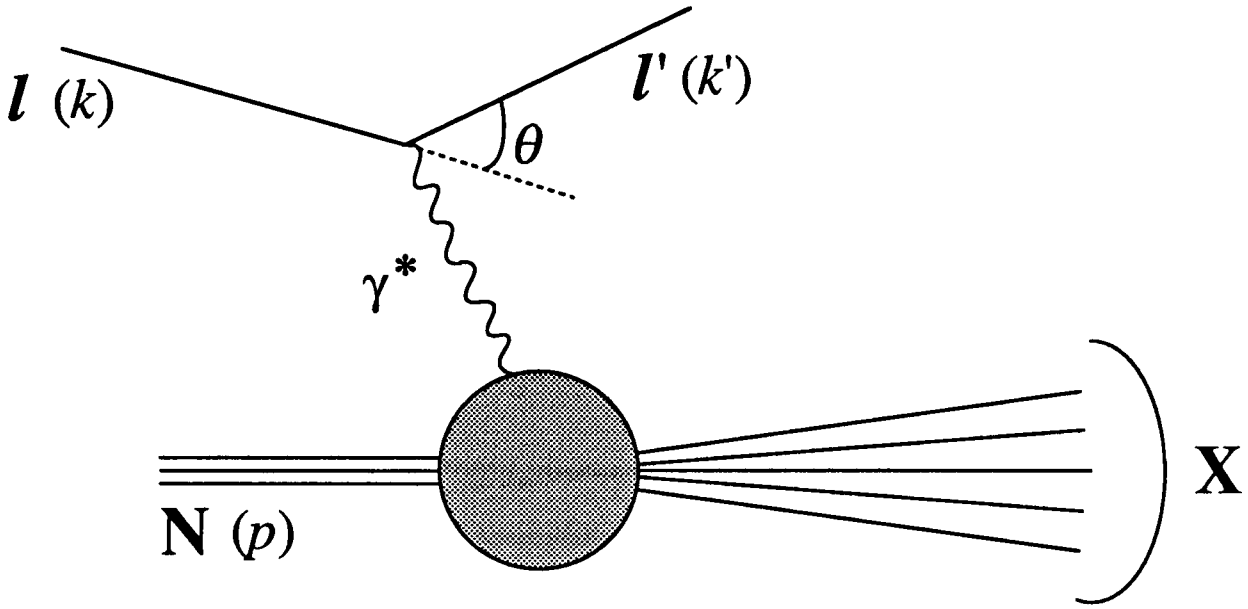

Fig.1

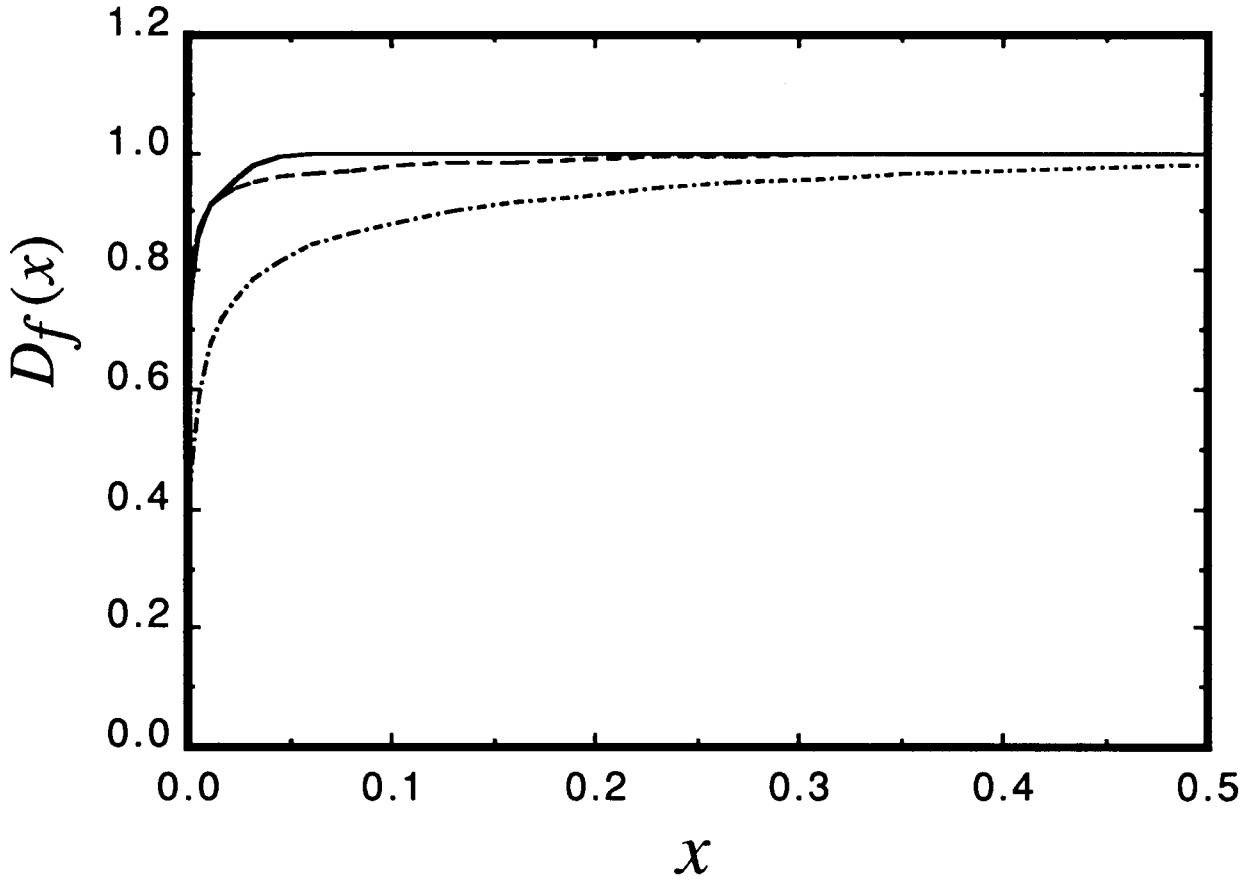

Fig.2

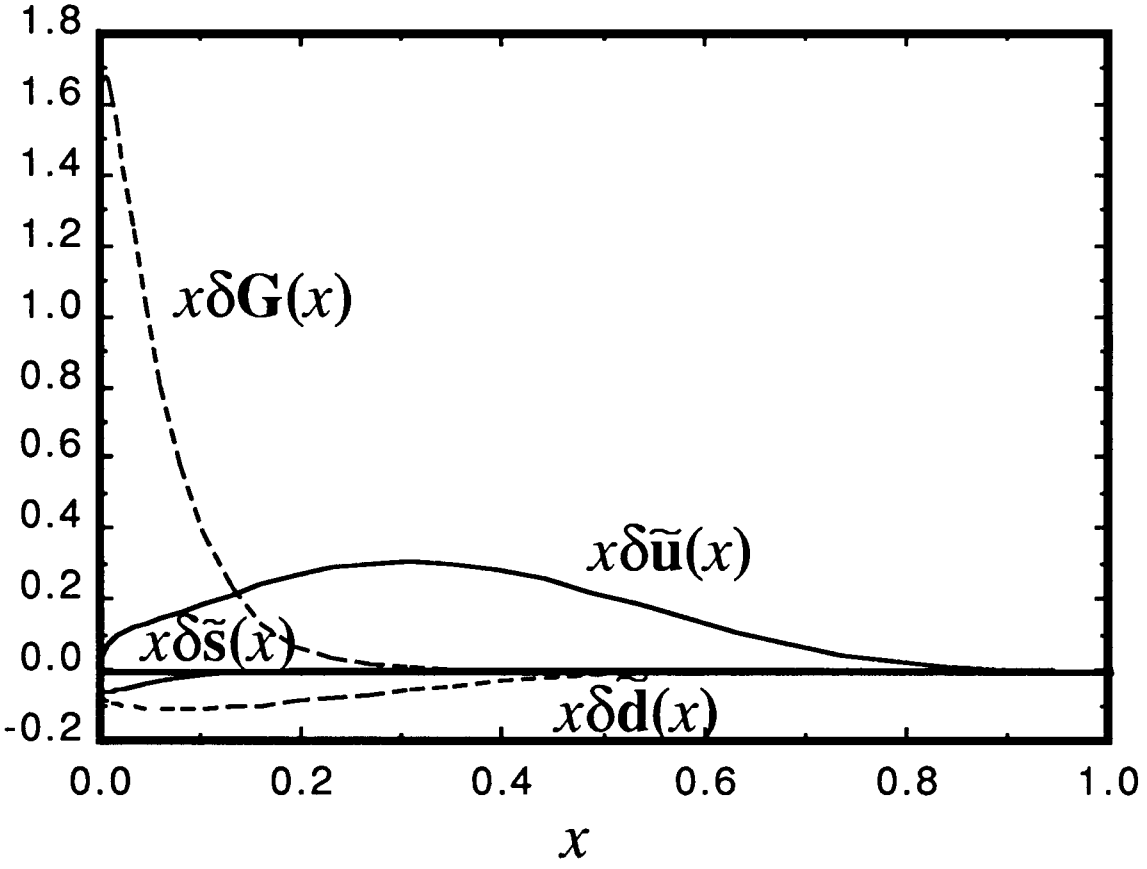
1.8
1.6
1.4
1.2
1.0
0.8
0.6
0.4
0.2
0.0
-0.2
0.0
0.2
0.4
0.6
0.8
1.0
x
xδG(x)
xδũ(x)
xδs̃(x)
xδd(x)

Fig.3

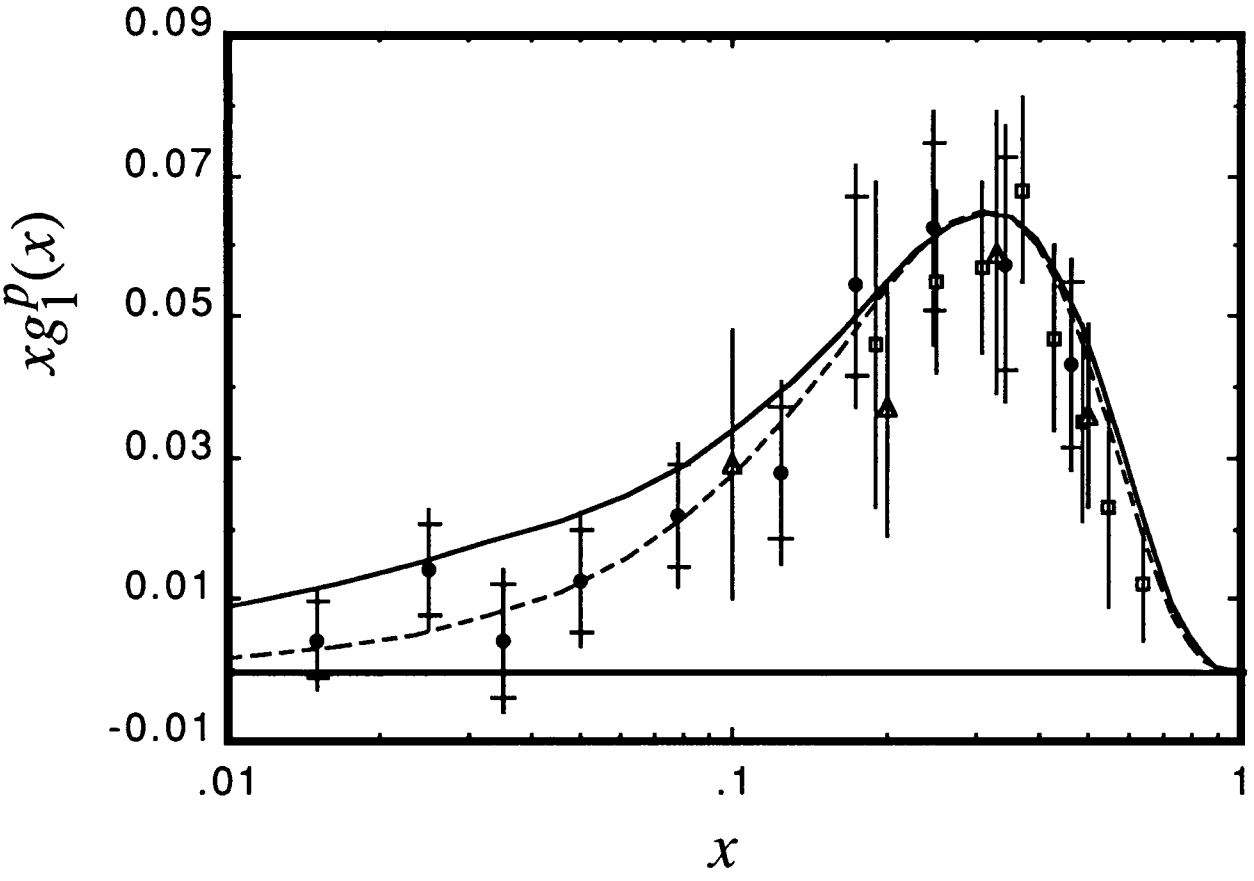
0.09
0.07
0.05
0.03
0.01
-0.01
.01
.1
1
x
$xg_1^p(x)$

Fig.4

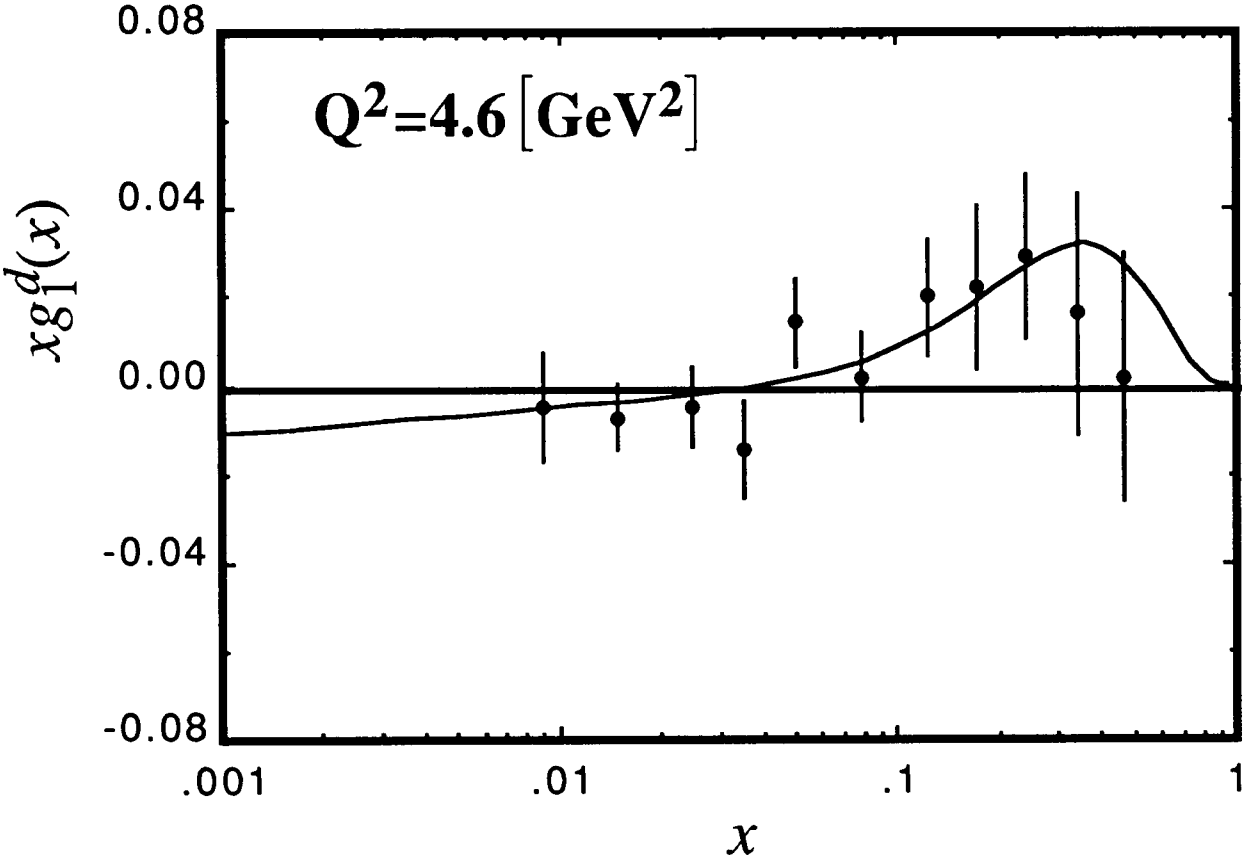

Fig.5

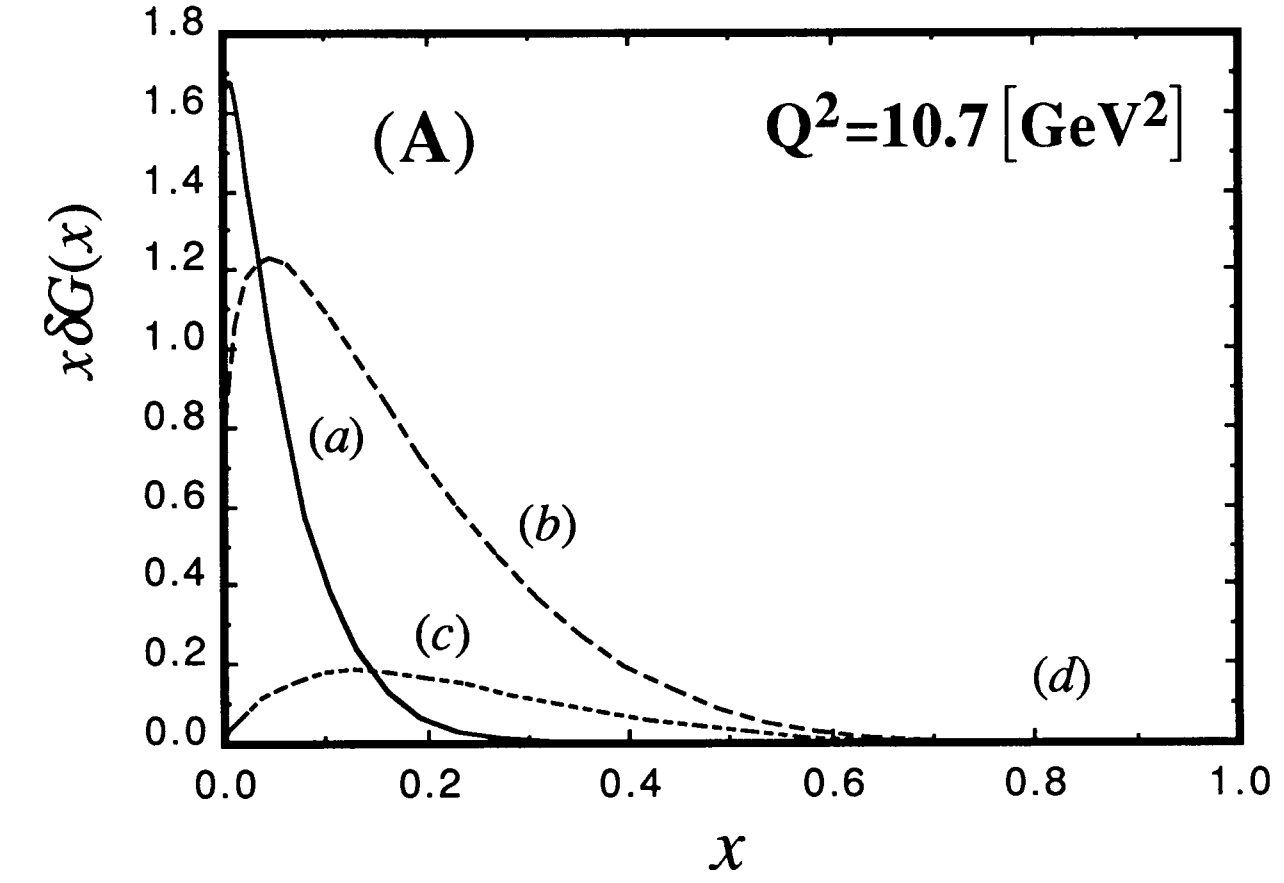
(A)
Q^2=10.7 [GeV^2]
$x\delta G(x)$
(a)
(b)
(c)
(d)
1.8
1.6
1.4
1.2
1.0
0.8
0.6
0.4
0.2
0.0
0.0
0.2
0.4
0.6
0.8
1.0
x

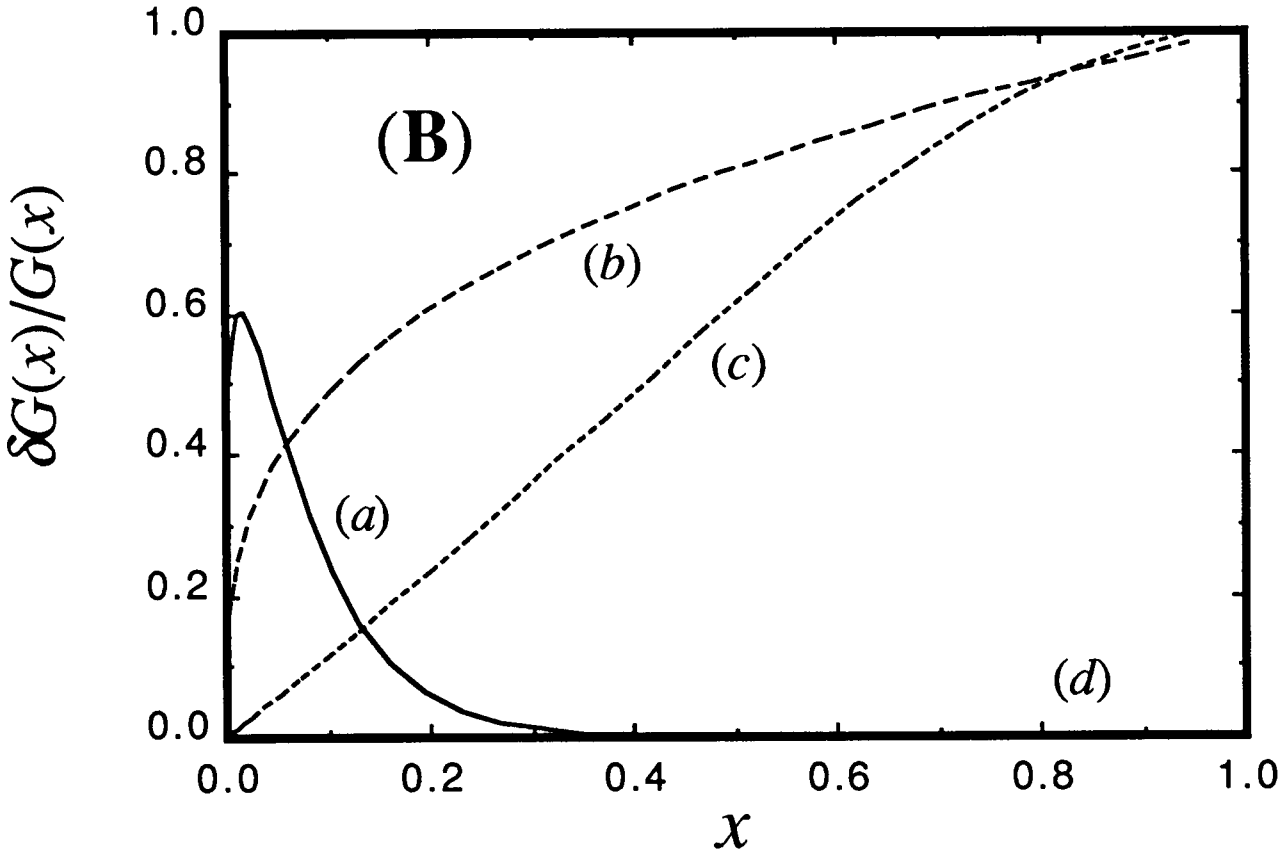
(B)
$\delta G(x)/G(x)$
(a)
(b)
(c)
(d)
1.0
0.8
0.6
0.4
0.2
0.0
0.0
0.2
0.4
0.6
0.8
1.0
x

Fig.6

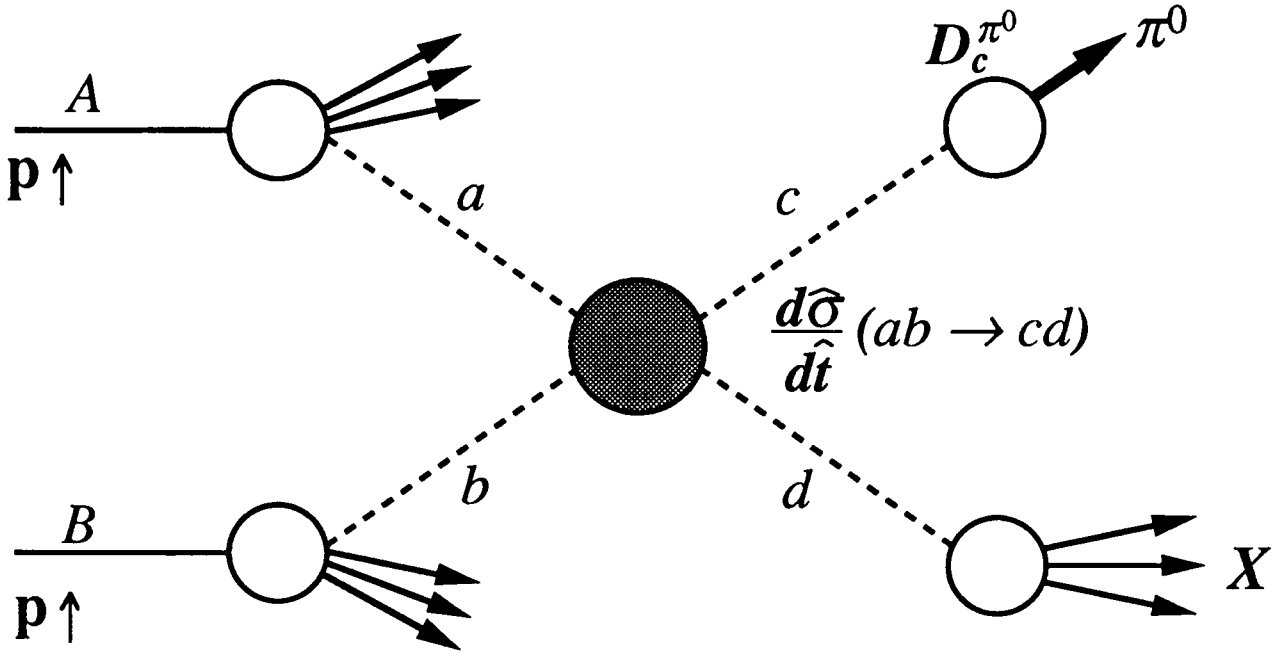

Fig.7

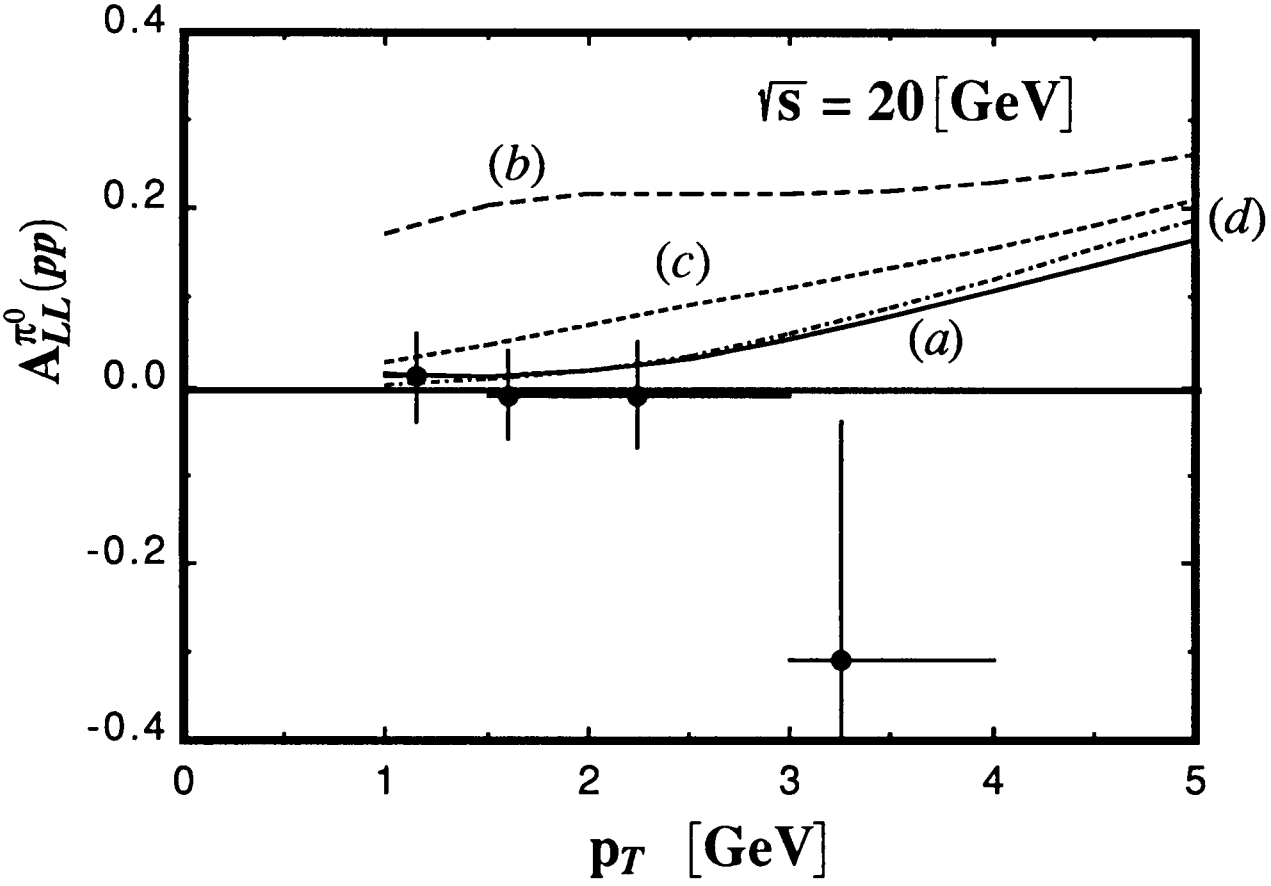
√s = 20 [GeV]
(b)
(c)
(d)
(a)
$A_{LL}^{\pi^0}(pp)$
0.4
0.2
0.0
-0.2
-0.4
0
1
2
3
4
5
p_T [GeV]

Fig.8

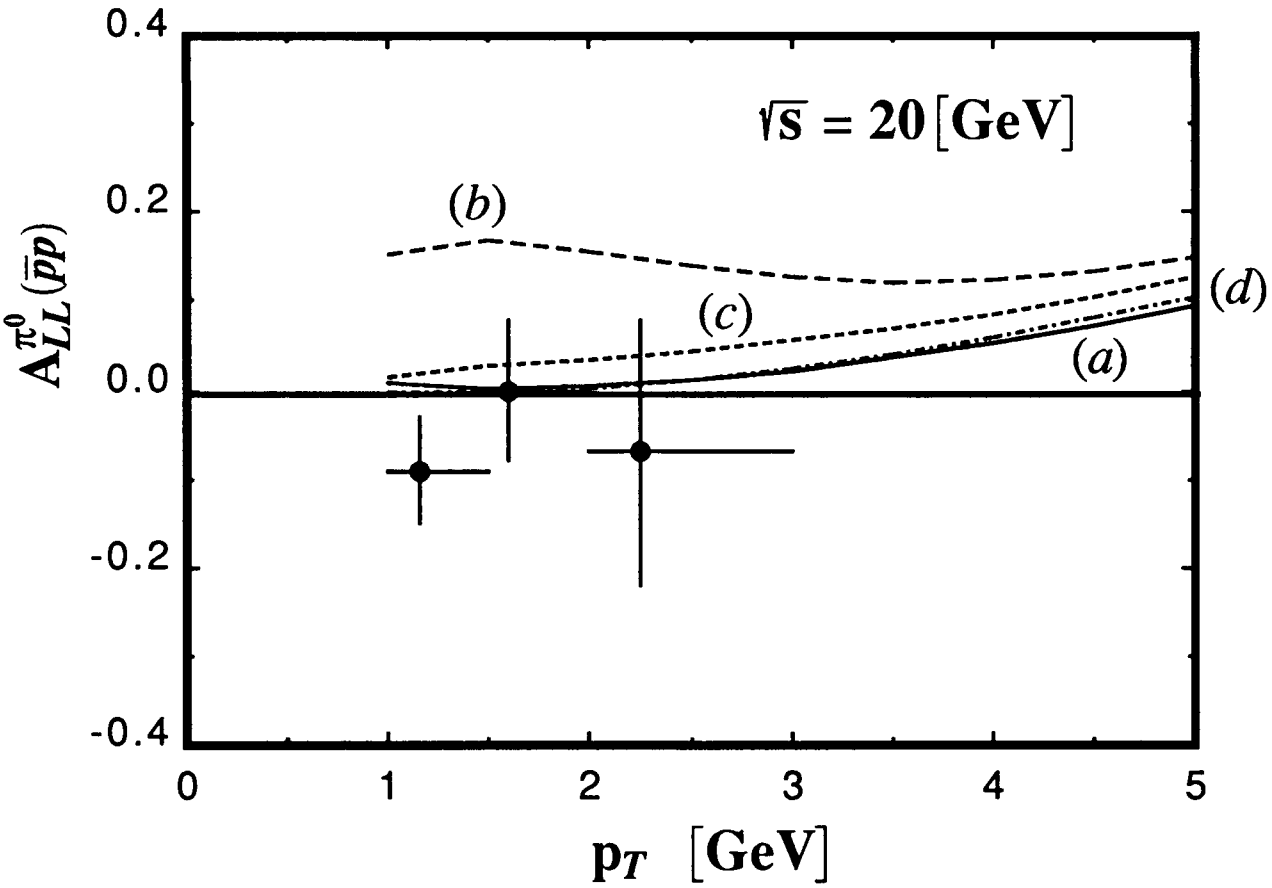
√s = 20 [GeV]
(b)
(c)
(d)
(a)
$A_{LL}^{\pi^0}(\bar{p}p)$
0.4
0.2
0.0
-0.2
-0.4
0
1
2
3
4
5
p_T [GeV]

Fig.9

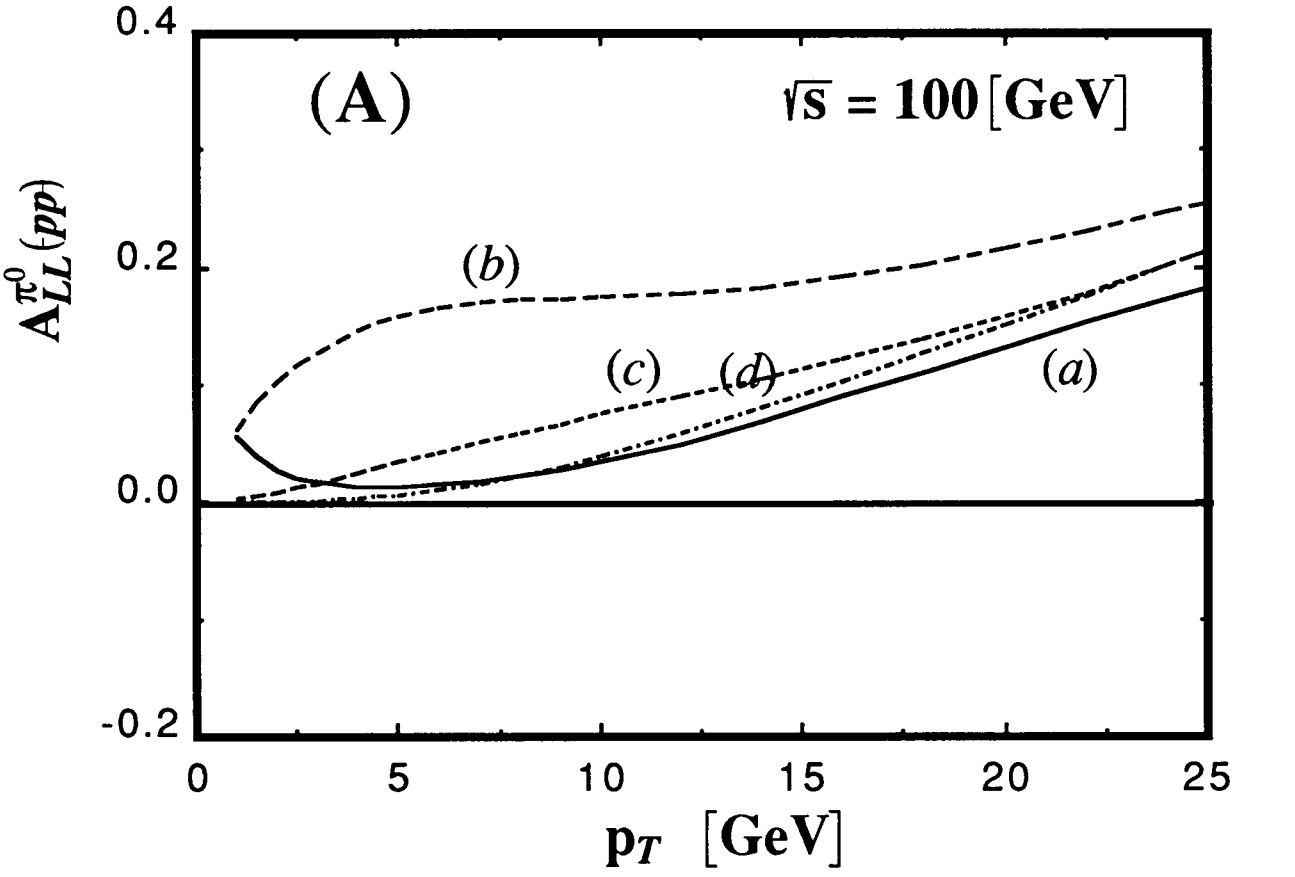
(A)
√s = 100 [GeV]
$A_{LL}^{\pi^0}(pp)$
(a)
(b)
(c)
(d)
0.4
0.2
0.0
-0.2
0
5
10
15
20
25
p_T [GeV]

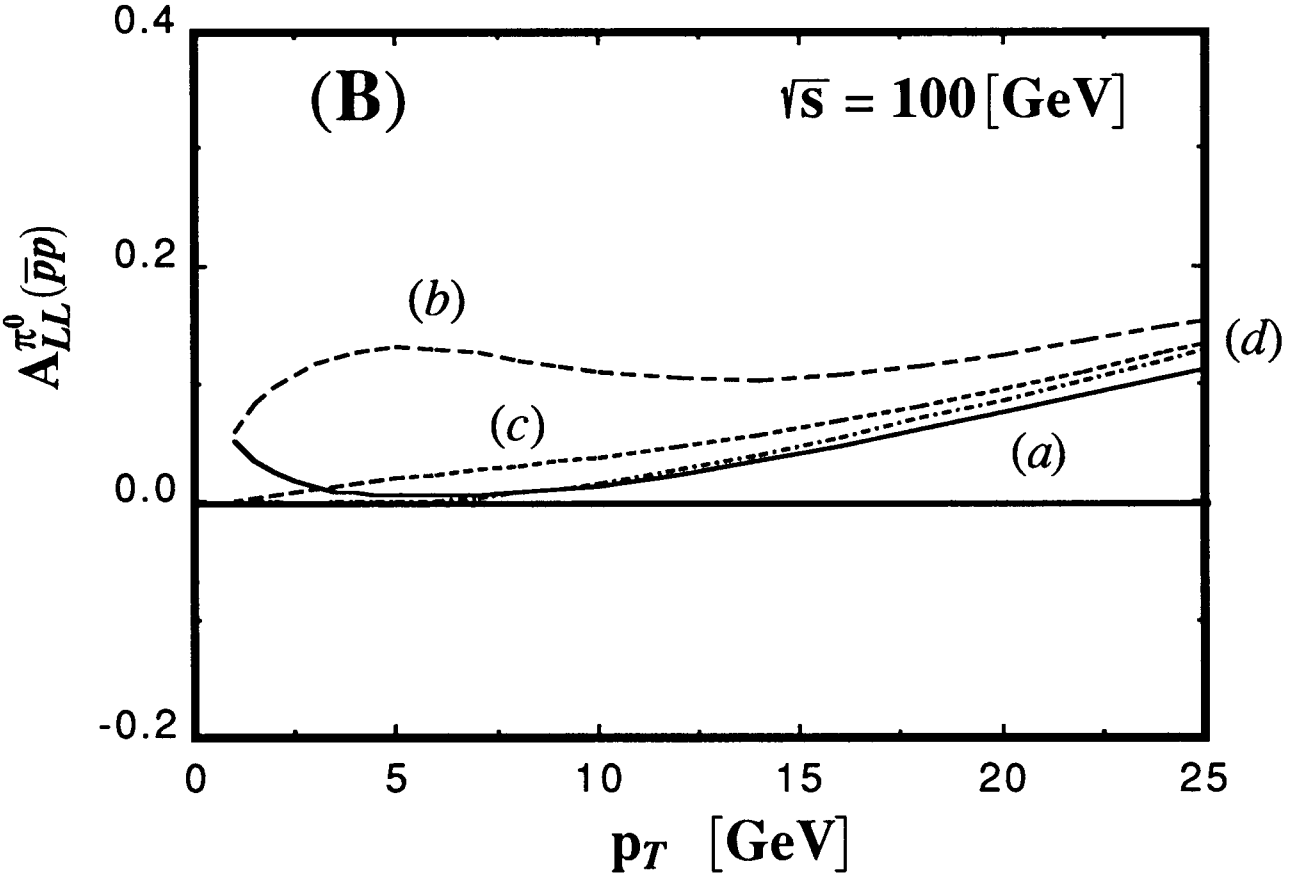
(B)
√s = 100 [GeV]
$A_{LL}^{\pi^0}(\bar{p}p)$
(a)
(b)
(c)
(d)
0.4
0.2
0.0
-0.2
0
5
10
15
20
25
p_T [GeV]

Fig.10

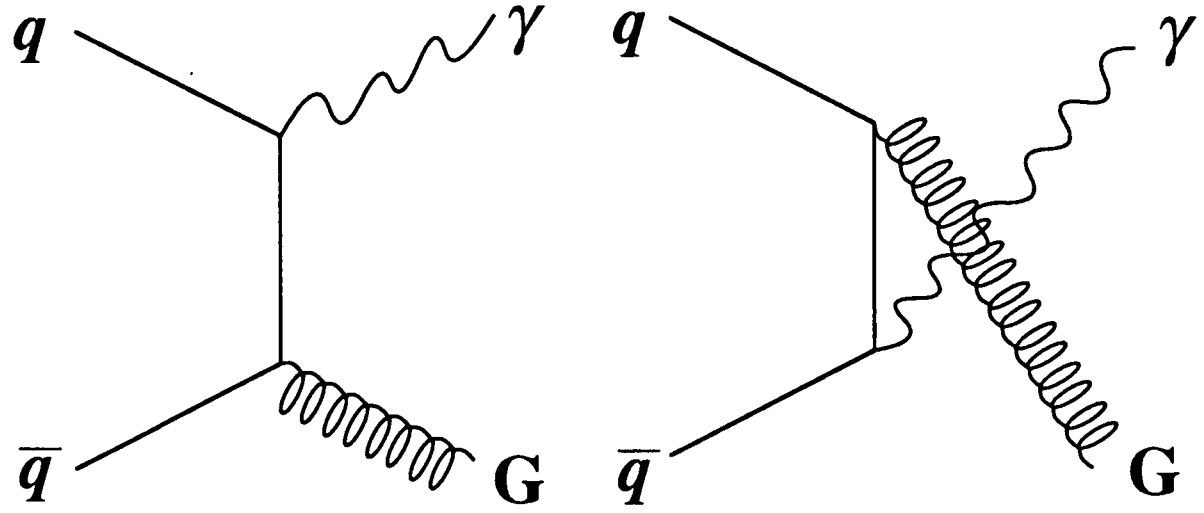

(A)

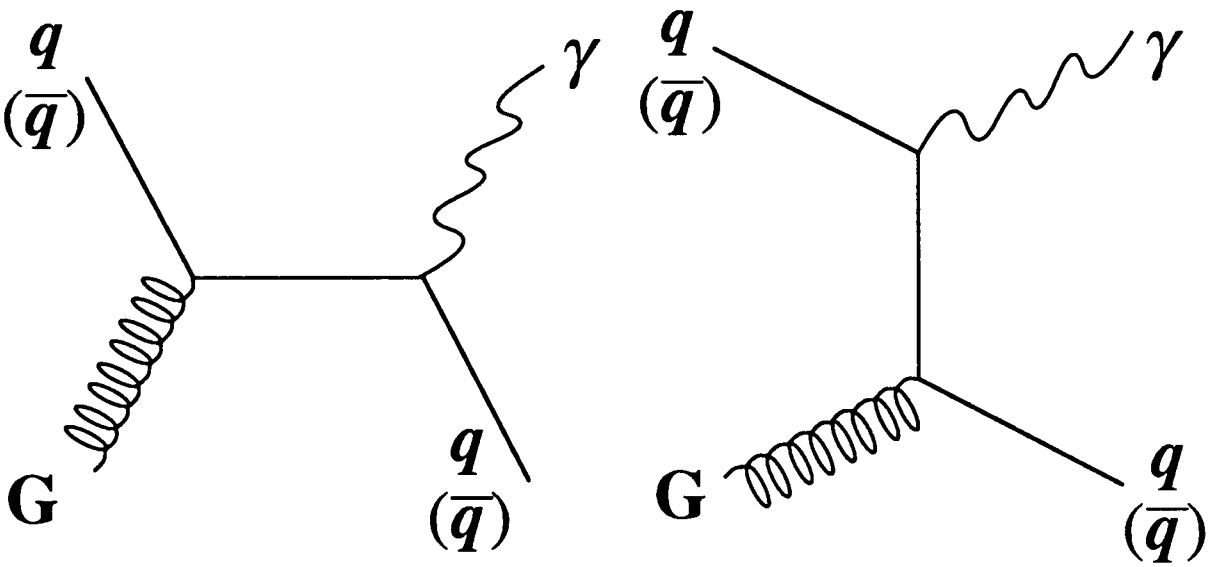

(B)

Fig.11

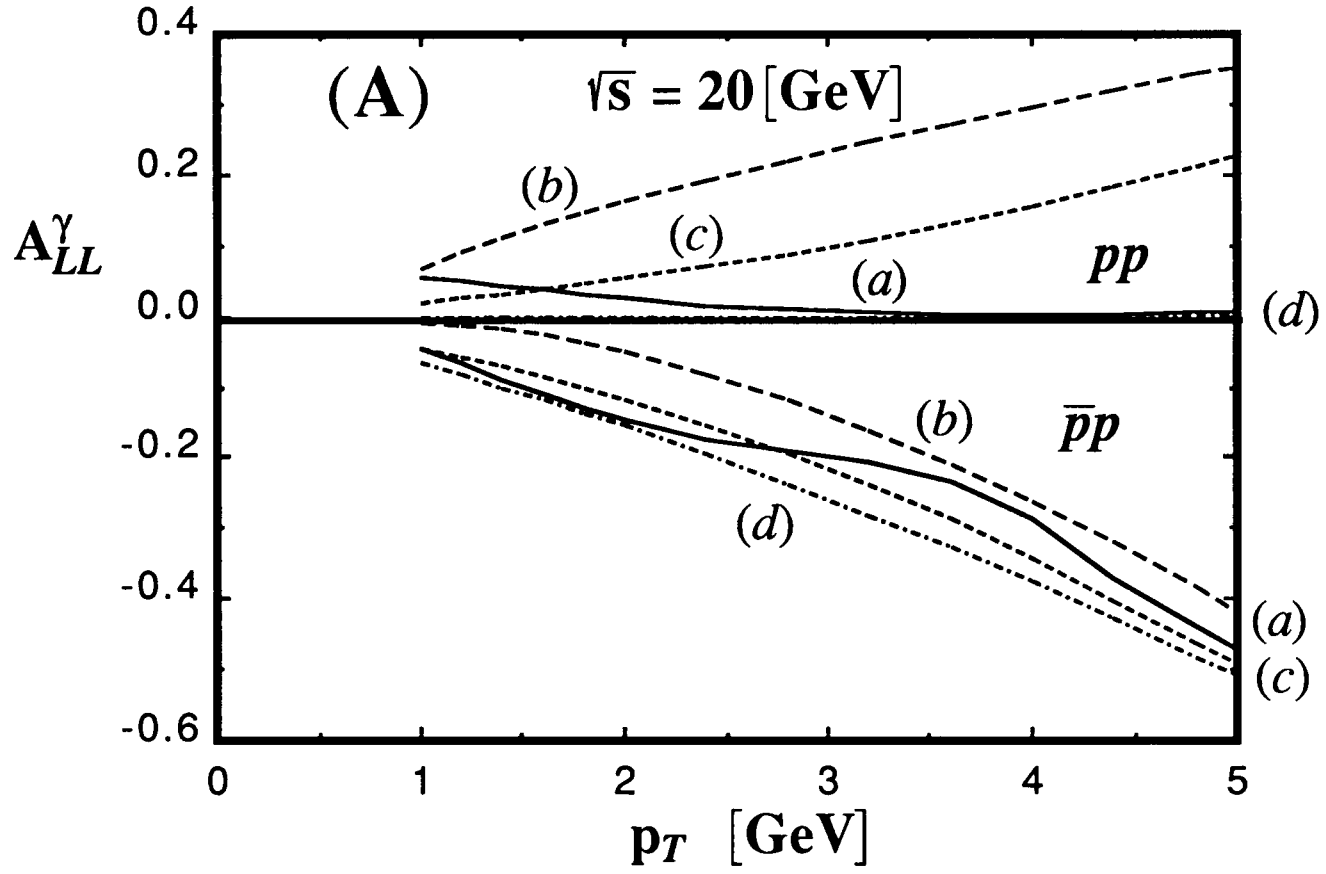
(A)
√s = 20 [GeV]
A_{LL}^{γ}
(b)
(c)
(a)
pp
(d)
(b)
p̄p
(d)
(a)
(c)
0.4
0.2
0.0
-0.2
-0.4
-0.6
0
1
2
3
4
5
p_T [GeV]

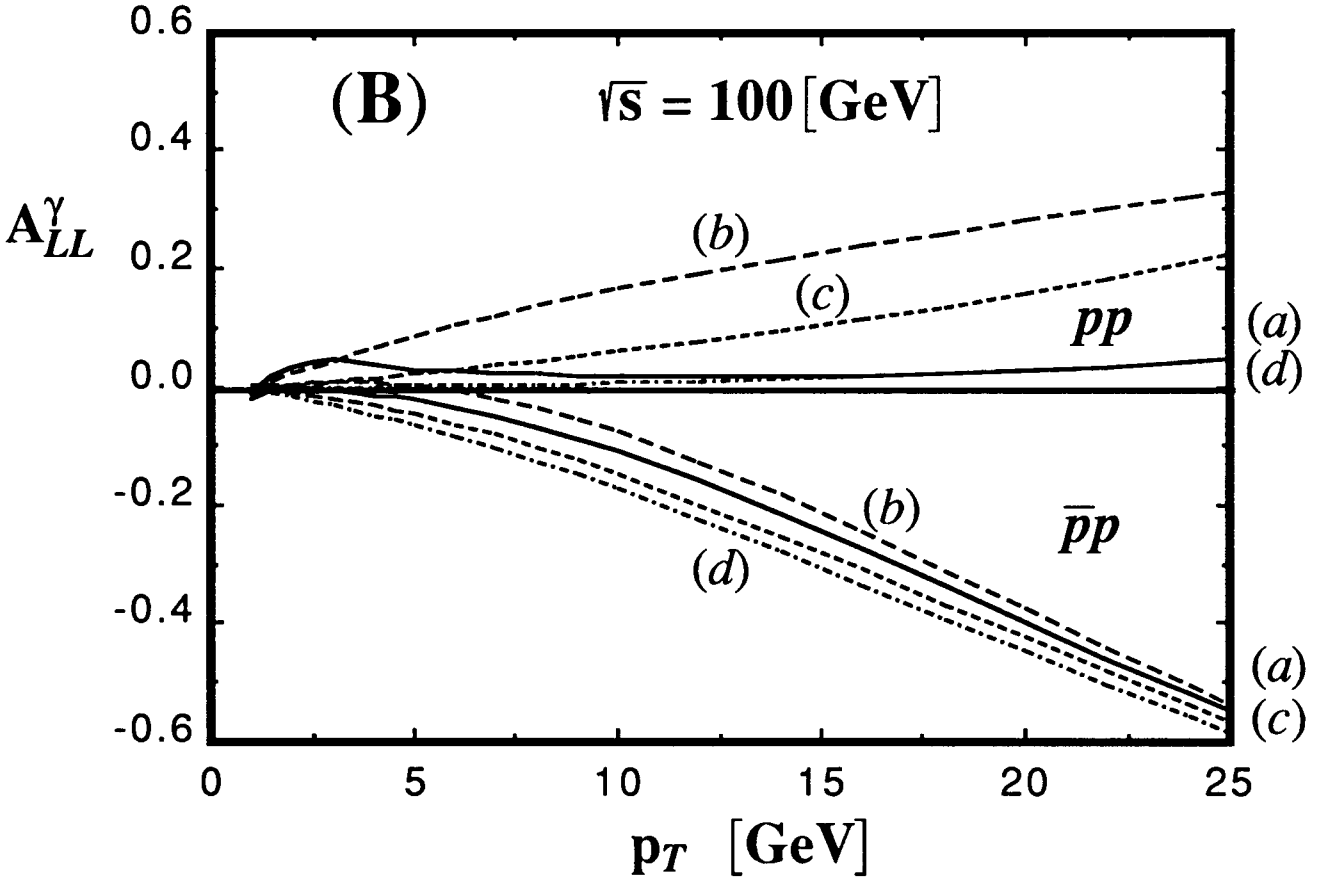
(B)
√s = 100 [GeV]
A_{LL}^{γ}
(b)
(c)
pp
(a)
(d)
(b)
p̄p
(d)
(a)
(c)
0.6
0.4
0.2
0.0
-0.2
-0.4
-0.6
0
5
10
15
20
25
p_T [GeV]

Fig.12

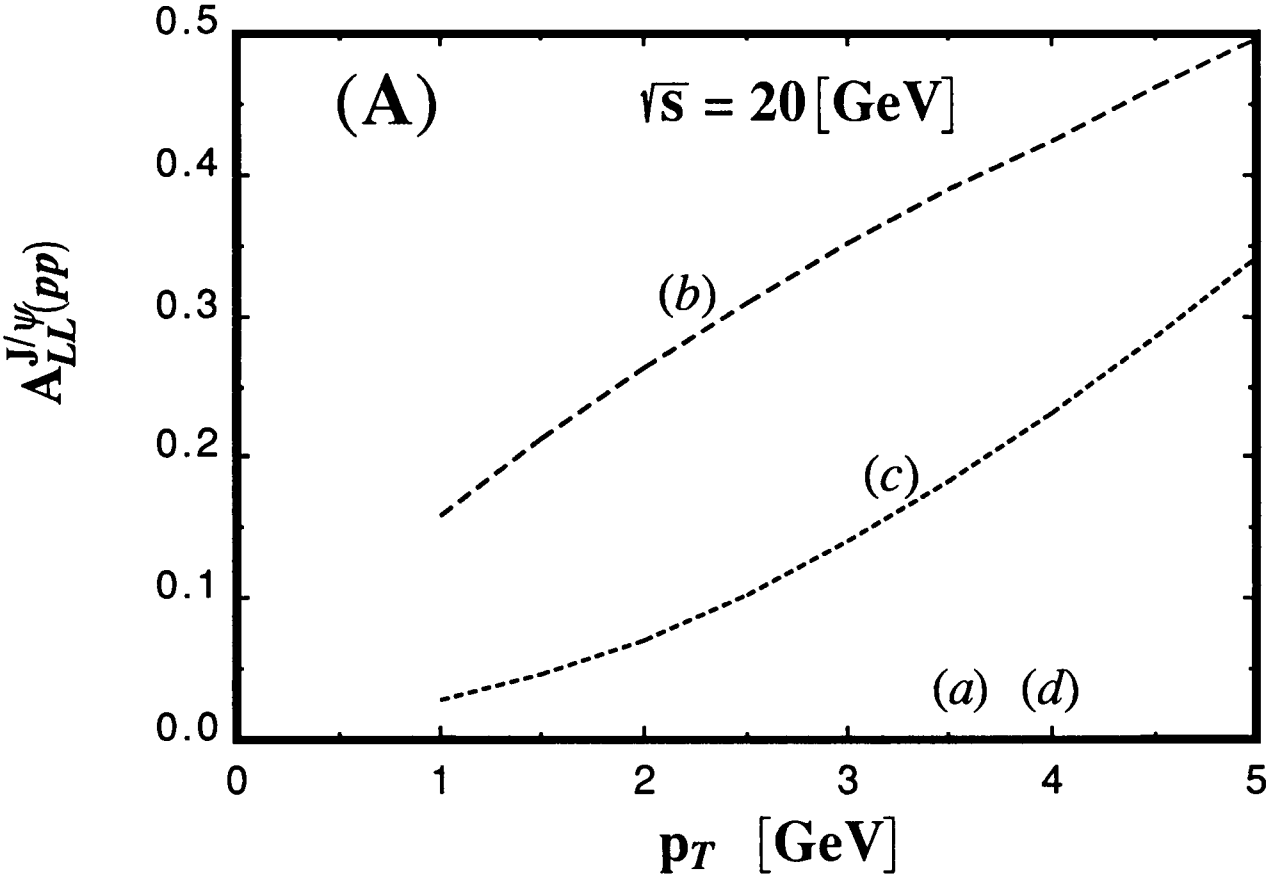
(A)
√s = 20 [GeV]
(b)
(c)
(a) (d)
0.5
0.4
0.3
0.2
0.1
0.0
0
1
2
3
4
5
$A_{LL}^{J/\psi(pp)}$
p_T [GeV]

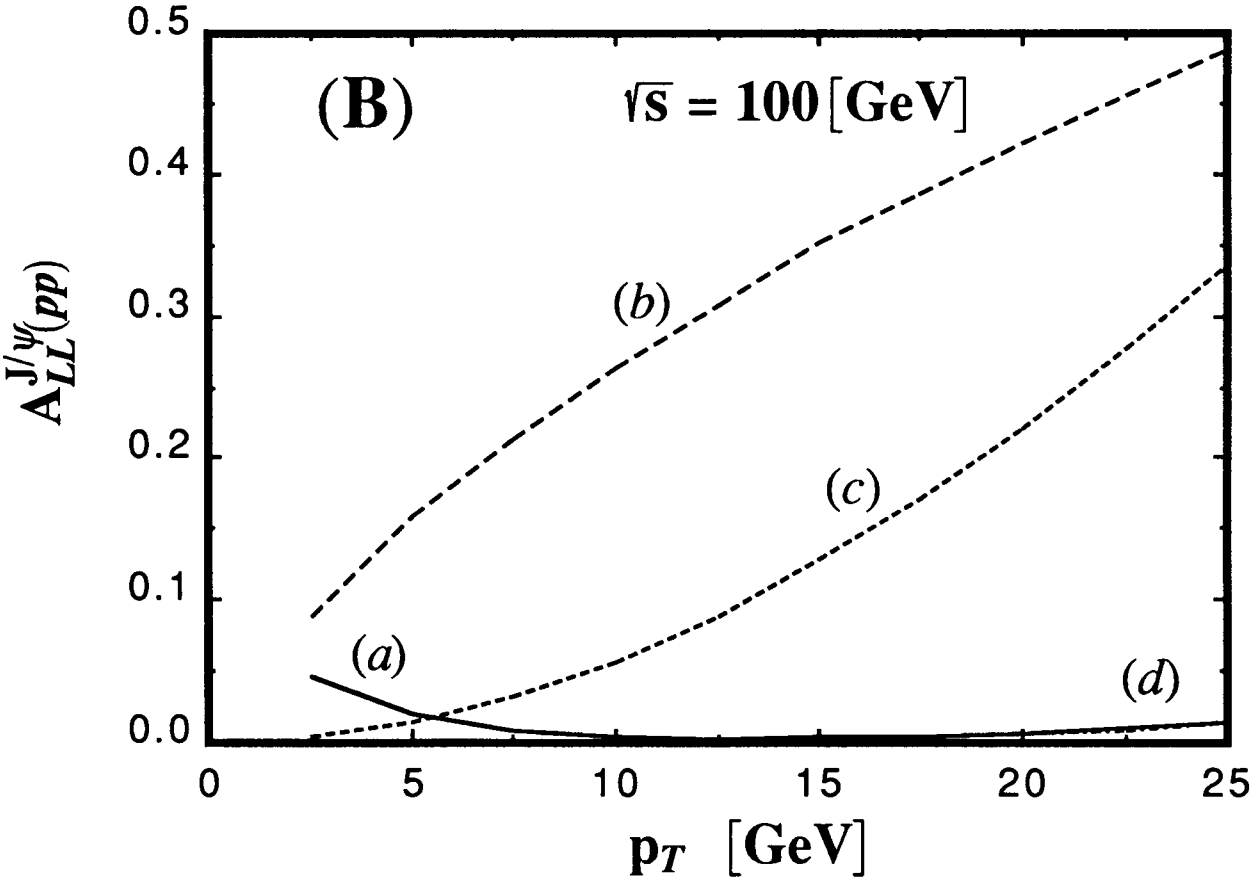
(B)
√s = 100 [GeV]
(b)
(c)
(a)
(d)
0.5
0.4
0.3
0.2
0.1
0.0
0
5
10
15
20
25
$A_{LL}^{J/\psi(pp)}$
p_T [GeV]

Fig.13

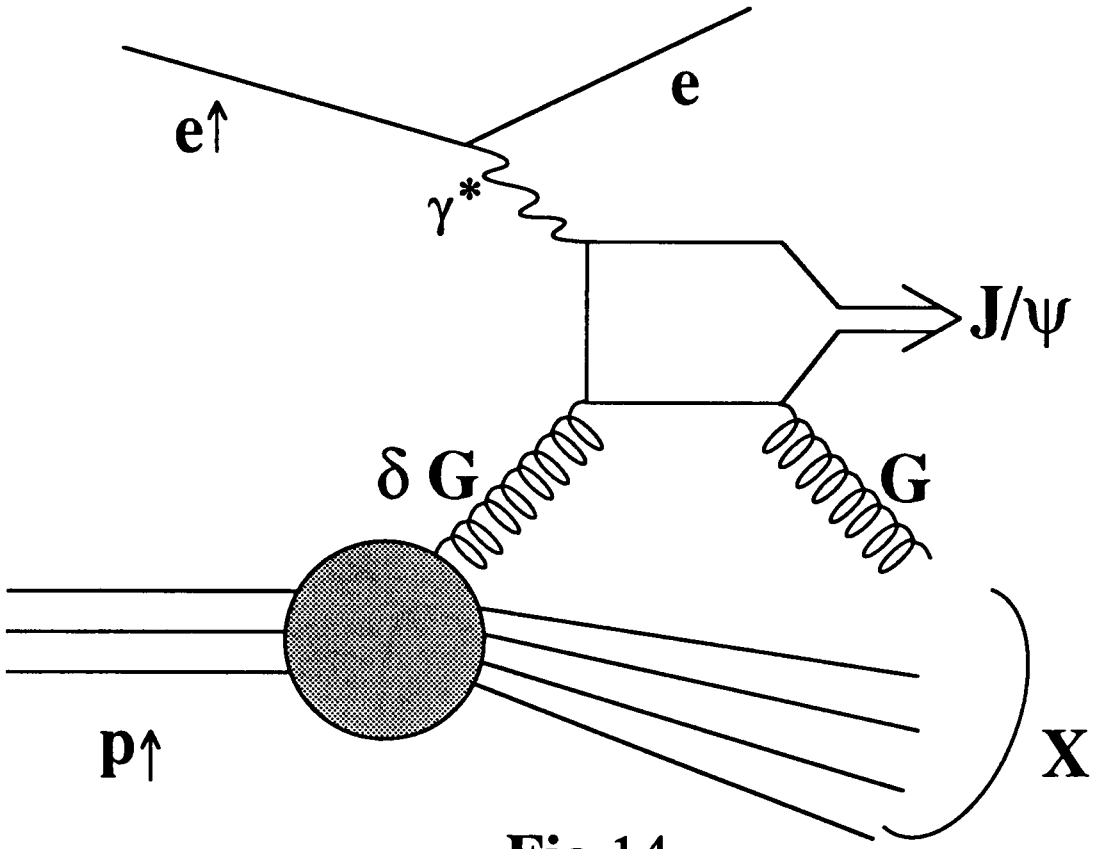
e↑
e
γ*
J/ψ
δ G
G
p↑
X

Fig.14

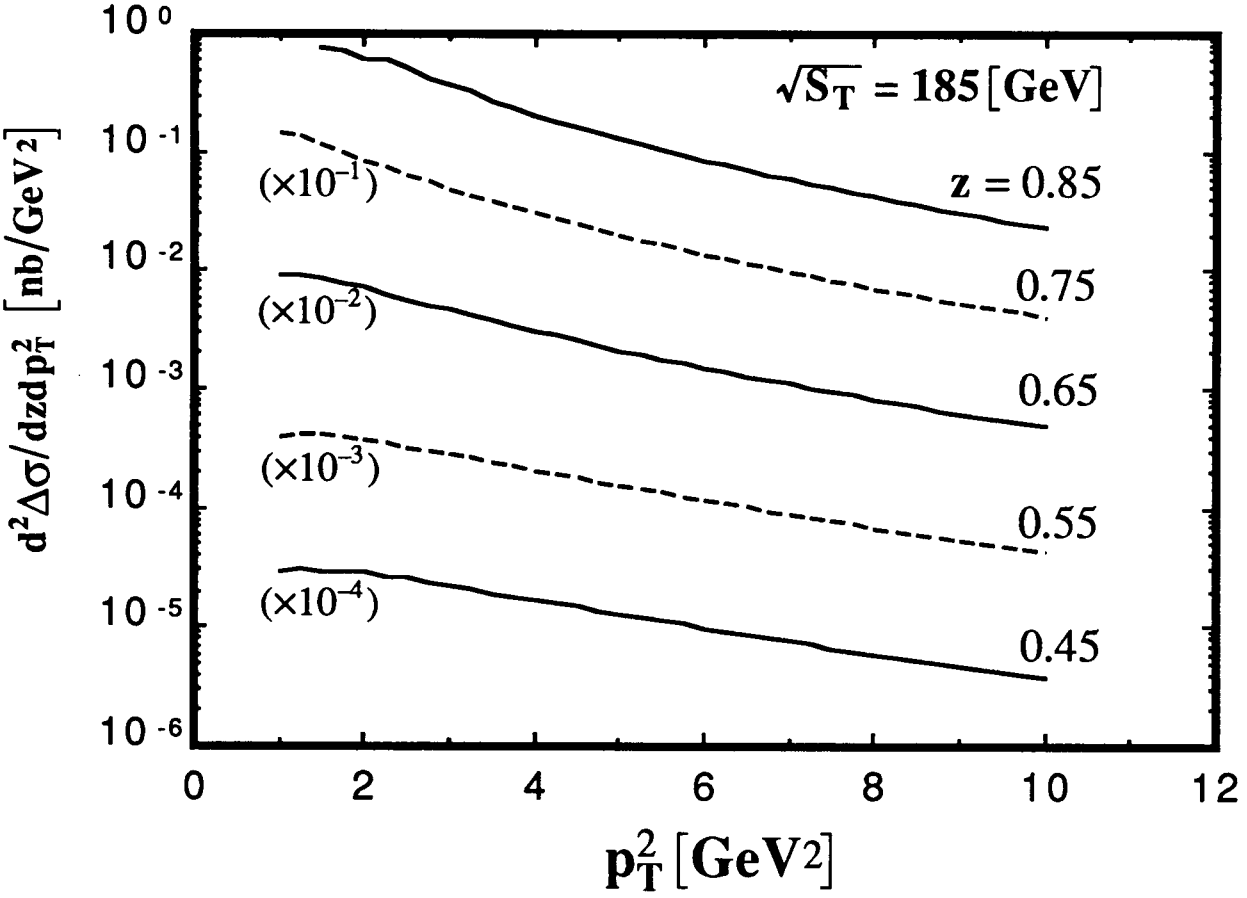
$\sqrt{S_T}$ = 185 [GeV]
z = 0.85
0.75
0.65
0.55
0.45
(×10⁻¹)
(×10⁻²)
(×10⁻³)
(×10⁻⁴)
d²Δσ/dzdp²T [nb/GeV²]
p²T [GeV²]
10 0
10 -1
10 -2
10 -3
10 -4
10 -5
10 -6
0
2
4
6
8
10
12

Fig.15

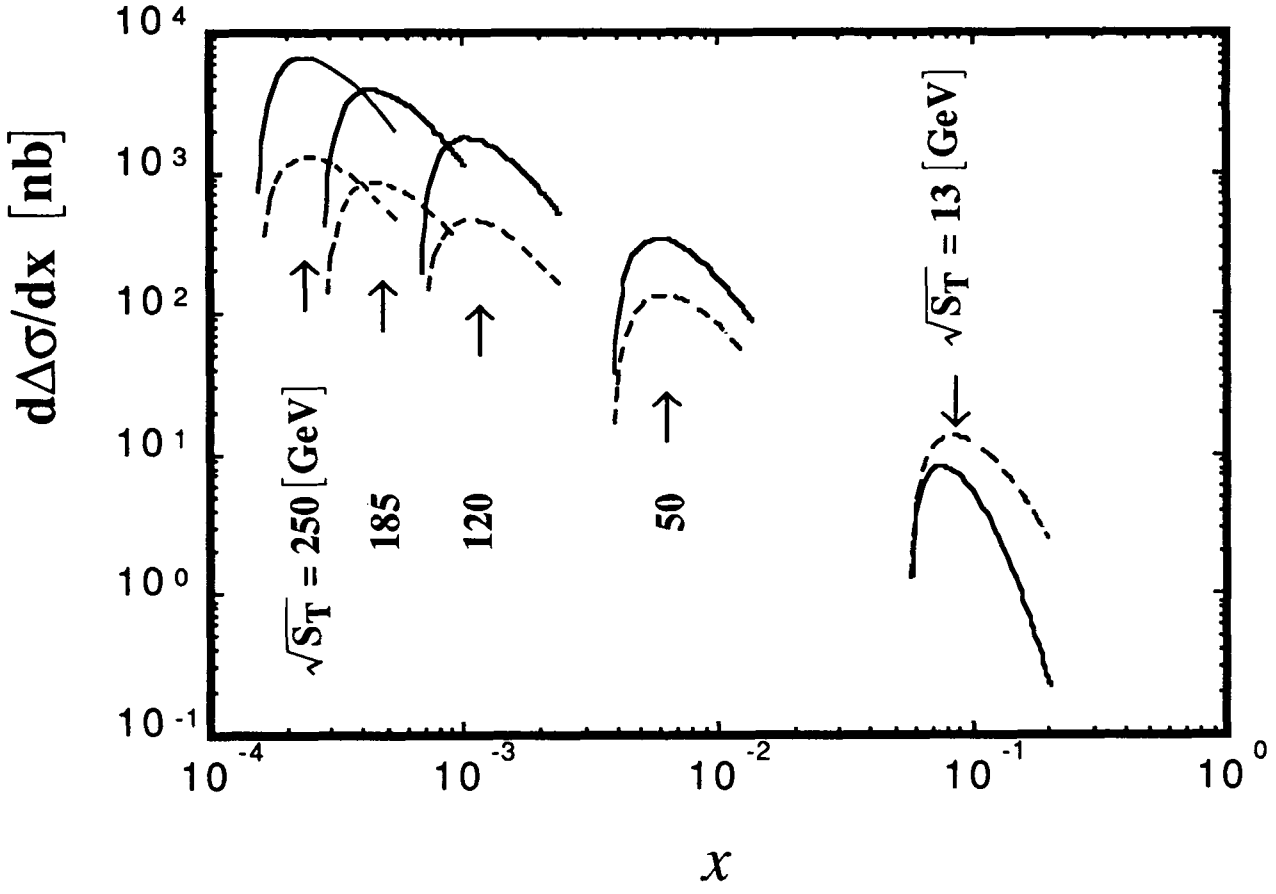
dΔσ/dx [nb]
10 4
10 3
10 2
10 1
10 0
10 -1
10 -4
10 -3
10 -2
10 -1
10 0
x
√S_T = 250 [GeV]
185
120
50
√S_T = 13 [GeV]

Fig.16